2010-10-06

Polymeric Monolithic Stationary Phases for Capillary Hydrophobic Interaction Chromatography

Yuanyuan Li
Brigham Young University - Provo

Polymeric Monolithic Stationary Phases for Capillary Hydrophobic Interaction Chromatography

Yuanyuan Li

A dissertation submitted to the faculty of
Brigham Young University
in partial fulfillment of the requirements for the degree of

Doctor of Philosophy

Milton L. Lee
Adam T. Woolley
Matthew R. Linford
Steven R. Goates
Barry M. Willardson

Department of Chemistry and Biochemistry

Brigham Young University

December 2010

ABSTRACT

Polymeric Monolithic Stationary Phases for Capillary Hydrophobic Interaction Chromatography

Yuanyuan Li

Department of Chemistry and Biochemistry
Doctor of Philosophy

Rigid poly[hydroxyethyl acrylate-*co*-poly(ethylene glycol) diacrylate] (Poly(HEA-*co*-PEGDA) monoliths were synthesized inside 75-μm i.d. capillaries by one-step UV-initiated copolymerization using methanol and ethyl ether as porogens. The optimized monolithic column was evaluated for hydrophobic interaction chromatography (HIC) of standard proteins. Six proteins were separated within 20 min with high resolution using a 20 min elution gradient, resulting in a peak capacity of 54. The performance of this monolithic column for HIC was comparable or superior to the performance of columns packed with small particles. Monoliths synthesized solely from PEGDA were also found to show excellent performance in HIC of proteins. Continuing efforts showed that rigid monoliths could be synthesized from PEGDA or poly(ethylene glycol) dimethacrylates (PEGDMA) containing different ethylene glycol chain lengths for HIC of proteins. Effects of PEG chain length, bi-porogen ratio and reaction temperature on monolith morphology and back pressure were investigated. Monoliths prepared from PEGDA 258 were found to provide the best chromatographic performance with respect to peak capacity and resolution. An optimized PEGDA 258 monolithic column was able to separate proteins using a 20-min elution gradient with a peak capacity of 62. The preparation of these in situ polymerized single-monomer monolithic columns was highly reproducible. The single-monomer synthesis approach clearly improves column-to-column reproducibility.

The highly crosslinked monolith networks resulting from single crosslinking monomers were found to enhance the surface area of the monolith and concentrations of mesopores. Thus, monolithic columns were developed from four additional crosslinking monomers, i.e., bisphenol A dimethacrylate (BADMA), bisphenol A ethoxylate diacrylate (BAEDA, EO/phenol = 2 or 4) and pentaerythritol diacrylate monostearate (PDAM) for RPLC of small molecules. Gradient elution of alkyl benzenes and alkyl parabens was achieved with high resolution using all monolithic columns. Porogen selection for the BADMA and PDAM was investigated in detail with the intention of obtaining data that could possiblly lead to a rational method for porogen selection.

Keywords: liquid chromatography, monolithic, hydrophobic interaction, capillary column, polymeric, diacrylate, dimethacrylate, poly(ethylene glycol), proteins, reversed phase, small molecules, bisphenol A dimethacrylate, bisphenol A ethoxylate diacrylate, pentaerythritol diacrylate monostearate, porogen selection

ACKNOWLEDGEMENTS

First and foremost, I give my thanks to my advisor, Dr. Milton L. Lee, for his consistent guidance, insights, patience, support and encouragement throughout my educational experience at Brigham Young University. I feel fortunate to have had the opportunity to study and perform research in his group. What I have learned from him is invaluable for my future career and personal life.

I would also like to thank the professors in the chemistry department for teaching me fundamentals and experimental skills in analytical chemistry. My graduate committee members, Dr. Matthew R. Linford, Dr. Adam T. Woolley, Dr. Steven R. Goates and Dr. Barry M. Willardson have provided critical evaluation and useful suggestions in my progress reports during my six-year PhD program. I also thank Dr. Karl F. Warnick and Dr. H. Dennis Tolley for their guidance and suggestions during my research.

Members in Dr. Lee's group are greatly acknowledged for their helpful discussions and friendship. In particular, I would like to thank Dr. Shu-ling Lin, Dr. Yansheng Liu, Dr. Binghe Gu and Dr. Xuefei Sun for their collaborations and helpful discussions. I give Susan Tachka and Sarah Holstine special thanks for their administrative support for all of us in Dr. Lee's group.

I express my gratitude to people in the department instrument shop and computer support office, especially Robert B. Hallock, Keith R. Kling and Michael Torrie. I also appreciate the opportunity and financial support offered by the Department of Chemistry and Biochemistry at Brigham Young University. The financial support from the National Institutes of Health is also gratefully acknowledged.

Last but not least, I would like to express my appreciation to my husband, Xueyuan Zhou, for his love and support, and my 3-year-old daughter, Yunqi (Anna), for the happiness she brings us. I also thank my parents and sisters for their continual love and support. I owe many thanks to all my tutors and friends, whose names are not mentioned here, who paved the way for me and provided encouragement throughout my life.

TABLE OF CONTENTS

LIST OF ABBREVIATIONS

AIBN	azobisisobutyronitrile
AMPS	2-acrylamido-2-methyl-1-propanesulfonic acid
ATRP	atom transfer radical polymerization
BADMA	bisphenol A dimethacrylate
BAEDA	bisphenol A ethoxylate diacrylate
BMA	butyl methacrylate
BMA-GDMA	poly(butyl methacrylate-*co*-glycerol dimethacrylate)
BVPE	1,2-bis(p-vinylphenyl)ethane
CEC	capillary electrochromatography
CLC	capillary liquid chromatography
DBC	dynamic binding capacity
DEGDMA	diethylene glycol dimethacrylate
DMF	dimethylformamide
DMPA	2,2-Dimethoxy-2-phenylacetophenone
DMSO	dimethyl sulfoxide
EDMA	ethylene glycol dimethacrylate
EPE-2800	poly(ethylene glycol)-*block*-poly(propylene glycol)-*block*-poly(ethylene glycol) (Mn = ~ 2800)
FITC	fluorecein isothiocyanate
GDMA	poly(glycerol dimethacrylate)
GMA-EDMA	poly(glycidyl methacrylate-*co*-ethylene dimethacrylate)

HEA	2-hydroxyethyl acrylate
HEA-PEGDA	poly[hydroxyethyl acrylate-*co*-poly(ethylene glycol) diacrylate]
HEMA	2-hydroxyethyl methacrylate
HEMA-EDMA	poly(2-hydroxyethyl methacrylate-*co*-ethylene dimethacrylate)
HIC	hydrophobic interaction chromatography
HILIC	hydrophilic-interaction chromatography
HPLC	high-performance liquid chromatography
IEC	ion-exchange chromatography
IPA	isopropyl alcohol
LC	liquid chromatography
MS-BVPE	poly[p-methylstyrene-*co*-1,2-(p-vinylphenyl)ethane]
PDAM	pentaerythritol diacrylate monostearate
PEG	poly(ethylene glycol)
PEGDA	poly(ethylene glycol) diacrylate
PEGDMA	poly(ethylene glycol) dimethacrylate
PEGMEA	polyethylene glycol methyl ether acrylate
PEP-2700	poly(propylene glycol)-*block*-poly(ethylene glycol)-*block*-poly(propylene glycol) (Mn = ~ 2700)
PPG	poly(propylene glycol)
PS-DVB	poly(styrene-*co*-divinylbenzene)
RPLC	reversed phase liquid chromatography
RSD	relative standard deviation
SEC	size exclusion chromatography

SEM	scanning electron microscopy
SEMA	2-sulphoethyl methacrylate
THF	tetrahydrofuran
TPM	3-(trimethoxysilyl)propyl methacrylate
TRIM	trimethylolpropane trimethacrylate
TVBS	tetrakis(4-vinylbenzyl)silane
UHPLC	ultrahigh pressure LC
VAL	2-vinyl-4,4-dimethylazlactone
XPS	X-ray photoelectron spectroscopy

LIST OF TABLES

LIST OF FIGURES

CHAPTER 1 BACKGROUND AND SIGNIFICANCE

1.1 Introduction

The chromatographic process involves the flow of a mobile phase through a stationary phase and selective distribution of analytes between the two phases. Thus, a stationary phase containing pores that are large enough to facilitate flow is an essential part of chromatography. As for high-performance liquid chromatography (HPLC), the hydraulic resistance of stationary phase to flow of mobile phase should be moderate, so that the analysis can be conducted within a reasonable time period, and a certain length of column can be used with a given pumping system. On the other hand, a fast and continuous exchange of solute molecules (mass transfer) between the mobile and the stationary phases is highly desirable to achieve high column efficiency. In a diffusion-controlled mass transfer process, a decrease in the diffusion distances can greatly reduce the resistance to mass transfer in the stationary phase. A small diffusion distance is even more important for large molecules since their diffusion coefficients are several orders of magnitude smaller than those of small molecules. At the same time, a large stationary phase surface area also contributes to fast mass transfer. These structural features together with the physical and chemical natures of mobile and stationary phases determine the characteristics of a chromatographic separation.

For packed columns, a logical way to reduce the diffusion path length has been to decrease the particle size. Column efficiency is directly proportional to the particle diameter according to the van Deemter equation.[1] However, as the particle size decreases, the permeability of the packed bed decreases proportionally. This results because as the particle size becomes smaller, the interstitial voids in the packed bed become smaller as well. The

pressure drop of a perfectly packed column is inversely proportional to the square of the particle diameter. Although packing density also contributes to column permeability, a less dense packing leads to a proportional increase in the number of defects in its bed, which consequently reduces the column efficiency. Ultrahigh pressure LC (UHPLC) pumps are now available, which makes it possible to achieve fast and high-resolution separations by utilizing sub-micron particles in packed columns;[2,3] however, further reduction in particle size is practically limited by the resulting backpressure; therefore, enhancement of column performance by simply reducing particle size is not practical. An alternative approach to achieve speedy analysis with similar column efficiency is through operating at higher temperature, since mobile phase viscosity decreases rapidly with increasing temperature.[4,5] Finally, monolithic beds, which were introduced two decades ago as chromatographic phases by Hjertén and Svec,[6-8] allow rapid analysis because of high column permeability.

Monolithic materials are continuous, porous structures characterized by mesopores and macropores. In terms of chromatography, a major advantage of monolithic columns is the ability to control and optimize separately the average sizes of the macropores or throughpores and the interconnected porous skeleton, which can be related to the particle diameter in packed columns.[9] Compared to packed columns, monolithic columns are absent of structural void volumes, and the microglobular skeleton is highly interconnected. This leads to more pores through which the mobile phase can flow. Therefore, most of the porous bed becomes available to the mobile phase, and mass transfer is facilitated by convective flow instead of pore diffusion. This difference in hydrodynamics allows high permeability and fast mass transfer. Furthermore, Monolithic columns are easy to prepare, and frits are no longer required to contain the packed bed. These characteristics make

monoliths particularly attractive for capillary liquid chromatography (CLC) and electrochromatography (CEC). They have been applied in most of the LC separation modes. Excellent reviews have appeared that describe the preparation of monoliths and their applications in LC.[9-16]

In this chapter, I focus on the synthesis of organic polymer monoliths as stationary phases for CLC, with emphasis on the two main concerns of designing a monolith for LC application, i.e., tailoring the surface chemistry to obtain the desired chromatographic selectivity, and optimizing the porous structure to allow the mobile phase to percolate through the monolithic bed at a reasonable pressure drop. I also review monoliths applied in CEC and microfluidic devices. Noteworthy to remember is that performance characteristics, such as stability, porosity and permeability, play a more important role in column performance in LC compared to CEC, because hydraulic pressure is used to drive the mobile phase.

The preparation of organic polymer monoliths in a capillary format is simple and straightforward. First, the inside wall of the capillary is treated so that the monolith can easily attach firmly to it to avoid gaps between the polymer and the capillary wall. The most widely used fused-silica capillary is usually treated with a bi-functional reagent through a silanization reaction, and the other functional group (e.g., vinyl group) can react with the monomer mixture to bind the polymer to the wall. Second, the capillary is filled with a homogeneous polymerization mixture, containing initiator, monomer(s) and porogen(s), and sealed at both ends with rubber stoppers, and the polymerization is initiated by heating or UV radiation. Monomers can be composed of functional monomer and crosslinking monomer, or a single functional crosslinking monomer. Porogens are present

to produce the porous structure, and they do not participate in the polymerization. When the polymerization is finished, the capillary is washed with appropriate solvent to remove the porogens and any other soluble compounds from the pores of the monolithic column. Third, if necessary, the polymeric monolith is modified with reagents to provide the desirable surface chemistry.

1.2 Capillary Surface Modification

Before introducing the polymerization mixture inside the fused-silica capillary column, the surface is modified with a bifunctional silanizing reagents with the purpose of preparing a mechanically stable column. Normally, vinyl silane, methacrylate silane or acrylate silane are used as coupling reagents, because they contain at least one functional group with a double bond that can react with the organic polymer, and functional groups that react with silanol groups on the capillary surface. Thus, after polymerization, monoliths are covalently attached to the capillary surface. This ensures that the monolith can withstand a relatively high pressure without being extruded from the capillary, and void channels caused by partial detachment are not formed between the monolith and the capillary wall due to shrinkage of the monolith during polymerization. Mechanical stability and radial homogeneity are two crucial features that influence column performance. Proper preparation of the capillary surface is, thus, important for achieving high quality separations. Generally, the procedures for capillary surface modification consist of capillary pre-treatment, silanization and drying. There are several detailed discussions in the literature concerning surface modification using 3-(trimethoxysilyl)propyl methacrylate (TPM) (synonym: [3-(methacryloyloxy)propyl] trimethoxysilane) as coupling agent,[17,18]

since TPM is the most widely used bifunctional compound for modifying the inner wall of fused-silica capillaries for monolith preparation.

Courtois et al. summarized and compared 3 pretreatments and 11 silanization methods that represented the most often used procedures for capillary surface modification.[17] The pretreatment procedures differed in base concentration, etching temperature and etching time, while the variables in the silanization step were concentration of the silane coupling agent (i.e., TPM), solvent used, silanization time and temperature, and presence (or not) of an inhibitor of vinyl polymerization during the silanization step. Capillaries of 1 mm i.d., rather than smaller diameter capillaries, were used to prepare monoliths with the purpose of performing all measurements using the same capillaries. Several important conclusions were addressed in this work. First, the etching step using alkaline solution increased the surface silanol concentration, resulting in an increase in the hydrophilicity of the capillary. Capillaries treated with 1 M NaOH/KOH at elevated temperature (120 ^{o}C) exhibited the lowest wetting angles together with the highest O/Si ratios measured by X-ray photoelectron spectroscopy (XPS). The lack of homogeneity of the capillary surface was observed prior to treatment, which made pre-treatment more important in order to obtain similar surface properties with capillaries from different batches and suppliers. Second, the etching step increased the roughness of the capillary surface. Roughness also contributed to adhesion of the monolith to the capillary wall as demonstrated by the firm adhesion of 1,6-hexanediol dimethacrylate polymer to a capillary that was only etched with KOH at higher temperature. Third, the TPM concentration was found to not be significant; however, a high TPM concentration could lead to polymerization, producing a TPM polymer layer in the capillary. The presence of water in

the silanization step resulted in weakly attached TPM and produced a thin layer of TPM gel on the capillary surface. The thin layer seemed to be retained by hydrophobic attraction rather than covalent bonding. Thus, this TPM gel could be easily washed away, which was confirmed by XPS measurements showing a lower carbon concentration after flushing with acetone. This work also revealed that procedures using acetone as solvent to dissolve TMP, which are frequently cited in the literature, did not give satisfactory results.

Vidič et al. studied the influence of glass surface modification on monolith attachment.[18] Different procedures for pre-treatment and silanization were investigated using three types of glass. Contact angles between the glass surface and water drop were measured to determine the concentration of silanol groups remaining on the surface after silanization. The pressure drop at which the monolith was dislodged was measured to evaluate the strength of monolith attachment to the capillary surface. It was found that the critical step in the glass surface modification procedure was the glass pre-treatment. Good results were obtained with glass boiled in water or 2 M HCl solution for 2.5 h or more. Among all tested silanization procedures, that using the 15% TPM in dried toluene solution gave the best results in most cases, which is in agreement with Courtois's work discussed above. A more recent study demonstrated that the use of toluene as solvent to dissolve TPM gave the most effective silanization compared to the other three commonly used solvents.[19] Since a pretreatment procedure such as etching or leaching might increase the surface roughness and consequently increase the strength of monolith attachment, the surface roughness was determined for both untreated and pre-treated glass boiled for 2.5 h in deionized water. The results showed no differences between the two samples, which indicated that the roughness of the pre-treated glass surface in water was not the reason for

better attachment of the monolith to the capillary wall. The author suggested that boiling resulted in formation of a thin layer containing with a unique chemical composition that may enhance the surface reactivity. Gu et al. followed a similar optimized procedure to treat the capillary inner surface.[20]

The above two procedures contained either etching or leaching in the pre-treatment step; however, in another work,[21] it was demonstrated that etching the columns with NaOH followed by a leaching treatment with HCl provided higher reproducibility than by either leaching or etching alone. Base on the above discussion, I recommend that the pre-treatment procedure include both etching and leaching steps. The complete, optimized procedure for capillary surface modification can be summarized as (1) washing step, in which a 5-m-long capillary was rinsed sequentially with ethanol and water to remove any impurities, (2) etching step, in which the capillary was filled with 1 M aqueous NaOH and heated to 120 ^{o}C for 3 h in a GC oven, (3) leaching step, in which the capillary was rinsed with water again, filled with 1 M HCl and heated to 110 ^{o}C for 3 h, (4) drying step, in which the capillary was rinsed with water and ethanol, and then dried at 120 ^{o}C for 1 h with a stream of nitrogen gas, (5) silanization step, in which the surface-activated capillary was filled with 15% (v/v) TPM in dry toluene at 35 ^{o}C overnight, and (6) drying step, in which the capillary was washed with toluene and acetone sequentially and then dried under a nitrogen gas purge at room temperature overnight.

It is worth mentioning that for a 10-μm i.d. capillary, an increase in the degree of silanization leads to the formation of a less porous layer on the surface.[22] The authors claimed that further increases in the extent of silanization using longer reaction time and/or higher temperatures should ultimately lead to the formation of a thick surface layer, leaving

little or no monomer available to form a monolithic structure in the center of the capillary. Examples were given that Yue et al. obtained a 10-μm i.d. PLOT capillary column after silanizing the capillary wall for 12 h at room temperature,[23] and Huang and Horvath also obtained a PLOT capillary column after silanizing the capillary at 120 ^{o}C for 6 h.[24] Although it was not mentioned, the selection of an appropriate solvent so that phase separation occurred early in the polymerization process was also an important factor in obtaining a PLOT column in both examples. In contrast, the effect of degree of silanization on monolith morphology was not observed for monoliths prepared in 50 μm I.D. capillaries that have a significantly larger volume-to-surface ratio. A similar confinement effect on monolith structure was reported in an earlier work.[25]

1.3 Initiation

There are a wide variety of techniques reported for the preparation of polymeric monoliths. They include radiation polymerization,[26,27] polymerization of high internal phase emulsions,[28,29] cryogels,[30,31] living polymerization,[32-36] polycondensation,[37,38] and preparation of monoliths from soluble polymers.[39,40] Svec recently published an excellent overview that describes various approaches used for the preparation of porous polymer monoliths.[10] In this section, I focus only on thermal-initiated and photo-initiated polymerizations, which are the most widely used methods for monolithic column preparation for chromatography.

1.3.1 Thermal-Initiated Polymerization

The early development of polymeric monoliths can be traced to techniques applied in the preparation of porous beads for packed columns using suspension polymerization. As

a result, thermal initiation was the first method used.[8,41,42] For example, the first successful rigid monolith applied as an HPLC separation medium was prepared in a stainless steel tube via thermal initiation.[8] In this approach, porous poly(glycidyl methacrylate-co-ethylene dimethacrylate) (GMA-EDMA)) was synthesized using GMA as functional monomer, EDMA as crosslinker monomer, cyclohexanol and dodecanol as porogens, and 1% 2,2'-azobisisobutyronitrile (AIBN) as thermal initiator. The epoxide group in the monolith was subsequently reacted with diethylamine to produce an anion-exchange monolith for protein analysis.

The effect of temperature in thermal-initiated monolith polymerization has been well studied and explained by Svec et al.[43-45] As a rule, higher polymerization temperature results in smaller pores. This is because the decomposition rate of the initiator, the number of growing radicals, and the overall polymerization rate are faster at higher temperature. A large number of free radicals form a large number of growing nuclei and microglobules of small size. When these small microglobules interconnect to form a monolith, smaller pores are generated. Temperature also affects the solvent quality. Higher temperature enhances dissolution of the polymer, since the mixing of a polymer with a solvent is an endothermic process. This results in later phase separation which leads to both nuclei and voids in larger sizes. In contrast to the effect of temperature on the nucleation rate, changes in solvent quality caused by an increase in temperature are not substantial in thermal-initiated polymerization.[45] Viklund et al. prepared GMA-EDMA and poly(styrene-co-divinylbenzene) (PS-DVB) monoliths via thermal-initiated polymerization.[45] Their work demonstrated that the pore size distributions of both monoliths shifted to smaller values with increased polymerization temperature which, consequently, led to an increase in

specific surface area. In thermal-initiated polymerization, temperature is a convenient variable that allows adjustment of the pore size distribution of a monolith without any change in the composition of the polymerization mixture. At the same time, the temperature of polymerization must be controlled carefully to obtain monoliths with reproducible and uniform porous structures.

The polymerization time also changes the porous properties of the monolith by influencing monomer conversion. In work conducted by Svec et al.,[44] it was observed that very large pores were characteristic of monoliths in early stages of polymerization, and the pore size distribution narrowed as polymerization progressed because the largest pores disappeared. In contrast, Trojer et al. found that decreasing the time of polymerization introduced a considerable fraction of mesopores in poly(p-methylstyrene-co-1,2-(p-vinylphenyl)ethane) (MS-BVPE) monoliths.[46] BET measurements revealed that the specific surface area increased from 26.8 to 77.2 m^2/g when the polymerization time was reduced from 24 h to 45 min. Separation of small molecules was tremendously enhanced using monoliths resulting from 45 min polymerization compared to those polymerized for 24 h. Although the reason for decrease in surface area with an increase in polymerization time was not given by the authors, it was most likely due to a less crosslinked monolithic network, since crosslinker conversion was observed to be higher than monomer conversion for short polymerization times, while they approached the same value with an increase in polymerization time. To ensure maximum monomer conversion and monolith rigidity, sufficient time is usually allowed for thermal-initiated polymerization and, thus, polymerization time is not widely used as an effective method to adjust the porous properties of a monolith.

Initiator concentration affects polymerization in a similar way as temperature. Higher concentration produces a larger number of free radicals and results in smaller microglobules and pores. For example, when AIBN concentrations was increased from 0.5% to 2%, the microglobule size decreased from 4.0 to 0.5 μm and permeability was one order smaller.[47]

The selection of polymerization temperature is also determined by the initiator decomposition temperature. AIBN is widely used for thermal initiation of polymer monoliths. Upon heating at ~ 60 ºC, AIBN decomposes to form free radicals, which can initiate the polymerization of most vinyl-containing monomers. Any monomer or solvent with boiling point above 60 ºC can potentially be used as a porogen to prepare monoliths. A temperature of ~ 60 ºC is also sufficient to decompose dibenzoyl peroxide. In contrast, 2,2,6,6-tetramethylpiperidyl-1-oxy requires a higher temperature of 130 ºC to decompose. The choice of initiator may also affect the features of the porous structures obtained. For example, replacement of AIBN by 2,2'-azobis- (2,4-dimethyl)valeronitrile in the preparation of poly(glycerol dimethacrylate) (GDMA) monoliths, while keeping the other reaction parameters constant, led to a decrease in population of mesopores and to formation of more macropores that, in turn, resulted in a decrease in the total surface area from 143 to 93 m^2/g.[48] Polymerization initiated by dibenzoyl peroxide produced monoliths with larger pores than AIBN, due to the slower decomposition rate of the initiator.[43]

1.3.2 Photo-Initiated Polymerization

Photo-initiated polymerization is the other widely used method for the preparation of polymer-based monoliths. Compared to thermal-initiated polymerization, a distinct advantage is that photopolymerization significantly shortens the polymerization time. When

UV-initiation was first used for monolith polymerization in 1997,[49] it took 60 min to complete reaction using eight 15 W fluorescent black light tubes; however, polymerizations can now be accomplished within several minutes when using UV lamps of 1000 W or higher. The fast reaction rate using photopolymerization is very useful in the optimization of the monolith, especially when hundreds of screening experiments must be conducted before finalizing the monolith composition and synthesis conditions. Another attractive feature of photoinitiation is the ability to selectively pattern monoliths within a specified space. Using a suitable mask, polymerization occurs only in the region that is exposed to UV irradiation.[50] This technique is widely used for microfluidic device applications.[51-54] Since photopolymerization is performed at room temperature, the range of solvents that can be used for preparation of monoliths is much broader than solvents used in thermally initiated processes. Volatile organic solvents such as methanol, tetrahydrofuran (THF), ethyl ether and hexane can also be used as porogens.[52,55-57] Broader selection of porogenic solvents enables more control over the morphology and pore size adjustment of a monolith. It was also claimed that photoinitiation can improve monolith uniformity compared to heat initiation. It is well known that free radical polymerization is an exothermic process. Using thermal polymerization, the heat generated cannot dissipate well, resulting in a temperature gradient along the radial direction of the tube (higher in the center than periphery). Because the morphology of the monolith, including surface area and through-pore diameter, is very sensitive to the temperature,[43] use of a temperature gradient during thermal initiation leads to nonuniformity, which in turn affects column efficiency.

Monolith synthesis using photopolymerization is simple to conduct. A monomer mixture similar to that used for thermal-initiated processes, containing initiator,

monomer(s) and porogen(s), is introduced into the mold and irradiated with UV light to initiate polymerization; however, a mold that is UV transparent and has a sufficiently small size in at least one dimension is required for effective photoinitiation. For capillary columns, this is readily achieved by using Teflon coated fused silica capillaries with small I.D. Quartz and glass chips also fulfill this requirement. UV transparent monomers and porogens are usually required for photopolymerization (i.e., monomers and porogens must not absorb UV radiation to any significant degree).[10]

The main factors that affect the photopolymerization reaction rate are the intensity and wavelength of the light source, as well as the nature and concentration of the initiator. The former is usually fixed once a UV lamp is chosen. Photoinitiators that are widely used for monolith preparation include AIBN,[52,58-61] 2-methoxy-2-phenylacetophenone (benzoin methyl ether)[49,62-64] and 2,2-dimethoxy-2-phenylacetophenone (DMPA).[20,53-57] AIBN can also be used for thermally initiated polymerization and comparative studies of both approaches have been reported.[65,66] They found that the photoinitiated monoliths exhibited approximately twice as high back pressure as those obtained by thermal initiation, indicating a difference in the porous structure. In contrast, only small differences in chromatographic performance were found for both types of monolithic capillary columns, which is reasonable since the surface chemistry is similar. The effect of initiator concentration on monolith morphology was reported. An increase in concentration from 0.2 to 1 wt% led to an increase in polymer density and, therefore, formation of a homogeneous porous structure,[67] while concentrations higher than about 3-4% led to cracks in the continuous polymer structure.[49] Although initiator type and concentration can be altered, they are not commonly used to adjust the pore size of the monolith.

UV-initiated polymerization is typically performed at room temperature; thus, temperature has not generally been used as an effective way to control pore as in thermal-initiated polymerization.[43-45] The effect of temperature on UV-initiated polymerization of monoliths has been described in recent papers.[57,68,69] In my work,[57] polymerization were conducted at room temperature and at approximately 0 °C to investigate the effect of low temperature on UV-initiated polymerization. The resulting monoliths exhibited different properties with regard to back pressure and morphology compared to those prepared at room temperature, demonstrating that temperature affects the nucleation rate and solvent properties, which subsequently affects the monolith properties, similar to thermal-initiated polymerization. These results suggest that in order to improve reproducibility, reaction temperature should also be considered in UV-initiated monolith preparation. This is especially important when polymerization within a specific area is required, such as in microchip fabrication, and lower temperature is utilized to avoid polymerization in other areas due to heating. The monolith morphology may differ if the monomer mixture composition is taken directly from synthesis methods conducted at room temperature.

1.4 Control of Chemistry

The ultimate goal of developing a separation medium is its applicability to separations. Thus, the surface chemistry should meet the desired application. For example, hydrophobic moieties are required for reversed phase and hydrophobic interaction chromatography, polar functionalities for normal phase and hydrophilic interaction chromatography, and ionizable groups for ion-exchange chromatography (IEC). Affinity chromatography requires unique reactive groups, while chiral functionalities are prerequisite for enantioselective separations. The desired monolithic stationary phase

selectivity can be incorporated through direct polymerization of functionalized monomers, or through surface modification of pre-formed monolithic matrices, including modification of reactive monoliths and grafting.

1.4.1 Monomers

Since there is initially only one phase in the polymerization solution, the range of monomers that can be used is much broader than for classical suspension polymerization, including water-soluble hydrophilic monomers. This greatly extends the variety of surface chemistries that can be obtained directly. One disadvantage of direct polymerization is that optimized polymerization conditions for one system cannot be transferred directly to another, and further experimentation is needed to re-optimize the polymerization. Despite this inconvenience, direct copolymerization of functional monomers provides the simplest approach to obtain the desirable surface chemistry. In single-step preparation of monolith, the chemistry of a monolith is largely controlled by choice of the monomers used in its preparation. Acrylamide, acrylate, methacrylate, styrene, norbornene, and their derivatives are mostly often used for the synthesis of monoliths. Figure 1.1 shows a few representative monomers that have been used for the preparation of rigid monoliths for LC applications. These monomers differ in chemical and physical properties, and can be divided into hydrophilic (acrylamide and methacrylamide, **1;** 2-hydroxyethyl acrylate and methacrylate, **2**), moderately hydrophilic [poly(ethylene glycol) methyl ether acrylate, **3**], hydrophobic (butyl methacrylate, **4**; styrene, **5**; N-isopropylacrylamide, **6**; norbornene, **7**), ionizable (2-acrylamido-2-methyl-1-propanesulfonic acid, **8**; phosphoric acid 2-hydroxyethyl methacrylate, **9;** acylic acid, **10**; (methacryloyloxy)ethyltrimethylammonium chloride, **11**; 2-(diethylamino)ethyl methacrylate, **12**), reactive (glycidyl methacrylate, **13**;

chloromethylstyrene, **14**; 2-vinyl-4,4-dimethylazlactone, **15**), zwitterionic [2-(N-3-sulfopropyl-N,N-dimethyl ammonium)ethyl methacrylate, **16**; 2-methacryloyloxyethyl phosphorylcholine, **17**], and protected (4-acetoxystyrene, **18**). In contrast to the various functional monomers, the number of useful crosslinking monomers is limited. Methylenebisacrylamide, **19**, is the most frequently used crosslinker with acrylamide monomers, while ethylene dimethacrylate, **20**, is used with acrylate and methacrylate monomers and divinylbenzene, **21**, is used with styrenic monomers. Crosslinking monomers 22 to 29 are less often used in monolith synthesis. A very recent report described a new technique to introduce functionality, i.e., rod-shaped hydroxyapatite nanoparticles were incorporated into the poly(2-hydroxyethyl methacrylate-co-ethylene dimethacrylate) (HEMA-EDMA) monolith by simply admixing them in the polymerization mixture followed by in situ polymerization.[70] This monolithic capillary column with embedded hydroxyapatite nanoparticles was used for protein separation and selective enrichment of phosphopeptides. Although the nanoparticles did not participate in the polymerization, they functioned similarly as functional monomer in the one-step copolymerization.

In conventional monolith design, both functional and crosslinking monomers are included, with the monomer providing the desired functionality and crosslinker serving to ensure rigidity. The functionality density can be controlled by altering the concentration of the functional monomer. For example, in the design of poly(butyl methacrylate-co-glycerol dimethacrylate) (BMA-GDMA) monoliths for HIC,[71] when the monomer/crosslinker ratio was 30/70, the resulting monolith did not function properly in the HIC mode, but was able to separate protein standards in the RP mode because the functionality density (i.e., butyl groups) was too high for HIC. When the author reduced the content of BMA to 10%,

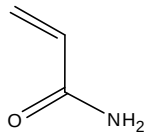

1
acrylamide

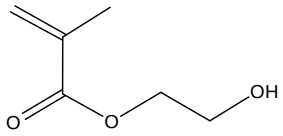

2
2-hydroxyethyl methacrylate

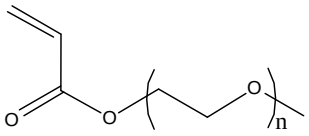

3
Poly(ethylene glycol) methyl ether acrylate

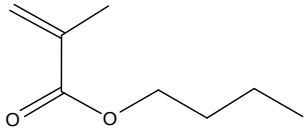

4
butyl methacrylate

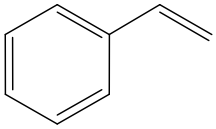

5
styrene

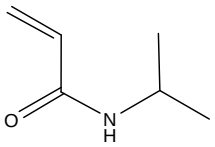

6
N-isopropylacrylamide

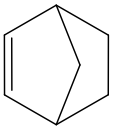

7
norbornene

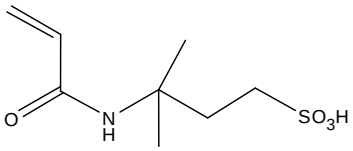

8
2-acrylamido-2-methyl-1-propanesulfonic acid

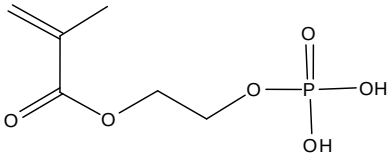

9
phosphoric acid 2-hydroxyethyl methacrylate

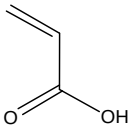

10
acylic acid

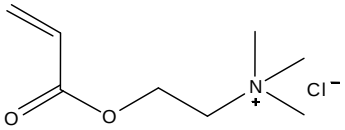

11
2-(acryloyloxy)ethyl trimethylammonium chloride

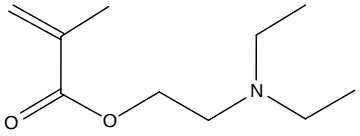

12
2-(diethylamino)ethyl methacrylate

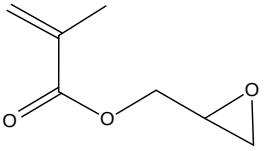

13
glycidyl methacrylate

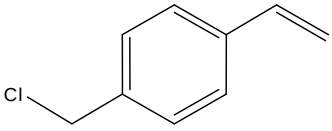

14
chloromethylstyrene

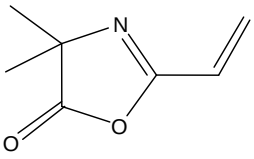

15
2-vinyl-4,4-dimethylazlactone

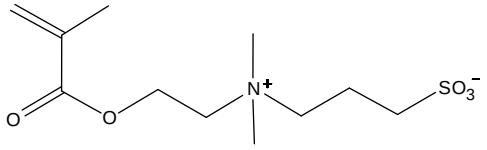

16
2-(N-3-Sulfopropyl-N,N-dimethyl ammonium)ethyl methacrylate

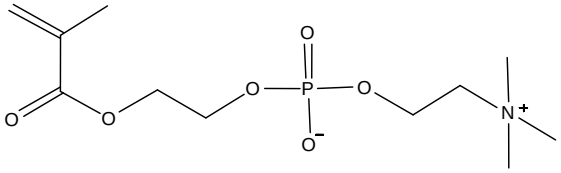

17
2-methacryloyloxyethyl phosphorylcholine

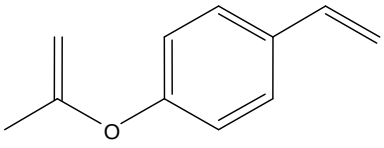

18
4-acetoxystyrene

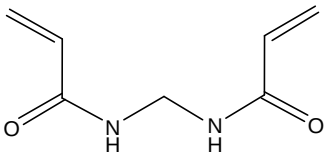

19
methylenebisacrylamide

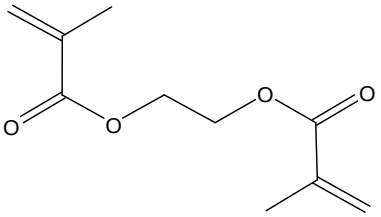

20
ethylene glycol dimethacrylate

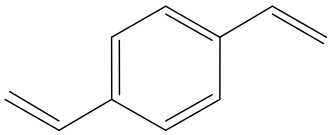

21
divinylbenzene

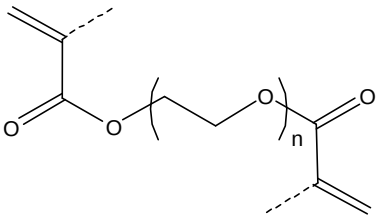

22
poly(ethylene glycol) diacrylate and dimethacrylate

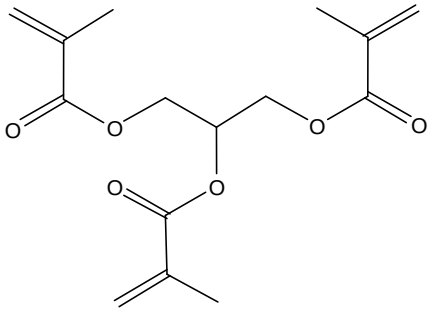

23
trimethylolpropane trimethacrylate

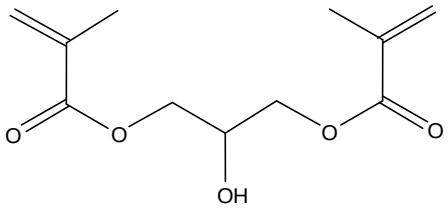

24
1,3-glycerol dimethacrylate

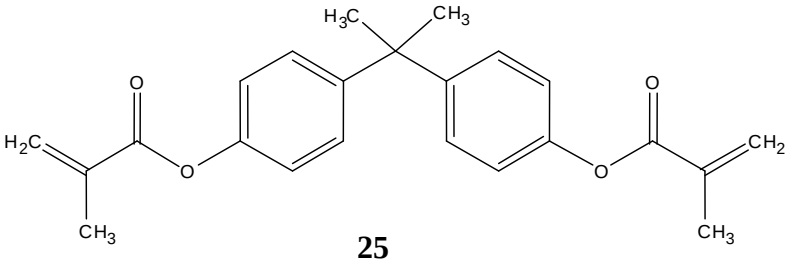

25
bisphenol A dimethacrylate

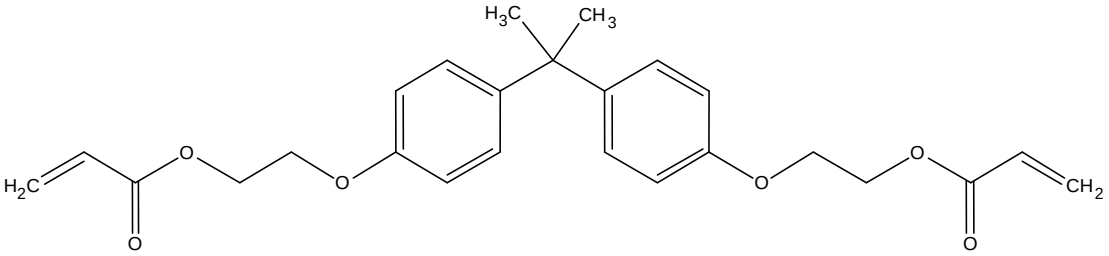

26
bisphenol A ethoxylate diacrylate, EO/phenol = 2 or 4

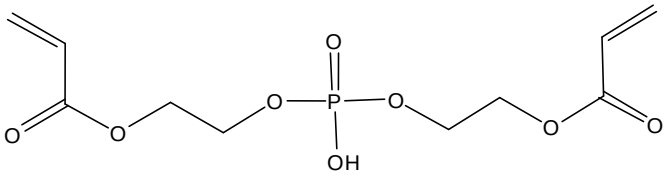

27
bis[2-(methacryloyloxy)ethyl] phosphate

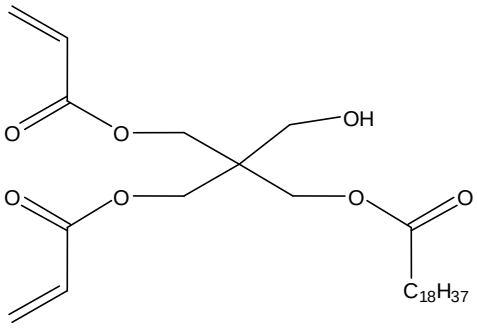

28
pentaerythritol diacrylate monostearate

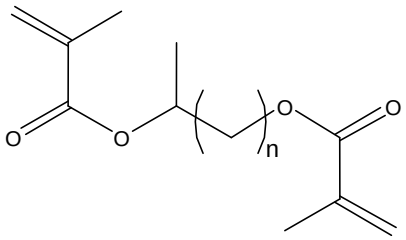

29
alkyl dimethacryalte

Figure 1.1. Chemical structures of common monomers used for the copolymerization of polymer monoliths.

separation according to the HIC mechanism was possible. In my design of poly[hydroxyethyl acrylate-*co*-poly(ethylene glycol) diacrylate] (HEA-PEGDA) monoliths for HIC, it was observed that an increase in the PEGDA concentration yielded monoliths with enhanced hydrophobicity.[56] This is because PEGDA is more hydrophobic than HEA, which makes PEGDA not only a crosslinker but also a functional monomer. In general, the ratio between monomer and crosslinker should be varied within a certain range, because too low concentration of crosslinker will result in monoliths lacking the necessary rigidity, while too high concentration will reduce the functionality density below that necessary for adequate interaction with the analytes.

Similar to a functional monomer, the crosslinker also plays an important role in monolith preparation. Variation in crosslinker concentration has a significant effect on the rigidity and porosity of the resulting monolith. The crosslinker is incorporated in the porous framework and remains as an integral part of the final monolithic backbone after polymerization. Thus, the surface properties of monoliths depend on the chemistry of both the monomer and the crosslinker. Research concerning the effect of the nature of the crosslinker on the properties of the resulting monoliths has arisen in recent years. For example, by replacing EDMA with PEGDA (M_n = 258) to copolymerize with polyethylene glycol methyl ether acrylate (PEGMEA), the monolith became moderately hydrophilic.[72] Compared to EDMA-based monoliths, PEGDA-based monoliths exhibited negligible nonspecific adsorption of proteins as demonstrated by clean fluorescent images obtained after flushing monoliths first loaded with fluorecein isothiocyanate (FITC)-labeled BSA. Using PEGDA-258 as crosslinking monomer, monoliths were synthesized for size exclusion,[72,73] cation-exchange,[20,74,75] anion-exchange[55] and hydrophobic interaction

chromatography[56,57] of proteins and peptides. These monoliths all demonstrated negligible or reduced nonspecific adsorption of biomolecules due to the presence of poly(ethylene glycol) (PEG) chains. Dimethacrylates with one, two or three PEG bridging moieties between methacrylate units have been copolymerized with BMA for reversed phase liquid chromatography (RPLC) of proteins.[76] The different crosslinkers do not significantly change the retention behavior of the column since the hydrophobicity of the stationary phase originates mainly from the butyl groups in the monomer and the hydrocarbon polymer backbone. In contrast, we synthesized a series of monoliths from single monomers of PEGDA and PEGDMA with different PEG chain lengths containing three or more ethylene glycol moieties.[57] The hydrophobicities of the monoliths decreased with an increase in PEG chain length, as demonstrated by HIC of proteins. In a recent study, stearyl methacrylate was copolymerized with alkyl dimethacrylates with different alkyl chain length and/or isomeric alkyl chains to demonstrate the role of the crosslinker on monolith properties.[19] The hydrophobicity of the monolith can be changed by varying the alkyl chain length and the branching groups in the crosslinker, as demonstrated by chromatograms of typical alkylbenzenes and protein standards.

A nontraditional approach to synthesize monoliths involves the use of only a cosslinking monomer, i.e., single-monomer system. Monolithic materials synthesized solely from crosslinking monomers have been reported for diacrylate and dimethacrylate,[57,77,78] divinylbenzene,[33,34] N,N-methylenebis(acrylamide),[79] glycerol dimethacrylate (GDMA),[48] 1,2-bis(p-vinylphenyl)ethane (BVPE),[80,81] and tetrakis(4-vinylbenzyl)silane (TVBS).[47,82] Compared to conventional two- or three-monomer systems, commercially available chemistries for single-monomer systems are not as rich, and the functionality density

cannot be adjusted by varying the ratio between monomer and crosslinker. However, optimization of the monolith polymerization is much easier, and column preparation is more reproducible. This process also has a number of other advantages. The highly crosslinked network results in higher rigidity, better mechanical stability and greater surface area as demonstrated in our report.[57] It allows preparation of monoliths that would be difficult to obtain using single step copolymerization of two monomers. For example, it is difficult to create a homogeneous polymerization mixture from monomers differing largely in polarity such as hydrophobic stearyl methacrylate and hydrophilic hydroxyethyl methacrylate. In contrast, monoliths from pentaerythritol diacrylate monostearate (PDAM) were successfully synthesized in my work for reversed phase chromatography of small molecules. My work also revealed that functionality density can be adjusted through control of the spacer length between the two acrylate ends.

1.4.2 Modification of Reactive Groups

Chemical modification of reactive groups offers another approach that allows the introduction of desirable functionality. Typically, a monolith with reactive groups is first prepared and, subsequently, pores of the monolith are filled with a reagent containing the desired chemistry and allowed to react. After reaction is complete, the monolith is flushed with a solvent to remove all remaining components before use. These procedures enable independent optimization of the synthesis of the monolith and its surface chemistry. Thus, it is possible to prepare a variety of functionalized monoliths from a single "universal" monolith, and tedious optimization of each of the new monomers is avoided. To conduct post-modification, including modification of reactive groups and grafting, the pre-formed monolith must be stable during modification (i.e., no excessive shrinking or swelling, and

no detachment from the column wall), even if harsh conditions such as high temperature and non-polar solvents are used. Furthermore, because the reaction must be carried out within the column, only reactions that proceed under warm reaction conditions to avoid forming insoluble product are suitable, and the modification process should preserve the hydrodynamic properties of the monolithic column.

Reactive monomers must be included in the polymerization mixture to provide reactive sites for further derivatization. Glycidyl methacrylate, chloromethylstyrene and 2-vinyl-4,4-dimethylazlactone (VAL) are three often used reactive monomers to copolymerize with corresponding crosslinkers to form reactive monoliths. For example, a poly(vinyl dimethylazlactone-co-acrylamide-co-ethylene dimethacrylate) monolithic support was used for immobilization of trypsin by a single reaction between azlatone and the amine group in trypsin.[83] High binding capacity and fast reactions both for immobilization (within 1 h) and protein digestion were obtained for this monolithic support. In continuing efforts, this group extended the azlactone chemistry to both capillary and microfluidic formats using UV-initiation methods.[84,85] The reaction of poly(chloromethylstyrene-co-divinylbenzene) with ethylenediamine and then with γ-gluconolactone completely switched the surface polarity from hydrophobic to hydrophilic.[86] GMA is a widely used functional methacrylate monomer. Since rigid GMA-EDMA monoliths were introduced in 1992 by Svec et al.,[8] various chemical reactions have been tried to convert the epoxy groups to specific functionalities for different separation modes. For example, based on amination, weak or strong anion exchangers were produced by reaction of epoxy groups with diethylamine and trimethylamine.[87,88] Through ring opening reaction of epoxides with sodium sulfite, GMA-EDMA monoliths were modified with

sulfonic acid functionalities to form cation exchangers for ion chromatography of inorganic cations.[89] Two other sulfonation methods were tried by Hutchinson et al. to modify GMA-EDMA monoliths.[90] The first approach was based on direct reaction of epoxy groups with 4-hydroxybenzene sulfonic acid in the presence of triethylamine at 60 ^{o}C. Alternatively, a multi-step reaction that included (i) ring-opening of the epoxy groups through reaction with thiobenzoic acid, (ii) formation of reactive thiol through reaction with methanol, and (iii) generation of sulfonic acid through oxidation of thiol by tert-butyl hydroperoxide. Other examples of surface modification of GMA-EDMA monoliths include introduction of hydrophobic functionalities through reaction with butanol, octanol or phenol under alkaline conditions,[41,42] and, reaction with ethylenediamine followed with chloroacetic acid or directly with iminodiacetic acid for a weak cation-exchange column.[91,92] Additionally, monoliths containing epoxy groups are also widely used for surface modification with specific ligands required for bioaffinity chromatography and enzyme immobilization.[93]

Recently, a new porous polymer monolithic capillary column was developed in Svec's group by modifying GMA-EDMA monoliths with gold nanoparticles that enabled the selective capture of cysteine-containing peptides. Thiol groups were introduced on the monolith surface through reaction of epoxide moieties with cysteamine for attachment of gold nanoparticles.[94] In their continuing work, this gold nanoparticle-modified GMA-EDMA monolithic column allowed easy switching between separation modes by a ligand exchange between octadecylthiol and sodium-2-mercaptoethanesulfonate for reversed phase and ion exchange chromatography of proteins.[95] Attachment of nanoparticles to the monolith was originally inspired by a modification technique for spherical beads, in which anionic latex nanoparticles were attached to sulfonated PS-DVB beads for ion

chromatography. In 2004, Hilder et al. synthesized a porous poly(butyl methacrylate-co-ethylene dimethacrylate-*co*-2-acrylamido-2-methyl-1-propanesulfonic acid) monolith, and then this monolith were modified with quaternary amine-functionalized latex particles via simple electrostatic binding with sulfonic acid groups. This monolith then enabled fast separation of carbohydrates.[96] Simultaneously, Haddad's group used a similar process that afforded a latex-coated polymer monolith used for the separation of anions in capillary electrochromatography (CEC) and micro HPLC.[97,98]

1.4.3 Grafting

The third approach, grafting, is another powerful method to introduce new functionalities in monoliths. In particular, grafting by deep UV has recently gained popularity. Grafting also enables control of porous properties of the monolith independently from management of its surface chemistry. Compared to the simple modification process shown in Section 1.4.2, in which only a single functionality is obtained by reacting each reactive site of the surface, the attachment of chains of a functional polymer to the reactive site at the surface of the pores would provide multiple functionalities, and better surface coverage would be expected. Furthermore, the grafted chains could also serve as new loci from which new chains could grow, ultimately leading to a highly branched structure. This would further increase the binding capacity of the resulting monolith. To conduct grafting, the requirements mentioned in Section 1.4.2 must be done. Furthermore, if photografting is performed, UV transparent molds and monomer solutions are required, and one dimension of the monolith must be shallow enough for effective initiation due to UV adsorption of the polymer matrix itself.

Grafting can be realized in several ways. First, monoliths prepared via ring-opening metathesis polymerization allow flexible grafting of various chromatographic ligands.[99,100] A variety of functionalities such as carboxylic acid, tertiary amine and cyclodextrin, have been grafted into a polynorbornene monolith. Second, grafting can be achieved through activation of stable free radicals on the surface of the monolith by heating to initiate the graft polymerization. Using this method, chloromethylstyrene and vinylpyridine have been successfully grafted to polystyrene monoliths.[32] Third, grafting can be performed through immobilization of initiators or vinyl-containing chemicals. The bulk monolith should be reactive to enable immobilization. For example, Tripp et al. immobilized a free radical azo initiator through reaction of 4,4'-azobis(4-cyanovaleric acid) with the chloromethyl functionality in a polychloromethylstyrene monolith.[101,102] This free radical initiator was then used to graft VAL onto the monolith to separate amines. For the poly(GMA) monolith, allylamine can be reacted with the epoxide group to form a pendant vinyl group. If a new monomer solution with initiator is added, grafting from the vinyl group in the poly(GMA) monolith will occur. Peters et al. used this approach to graft N-isopropylacrylamide, and obtained a unique monolith whose hydrophobicity was thermally responsive.[103] Fourth, grafting can be achieved via atom transfer radical polymerization (ATRP). Monolithic columns based on poly(chloromethylstyrene-co-divinylbenzene) grafted with poly(N-isopropylacrylamide) via ATRP were recently used for the separation of proteins in the hydrophobic interaction mode.[104] Finally, grafting is realized via UV irradiation. This is a universal approach and very popular today. If a polymer is irradiated with deep UV at 200-300 nm, hydrogen abstraction occurs, leaving an active radical on the polymer substrate.[105,106] This energy rich radical then initiates propagation reactions leading to

grafting from the surface. Using this approach, 2-acrylamido-2-methyl-1-propanesulfonic acid (AMPS), VAL and BMA were grafted onto a poly(BMA) monolith.[50,107,108] A similar method was used to prepare reactive supports with enhanced biocompatibility from GMA-EDMA monoliths. After hydrolysis of the epoxide group to a diol, poly(ethylene glycol) methacrylate was grafted within the pores and, in the next step, the pore surface was activated by photografting VAL. This monolith was then used for fabrication of active immobilized enzyme microreactors,[109,110] and for preparation of ion-exchange columns.[111]

1.5 Control of Morphology

For monolithic columns used in capillary HPLC, both large surface area and good permeability are desirable. A large surface area provides more active sites for effective interactions and high efficiency, and good permeability allows faster processing and moderate back-pressure. The porosity is the most important morphology characteristic. It reflects the size and organization of both microglobules and clusters and depends on the compositions of the polymerization mixture and the reaction conditions. There are three types of pores present in polymeric monoliths: nanopores (<2 nm), mesopores (between 2 and 50 nm) and macropores (i.e., throughpores, >50 nm). The surface area is mainly determined by the nanopores and mesopores, while the permeability is mainly determined by the average diameter of the macropores (throughpores). After the monomers are selected, attention is then focused on development of a stable monolithic column with high surface area and good permeability.

The pore size distribution of a polymer monolith can be adjusted by several variables. Those related to the components of the polymerization mixture include initiator type and concentration, total monomer to total porogen ratio, monomer to crosslinker ratio,

porogen nature and ratio of porogens if more than one porogen is used. Others that may affect the porosity of the monolith are polymerization temperature and time in thermal-initiated polymerization, and light wavelength and density as well as temperature in photo-initiated polymerization, which have been discussed in the previous section. I have also included brief discussion concerning the effect of initiator nature and concentration on monolith morphology in the previous section. As a general rule, a decrease in initiator can increase the permeability of the monolith; however, a longer time is required to complete the polymerization, and sometimes the resulting monolith lacks rigidity. A further increase in initiator concentration often leads to rapid decrease in pore size because of the increased number of free radicals. For monolith synthesis, the concentration of initiator is usually set at 1 ~ 1.5% of the total monomer. Compared to initiator nature and concentration, the other three components of the precursor solution are more often used to alter the monolith morphology. These are discussed in more detail in the following sections.

1.5.1 Porogens

Among all variables used to adjust monolith porosity, the choice of porogenic solvents and their ratio is the most powerful tool. Unlike other variables such as monomer ratio or type of initiator, altering the porogens does not affect the chemical composition of the monolith. The mechanism of pore formation using porogens is based on differential phase separation during polymerization induced by the porogenic solvents with different thermodynamic properties. Polymerization takes place via initiating the homogeneous precursor solution. After the polymer chains grow to a certain molecular weight and/or crosslink to a certain degree, they become insoluble in the polymerization mixture, the polymer chains precipitate and phase separation occurs. In general, poor solvents will

generate a monolith with larger pores due to earlier onset of phase separation. Good solvents, on the other hand, yield monoliths with small pores, resulting in higher back pressure.

Although modern monolith techniques have been studied for two decades, to date, there is still no generally accepted theory proposed for porogen selection. Selection of appropriate porogens still must primarily depend on experiments and experience. In spite of this, several basic requirements for the design and selection of porogens are essential. First, the porogen or porogen combination must be miscible with all reagent components. A homogeneous monomer solution is a prerequisite for developing a good monolith. Second, it is desirable that both poor and good solvents are included in the polymerization mixture, so that the permeability can be adjusted by varying the ratio between the two types of porogens. At the same time, it is better that the solvent strengths of the two types of porogens are not excessively different, or the column back pressure will be too sensitive to the porogen ratio and the reproducibility of column preparation will suffer. Finally, the porogen must be compatible with the initiation technique. For example, in thermal initiation, the boiling point of the solvent should be higher than the polymerization temperature. In photoinitiation, it is generally recommended that only UV transparent solvents be utilized.

The properties of the monomers decide the selection of porogens and their ratios. For example, GMA-EDMA monoliths with a mean pore size of 1 μm are usually obtained by thermal polymerization with the use of a porogen mixture containing 20% dodecanol and 80% cyclohexanol. In contrast, a much higher amount of less polar dodecanol is required for the preparation of HEMA monoliths with similar pore size.[112] Merhar et al.

investigated the effect of monomer nature on pore structure of synthesized monoliths.[113] For this purpose, a GMA/EDMA mixture was used to synthesize the basic monolith, and then 5% or 15% GMA was replaced with eight other monomers, including hydroxypropyl methacrylate, 2-diethylaminoethyl methacrylate, 2-dimethylaminoethyl methacrylate, as well as with different alkylmethacrylates from C-2 to C-18. It was found that the pore radius decreased significantly with increasing hydrophilicity as well as with decreasing hydrophilicity (increasing hydrophobicity) of the monomer with regard to the GMA monolith. I systematically investigated the copolymerization of HEMA, HEA, PEGDA, and EDMA, and found that porogens suitable for formation of rigid HEA/PEGDA monoliths were not effective for HEMA/PEGDA, and vice versa, despite the slight differences between the two sets of monomers.[56] Thus, how to select the appropriate porogenic solvents in an efficient way once the monomers are selected to design a monolithic stationary phase is still largely empirical, and more efforts must be made in this area.

Dipole moment or polarity is a solvent property often cited when selecting the porogenic solvents. In work conducted by Courtois et al.,[64] it was predicted that porogens that possess high dipole moment values were likely to produce monoliths of small median pore diameter for the monomer system containing GMA, triethylene glycol dimethacrylate and trimethylol-propane trimethacrylate. Another solvent property proposed as a guideline for porogen selection is the solubility parameter (δ) values of monomers and solvents.[19] Solubility is an often-used guideline in selecting the appropriate solvents for preparing macroporous copolymer beads.[114] If the solvent has a similar δ value as the monomer, the solvent can be considered to be a good solvent, while large difference between the two δ values indicates a poor solvent for the monomer. In Chapter 4, different solvents for

bisphenol A dimethacrylate (BADMA) monolith synthesis, including toluene, THF, dimethylformamide (DMF), dimethyl sulfoxide (DMSO), decanol, dodecanol, ethyl ether, acetonitrile, isopropyl alcohol (IPA), methanol and cyclohexanol were investigated. The solvent properties of polarity and solubility were used as guidelines for porogen selection. My investigation indicated that neither of them could be the only property contributing to the porogen effect. To rationally select the porogenic solvents, a more complicated strategy must be applied and additional properties of the solvents must be considered. However, if the porogenic solvents are similar in other properties, polarity provides a good guideline to predict porogen behavior.

Although a wide variety of solvents or their mixtures could be potential porogens for monolith preparation, relatively few porogens have been used. This is not surprising, since researchers still prefer to look for appropriate porogenic solvents based on their experience and the published work of others. Some porogen mixtures described during the early years of monolith development still remain popular. For example, mixtures of toluene or THF with long-chain alcohols have been routinely used for the preparation of monoliths from styrene and divinylbenzene[45,115-120] Similarly, a mixture of cyclohexanol and dodecanol, initially used for the synthesis of monoliths from GMA and EDMA,[8] remains popular for this monolith,[121-123] as well as for monoliths from other monomers such as BMA-EDMA,[124] lauryl methacrylate-EDMA,[125] HEMA-EDMA,[25,126] and glyceryl monomethacrylate with EDMA or TRIM.[127] Other solvents were evaluated for preparation of GMA-EDMA monoliths by Zhu et al.[128] Combination of 1,4-butanediol and dimethylsulfoxide was found to produce monoliths with high permeability. Santora et al. reported poly(divinylbenzene), PS-DVB, poly(EDMA) and poly(methyl methacrylate-*co*-

ethylene dimethacrylate) monolithic materials using single solvent porogens including THF, acetonitrile, toluene, chlorobenzene, hexane, methanol, DMF, and methyl-t-butyl ether.[129] Huang et al. used 1-propanol and formamide as porogens to synthesize PS-DVB monoliths for peptide analysis in capillary liquid chromatography-electrospray ionization mass spectrometry.[130] Another widely-adopted porogen system containing 1,4-butanediol and 1-propanol was originally recommended by Peters et al. for the preparation of monoliths from EDMA and BMA for LC and CEC.[131-133] This mixture was later used for monolith synthesis from BMA-EDMA,[134,135] GMA-EDMA,[89] ethylene dimethacrylate-lauryl methacrylate-[2-(methacryloyloxy)ethyl] trimethyl ammonium chloride,[136] as well as BMA with different ethylene glycol dimethacrylates.[76] Similar mixtures containing *tert*-butanol and 1,4-butanediol were used as porogens to copolymerize stearyl methacrylate with different alkyl dimethacrylates.[19] Noteworthy is that swiftness and convenience of column preparation using UV-initiated polymerization makes it feasible to test many porogenic solvents within a reasonable time period.

In addition to common organic solvents as porogens, solutions of a polymer in a solvent can also work as porogens. For example, polyethylene glycol (PEG) or polypropylene glycol (PPG) of different molecular weights have been used as co-porogen to prepare poly(acrylamide-*co*-methylenebisacrylamide) monoliths.[137] Novotny's group used a solution of PEG (Mn = 10000) in N-methylformamide or formamide to prepare a macroporous matrix for CEC from a polymerization mixture consisting of acrylamide, methylene-bisacrylamide, acrylic acid (or vinylsulfonic acid), and alkyl acrylates.[138] A systematic study described the use of PEG with a molar mass of 4,000–20,000 dissolved in 2-methoxy-ethanol for the preparation of glycidyl methacrylate-co-trimethylolpropane

trimethacrylate-co-triethylene glycol dimethacrylate) monoliths for hydrophobic interaction chromatography (HIC) of proteins.[64] It was found that longer PEG chains produced pores of larger size with a concomitant decrease in the surface area. PEG or PPG solutions were also reported as porogens in forming monolithic materials from PEG-containing crosslinking monomers.[77,78] Li et al. used poly(propylene glycol)-block-poly(ethylene glycol)-blockpoly(propylene glycol) triblock copolymer and diethyl ether as porogens to prepare monolithic poly(ethylene glycol methyl ether acrylate-co-polyethylene glycol diacrylate) capillary columns.[73] These columns were tested for size exclusion chromatography (SEC) of proteins and peptides. Triblock copolymers were recently used as an intermediate porogen in the formation of poly(PADM) monoliths for reversed phase chromatography of small molecules. Polystyrene is another polymer family that has been used as porogens in monolith synthesis. A combination of high molecular mass polystyrene and chlorobenzene was used for the preparation of poly(GDMA) monoliths, which were able to separate small molecules due to the presence of a concentration of mesopores.[48] Mixtures of polystyrene dissolved in toluene and poly(dimethylsiloxane) dissolved in hexane was tested by Sinitsyna et al. to prepare GMA-EDMA monolithic layers.[139]

Another atypical porogen is supercritical carbon dioxide. This porogen is attractive since it is nontoxic, nonflammable and inexpensive. Furthermore, the solvating power can be adjusted by applying different pressures, and the porogen simply evaporates with no need for washing after polymerization is completed. Using EDMA and trimethylolpropane trimethacrylate (TRIM) as model monomers, monoliths with a broad range of through-pore diameters (20 nm - 8 μm) have been prepared.[140,141] The authors found a direct dependence of properties such as pore size, pore volume, and surface area on CO_2 pressure. However,

special equipment was required for the application of high pressures in the range of 15 - 30 MPa for the synthesis, and no applications of the resultant chromatographic column technology have been reported.

1.5.2 Monomer Ratio

In contrast to the porogenic solvents which affect the porous structures of the monoliths but not their compositions, a change in monomer to crosslinker ratio affects both the porous properties and chemical compositions. Similar to the effect of poor solvent, the crosslinker contributes to early phase separation because of greater crosslinking in the early stages of the polymerization process. Since crosslinking reduces swelling, the nuclei remain relatively small in size. The pre-microglobules can still capture nuclei generated during the later stages of polymerization, but true coalescence does not occur. Thus, the final porous structure is composed of small microglobules and small voids. As a result, the pore size distribution usually shifts toward smaller pore sizes as the percentage of crosslinker is increased, which has been demonstrated by various monomer mixtures such as GMA/EDMA and styrene/divinylbenzene.[41,45] Noteworthy, if the monomer and crosslinker are vastly different in chemical and physical properties, variations in their ratio change the properties of the monomer mixture and, consequently, change the porogen effect that may also contribute to the resulting porous structure. For example, for the preparation of HEA-PEGDA monoliths, an increase was observed in column backpressure as the ratio of PEGDA/HEA was decreased from 1.37:1 to 1:1 while keeping the porogen composition constant.[56] This resulted because, with more concentrated HEA, methanol became a better solvent for the monomer mixture, and phase separation occurred in a later stage of polymerization, resulting in monoliths with smaller macropores.

Additionally, the proportion of crosslinker also affects the rigidity and homogeneity of the monolith. As a general rule, monoliths prepared from mixtures containing a high content of crosslinking monomer have greater rigidity and enhanced homogeneity because of the highly crosslinked network. Adding more crossliking monomer can also lead to monoliths with larger surface areas, since smaller microglobules are formed.[129] However, increasing the relative amount of crosslinking monomer may not be suitable for preparation of monoliths in which both high functionality concentration and large surface area are desirable. In contrast, the single-monomer synthesis approach is well suited for the preparation of monoliths for this purpose, since only functionalized crosslinking monomer is included in the synthesis. Although the porosity of the monoliths can no longer be adjusted through changing the ratio of monomer to crosslinker, a broader range of porogen to monomer ratio can be applied without affecting homogeneity or rigidity.

Applications of polymer monolithic stationary phases are particularly useful for the separation of high-molecular-weight compounds such as proteins and nucleic acids.[118,142] This is because the highly porous structure and absence of small mesopores make polymer monoliths suitable for fast mass transfer of large molecules. In contrast, efficient separation of small molecules on polymer monoliths is less frequently observed because of low surface area that limits interaction of analytes with the stationary phase. There have been several reports of methacrylate monoliths for separation of small molecules.[135,143,144] Several new approaches were recently explored to prepare polymer monoliths with larger surface areas, including termination of the polymerization reaction at an early stage,[46] copolymerization of different alkyl dimethacrylates with stearyl methacrylate,[19] and hypercrosslinking.[145] As previously discussed, synthesis from a single functional

crosslinking monomer is another approach to effectively increase the surface area and the concentration of desirable mesopores in the monolith, which has been demonstrated in several reports. Monoliths from BVPE and TVBS were successfully used for separation of both low and high molecular weight analytes due to the presence of relatively high fractions of mesopores and small macropores ranging from 5 to 400 nm.[47,80] Since both monomers could not be easily dissolved in the porogenic solvents (i.e., toluene and decanol), heating was used to facilitate dissolution, and only thermally initiated polymerization could be used. I synthesized several monoliths from single crosslinking monomers including bisphenol A dimethacrylate, bisphenol A ethoxylate diacrylate (BAEDA, EO/phenol = 2 or 4) and PDAM, which are described in Chapter 4. Due to the enhanced surface areas resulting from highly crosslinked structures, effective separations of alkyl benzenes and alkyl parabens with high resolution were demonstrated using these columns.

1.5.3 Monomer to Porogen Ratio

Variation in total monomer to total porogen ratio is a straightforward method to adjust the pressure drop of a monolith; the lower the percentage of monomers in the polymerization mixture, the higher the permeability of the resulting monolith. The effect of monomer concentration on the properties of the final polymer was recently demonstrated by Trojer et al. for poly(p-methylstyrene-co-1,2-(p-vinylphenyl)ethane) monoliths.[46] The macropore distribution shifted from 8.78 to 0.09 μm when the total monomer to porogen ratio was increased from 35% to 45% (v/v). This can be explained by a larger number of nuclei formed via irradiation of more concentrated monomers. When high density nuclei compete for the monomer, their sizes grow much less before they touch each other. Smaller voids are consequently formed between microglobules in the clusters of the final monolithic

polymer, resulting in smaller macropores. Thus, to guarantee a reasonable solvent flow within the operating pressure limits of HPLC instrumentation, the monomer to porogen ratio should not be high (< 50% in most cases). At the same time, although a decrease in the initial monomer concentration produces larger macropores, it decreases the density and rigidity of the monolith as well. Actually, it was observed that monolithic polymers were not formed at low monomer concentration (< 0.5 g/mL) for synthesis of TRIM, and the resulting product was a powder.[141] Decreased rigidity due to lower initial monomer concentration was also demonstrated in the synthesis of poly(triethylene glycol dimethacrylate) monoliths.[57] Monoliths prepared from a monomer concentration of 32.2 wt% could be stored dry. When the monomer concentration decreased to 20.2 wt%, the monolith exhibited lower backpressure and was not able to be regenerated after drying. Eeltink et al. reported on low-density methacrylate monoliths for CEC, which were prepared using a total monomer content of 20%.[143] Only column efficiency was measured to compare the low-density monoliths with high-density monoliths. No separations were shown in this report.

1.6 Dissertation Overview

Chapter 2 reports the preparation and evaluation of a polymer monolith for use in HIC of proteins. HEA was used as monomer and PEGDA (Mn = 258) as crosslinker. PEGDA was found to function as crosslinker and functional monomer at the same time. The optimized monolith was able to separate six protein standards with high resolution using a 20 min elution gradient, resulting in a peak capacity of 54. Porogen selection for the synthesis of monoliths from copolymerization between HEMA, HEA, EDMA and PEGDA was also investigated in this chapter. Chapter 3 describes the preparation of two series of

monolithic columns from PEGDA or PEGDMA with different PEG chain lengths. The porogen ratio was varied to adjust the column back pressure. Polymerization at room temperature and approximately 0 ^{o}C was investigated to determine the effect of temperature on monolith morphology in UV-initiated polymerization. All monoliths were evaluated for HIC of proteins. The optimized poly($PEGDA_{258}$) monolith was used to analyze commercial trypsin inhibitor samples. The work described in this chapter demonstrated several advantages with respect to monolith synthesis using a single-monomer system, including excellent column-to-column reproducibility, rigidity, and mechanical stability, as well as easy optimization. The highly crosslinked monolith network resulting from using a single crosslinking monomer also enhanced the surface area and concentration of mesopores. Thus, monoliths prepared solely from four crosslinking monomers, i.e., BADMA, BAEDA (EO/phenol = 2 or 4) and PDAM, for RPLC of small molecules were described in Chapter 4. Gradient elution of alkyl benzenes and alkyl parabens with high resolution was achieved using all monolithic columns. The porogen selection for BADMA and PDAM was investigated with the intention of obtaining data that could possiblly lead to a method for rational porogen selection. Chapter 5 presents some proposed future directions in polymer monolith development using single crosslinking monomers.

1.7 References

1. Van Deemter, J. J.; Zuiderweg, F. J.; Klinkenberg, A *Chem. Eng. Sci.* **1995,** *50,* 3869-3882.
2. MacNair, J. E.; Lewis, K. C.; Jorgenson, J. W. *Anal. Chem.* **1997,** *69*, 983-989.
3. Wu, N.; Collins, D. C.; Lippert, J. A.; Xiang, Y.; Lee, M. L. *J. Microcolumn Sep.* **2000,** *12*, 462-469.
4. Wang, X.; Barber, W. E.; Carr, P. W. *J. Chromatogr. A* **2006,** *1107*, 139-151.
5. Yang, X.; Ma, L.; Carr, P. W. *J. Chromatogr. A* **2005,** *1079*, 213-220.
6. Hjerten, S.; Liao, J.; Zhang, R. *J. Chromatogr.* **1989,** *473*, 273-275.

7. Liao, J.; Zhang, R.; Hjerten, S. *J. Chromatogr.* **1991,** *586*, 21-26.
8. Svec, F.; Frechet, J. M. J. *Anal. Chem.* **1992,** *64*, 820-822.
9. Guiochon, G. *J. Chromatogr. A* **2007,** *1168*, 101-168.
10. Svec, F. *J. Chromatogr. A* **2010,** *1217*, 902-924.
11. Vlakh, E. G.; Tennikova, T. B. *J. Chromatogr. A* **2009,** *1216*, 2637-2650.
12. Vlakh, E. G.; Tennikova, T. B. *J. Sep. Sci.* **2007,** *30*, 2801-2813.
13. Smith, N. W.; Jiang, Z. *J. Chromatogr. A* **2008,** *1184*, 416-440.
14. Wu, R.; Hu, L.; Wang, F.; Ye, M.; Zou, H. *J. Chromatogr. A* **2008,** *1184*, 369-392.
15. Svec, F. *J. Sep. Sci.* **2004,** *27*, 747-766.
16. Svec, F. *J. Sep. Sci.* **2004,** *27*, 1419-1430.
17. Courtois, J.; Szumski, M.; Bystrom, E.; Iwasiewicz, A.; Shchukarev, A.; Irgum, K. *J. Sep. Sci.* **2006,** *29*, 325-325.
18. Vidic, J.; Podgornik, A.; Strancar, A. *J. Chromatogr. A* **2005,** *1065*, 51-58.
19. Xu, Z.; Yang, L.; Wang, Q. *J. Chromatogr. A* **2009,** *1216*, 3098-106.
20. Gu, B.; Li, Y.; Lee, M. L. *Anal. Chem.* **2007,** *79*, 5848-5855.
21. Cifuentes, A.; Canalejas, P.; Ortega, A.; Diez-Masa, J. C. *J. Chromatogr. A* **1998,** *823*, 561-571.
22. Nischang, I.; Svec, F.; Frechet, J. M. J. *Anal. Chem.* **2009,** *81*, 7390-7396.
23. Yue, G.; Luo, Q.; Zhang, J.; Wu, S.; Karger, B. L., *Anal. Chem.* **2007,** *79*, 938-946.
24. Huang, X.; Horvath, C. *J. Chromatogr. A* **1997,** *788*, 155-164.
25. He, M.; Zeng, Y.; Sun, X.; Harrison, D. J. *Electrophoresis* **2008,** *29*, 2980-2986.
26. Vizioli, N. M.; Rusell, M. L.; Carbajal, M. L.; Carducci, C. N.; Grasselli, M. *Electrophoresis* **2005,** *26*, 2942-2948.
27. Bandari, R.; Knolle, W.; Prager-Duschke, A.; Glasel, H. R.; Buchmeiser, M. R. *Macromol. Chem. Physic.* **2007,** *208*, 1428-1436.
28. Krajnc, P.; Leber, N.; Stefanec, D.; Kontrec, S.; Podgornik, A. *J. Chromatogr. A* **2005,** *1065*, 69-73.
29. Yao, C.; Qi, L.; Jia, H.; Xin, P.; Yang, G.; Chen, Y. *J. Mater. Chem.* **2009,** *19*, 767-772.
30. Yao, K.; Yun, J.; Shen, S.; Chen, F. *J. Chromatogr. A* **2007,** *1157*, 246-251.
31. Dainiak, M. B.; Galaev, I. Y.; Mattiasson, B. *J. Chromatogr. A* **2006,** *1123*, 145-150.
32. Meyer, U.; Svec, F.; Frechet, J. M. J.; Hawker, C. J.; Irgum, K. *Macromolecules* **2000,** *33*, 7769-7775.
33. Kanamori, K.; Nakanishi, K.; Hanada, T. *Adv. Mater.* **2006,** *18*, 2407-2411.
34. Hasegawa, J.; Kanamori, K.; Nakanishi, K.; Hanada, T.; Yamago, S. *Macromolecules* **2009,** *42*, 1270-1277.
35. Kanamori, K.; Hasegawa, J.; Nakanishi, K.; Hanada, T. *Macromolecules* **2008,** *41*, 7186-7193.
36. Mayr, B.; Holzl, G.; Eder, K.; Buchmeiser, M. R.; Huber, C. G. *Anal. Chem.* **2002,** *74*, 6080-6087.

37. Hosoya, K.; Hira, N.; Yamamoto, K.; Nishimura, M.; Tanaka, N. *Anal. Chem.* **2006,** *78*, 5729-5735.
38. Peskoller, C.; Niessner, R.; Seidel, M. *J. Chromatogr. A* **2009,** *1216*, 3794-3801.
39. Mai, N. A.; Duc, N. T.; Irgum, K. *Chem. Mater.* **2008,** *20*, 6244-6247.
40. Nguyen, A. M.; Nordborg, A.; Shchukarev, A.; Irgum, K. *J. Sep. Sci.* **2009,** *32*, 2619-2628.
41. Tennikova, T. B.; Belenkii, B. G.; Svec, F. *J. Liq. Chromatogr.* **1990,** *13*, 63-70.
42. Tennikova, T. B.; Bleha, M.; Svec, F.; Almazova, T. V.; Belenkii, B. G. *J. Chromatogr.* **1991,** *555*, 97-107.
43. Svec, F.; Frechet, J. M. J. *Macromolecules* **1995,** *28*, 7580-7582.
44. Svec, F.; Frechet, J. M. J. *Chem. Mater.* **1995,** *7*, 707-715.
45. Viklund, C.; Svec, F.; Frechet, J. M. J.; Irgum, K. *Chem. Mater.* **1996,** *8*, 744-750.
46. Trojer, L.; Bisjak, C. P.; Wieder, W.; Bonn, G. K. *J. Chromatogr. A* **2009,** *1216*, 6303-6309.
47. Lubbad, S. H.; Buchmeiser, M. R. *J. Sep. Sci.* **2009,** *32*, 2521-2529.
48. Aoki, H.; Kubo, T.; Ikegami, T.; Tanaka, N.; Hosoya, K.; Tokuda, D.; Ishizuka, N. *J. Chromatogr. A* **2006,** *1119*, 66-79.
49. Viklund, C.; Ponten, E.; Glad, B.; Irgum, K.; Horstedt, P.; Svec, F. *Chem. Mater.* **1997,** *9*, 463-471.
50. Peterson, D. S.; Rohr, T.; Svec, F.; Frechet, J. M. J. *Anal. Chem.* **2003,** *75*, 5328-5335.
51. Stachowiak, T. B.; Svec, F.; Frechet, J. M. J. *J. Chromatogr. A* **2004,** *1044*, 97-111.
52. Yu, C.; Xu, M. C.; Svec, F.; Frechet, J. M. J. *J. Polym. Sci. Part A-Polym. Chem.* **2002,** *40*, 755-769.
53. Sun, X.; Yang, W.; Pan, T.; Woolley, A. T. *Anal. Chem.* **2008,** *80*, 5126-5130.
54. Yang, W.; Sun, X.; Wang, H.; Woolley, A. T. *Anal. Chem.* **2009,** *81*, 8230-8235.
55. Li, Y.; Gu, B.; Tolley, H. D.; Lee, M. L. *J. Chromatogr. A* **2009,** *1216*, 5525-5532.
56. Li, Y.; Tolley, H. D.; Lee, M. L. *Anal. Chem.* **2009,** *81*, 9416-9424.
57. Li, Y.; Tolley, H. D.; Lee, M. L. *J. Chromatogr. A* **2010,** *1217*, 4934-4945.
58. Throckmorton, D. J.; Shepodd, T. J.; Singh, A. K. *Anal. Chem.* **2002,** *74*, 784-789.
59. Augustin, V.; Jardy, A.; Gareil, P.; Hennion, M. C. *J. Chromatogr. A* **2006,** *1119*, 80-87.
60. Augustin, V.; Proczek, G.; Dugay, J.; Descroix, S.; Hennion, M. C. *J. Sep. Sci.* **2007,** *30*, 2858-65.
61. Proczek, G.; Augustin, V.; Descroix, S.; Hennion, M. C. *Electrophoresis* **2009,** *30*, 515-524.
62. Bandilla, D.; Skinner, C. D. *J. Chromatogr. A* **2003,** *1004*, 167-179.
63. Bedair, M.; Oleschuk, R. D. *Analyst* **2006,** *131*, 1316-1321.
64. Courtois, J.; Bystrom, E.; Irgum, K. *Polymer* **2006,** *47*, 2603-2611.

65. Geiser, L.; Eeltink, S.; Svec, F.; Frechet, J. M. J. *J. Chromatogr. A* **2007,** *1140* , 140-146.
66. Bernabe-Zafon, V.; Canto-Mirapeix, A.; Simo-Alfonso, E. F.; Ramis-Ramos, G.; Herrero-Martinez, J. M. *Electrophoresis* **2009,** *30*, 1929-1936.
67. Khimich, G. N.; Tennikova, T. B. *Russ. J. Appl. Chem.* **2005,** *78*, 623-627.
68. Szumski, M.; Buszewski, B. *J. Sep. Sci.* **2009,** *32*, 2574-2581.
69. Hirano, T.; Kitagawa, S.; Ohtani, H. *Anal. Sci.* **2009,** *25*, 1107-1113.
70. Krenkova, J.; Lacher, N. A.; Svec, F. *Anal. Chem.* **2010** *Article ASAP*.
71. Hemstrom, P.; Nordborg, A.; Irgum, K.; Svec, F.; Frechet, J. M. J. *J. Sep. Sci.* **2006,** *29*, 25-32.
72. Gu, B.; Armenta, J. M.; Lee, M. L. *J. Chromatogr. A* **2005,** *1079*, 382-391.
73. Li, Y.; Tolley, H. D.; Lee, M. L. *Anal. Chem.* **2009,** *81*, 4406-4413.
74. Gu, B.; Chen, Z.; Thulin, C. D.; Lee, M. L. *Anal. Chem.* **2006,** *78*, 3509-3518.
75. Chen, X.; Tolley, H. D.; Lee, M. L. *J. Sep. Sci.* **2009,** *32*, 2565-2573.
76. Nordborg, A.; Svec, F.; Frechet, J. M. J.; Irgum, K. *J. Sep. Sci.* **2005,** *28*, 2401-2406.
77. Kubo, T.; Kimura, N.; Hosoya, K.; Kaya, K. *J. Polym. Sci. Part A-Polym. Chem.* **2007,** *45*, 3811-3817.
78. Wu, Z.; Frederic, K. J.; Talarico, M.; De Keel, D. *Can. J. Chem. Eng.* **2009,** *87*, 579-583.
79. Hasegawa, J.; Kanamori, K.; Nakanishi, K.; Hanada, T.; Yamago, S. *Macromol. Rapid. Comm.* **2009,** *30*, 986-990.
80. Greiderer, A.; Ligon, S. C.; Huck, C. W.; Bonn, G. K. *J. Sep. Sci.* **2009,** *32*, 2510-2520.
81. Greiderer, A.; Trojer, L.; Huck, C. W.; Bonn, G. K. *J. Chromatogr. A* **2009,** *1216*, 7747-7754.
82. Lubbad, S. H.; Buchmeiser, M. R. *J. Chromatogr. A* **2010,** *1217*, 3223-3230.
83. Xie, S.; Svec, F.; Frechet, J. M. J. *Biotechnol. Bioeng.* **1999,** *62*, 30-35.
84. Peterson, D. S.; Rohr, T.; Svec, F.; Frechet, J. M. J. *J. Proteome. Res.* **2002,** *1*, 563-568.
85. Peterson, D. S.; Rohr, T.; Svec, F.; Frechet, J. M. J. *Anal. Chem.* **2002,** *74*, 4081-4088.
86. Wang, Q.; Svec, F.; Frechet, J. M. J. *Anal. Chem.* **1995,** *67* (3), 670-674.
87. Svec, F.; Frechet, J. M. J. *Biotechnol. Bioeng.* **1995,** *48*, 476-480.
88. Sykora, D.; Svec, F.; Frechet, J. M. J. *J. Chromatogr. A* **1999,** *852*, 297-304.
89. Ueki, Y.; Umemura, T.; Li, J. X.; Odake, T.; Tsunoda, K. *Anal. Chem.* **2004,** *76*, 7007-7012.
90. Hutchinson, J. P.; Hilder, E. F.; Shellie, R. A.; Smith, J. A.; Haddad, P. R. *Analyst* **2006,** *131*, 215-221.
91. Wei, Y.; Huang, X.; Liu, R.; Shen, Y.; Geng, X. *J. Sep. Sci.* **2006,** *29*, 5-13.

92. Luo, Q.; Zou, H.; Xiao, X.; Guo, Z.; Kong, L.; Mao, X. *J. Chromatogr. A* **2001,** *926*, 255-264.
93. Svec, F. *Electrophoresis* **2006,** *27*, 947-961.
94. Xu, Y.; Cao, Q.; Svec, F.; Frechet, J. M. J. *Anal. Chem.* **2010,** *82*, 3352-3358.
95. Cao, Q.; Xu, Y.; Liu, F.; Svec, F.; Frechet, J. M. J. *Anal. Chem.* **2010,** *82*, 7416-7421.
96. Hilder, E. F.; Svec, F.; Frechet, J. M. J. *J. Chromatogr. A* **2004,** *1053*, 101-106.
97. Hutchinson, J. P.; Zakaria, P.; Bowiet, A. R.; Macka, M.; Avdalovic, N.; Haddad, P. R. *Anal. Chem.* **2005,** *77*, 407-416.
98. Zakaria, P.; Hutchinson, J. P.; Avdalovic, N.; Liu, Y.; Haddad, P. R. *Anal. Chem.* **2005,** *77*, 417-423.
99. Sinner, F.; Buchmeiser, M. R. *Macromolecules* **2000,** *33*, 5777-5786.
100. Sinner, F. M.; Buchmeiser, M. R. *Angew. Chem. Int. Edit.* **2000,** *39*, 1433-1436.
101. Tripp, J. A.; Stein, J. A.; Svec, F.; Frechet, J. M. J. *Org. Lett.* **2000,** *2*, 195-198.
102. Tripp, J. A.; Svec, F.; Frechet, J. M. J. *J. Comb. Chem.* **2001,** *3*, 216-223.
103. Peters, E. C.; Svec, F.; Frechet, J. M. J. *Adv. Mater.* **1997,** *9*, 630-633.
104. Zhang, R.; Yang, G.; Xin, P.; Qi, L.; Chen, Y. *J. Chromatogr. A* **2009,** *1216*, 2404-2411.
105. Ranby, B.; Yang, W.; Tretinnikov, O. *Nucl. Instrum. Meth. B* **1999,** *151*, 301-305.
106. Kato, K.; Uchida, E.; Kang, E. T.; Uyama, Y.; Ikada, Y. *Prog. Polym. Sci.* **2003,** *28*, 209-259.
107. Rohr, T.; Hilder, E. F.; Donovan, J. J.; Svec, F.; Frechet, J. M. J. *Macromolecules* **2003,** *36*, 1677-1684.
108. Hilder, E. F.; Svec, F.; Frechet, J. M. J. *Anal. Chem.* **2004,** *76*, 3887-3892.
109. Krenkova, J.; Lacher, N. A.; Svec, F. *Anal. Chem.* **2009,** *81*, 2004-2012.
110. Krenkova, J.; Lacher, N. A.; Svec, F. *J. Chromatogr. A* **2009,** *1216*, 3252-3259.
111. Krenkova, J.; Gargano, A.; Lacher, N. A.; Schneiderheinze, J. M.; Svec, F. *J. Chromatogr. A* **2009,** *1216*, 6824-6830.
112. Xie, S.; Svec, F.; Frechet, J. M. J. *Chem. Mater.* **1998,** *10*, 4072-4078.
113. Merhar, M.; Podgornik, A.; Barut, M.; Zigon, M.; Strancar, A. *J. Sep. Sci.* **2003,** *26*, 322-330.
114. Okay, O. *Prog. Polym. Sci.* **2000,** *25*, 711-779.
115. Moore, R. E.; Licklider, L.; Schumann, D.; Lee, T. D. *Anal. Chem.* **1998,** *70*, 4879-84.
116. Xiong, B.; Zhang, L.; Zhang, Y.; Zou, H.; Wang, J. *J. High. Res. Chrom.* **2000,** *23*, 67-72.
117. Jin, W.; Fu, H. J.; Huang, X.; Xiao, H.; Zou, H., *Electrophoresis* **2003,** *24*, 3172-3180.
118. Premstaller, A.; Oberacher, H.; Huber, C. G. *Anal. Chem.* **2000,** *72*, 4386-93.
119. Walcher, W.; Oberacher, H.; Troiani, S.; Holzl, G.; Oefner, P.; Zolla, L.; Huber, C. G. *J. Chromatogr. B* **2002,** *782*, 111-125.

120. Oberacher, H.; Huber, C. G. *Trend. Anal. Chem.* **2002,** *21*, 166-174.
121. Dong, X.; Dong, J.; Ou, J.; Zhu, Y.; Zou, H. *Electrophoresis* **2006,** *27*, 2518-25.
122. Okanda, F. M.; El Rassi, Z. *Electrophoresis* **2006,** *27*, 1020-1030.
123. Danquah, M. K.; Forde, G. M. *J. Chromatogr. A* **2008,** *1188*, 227-233.
124. Eeltink, S.; Hilder, E. F.; Geiser, L.; Svec, F.; Frechet, J. M.; Rozing, G. P.; Schoenmakers, P. J.; Kok, W. T. *J. Sep. Sci.* **2007,** *30*, 407-13.
125. Le Gac, S.; Carlier, J.; Camart, J. C.; Cren-Olive, C.; Rolando, C. *J. Chromatogr. B* **2004,** *808*, 3-14.
126. Hradil, J.; Horak, D. *React. Funct. Polym.* **2005,** *62*, 1-9.
127. Zhong, H. W.; El Rassi, Z. *J. Sep. Sci.* **2009,** *32*, 10-20.
128. Zhu, G.; Yang, C.; Zhang, L.; Liang, Z.; Zhang, W.; Zhang, Y. *Talanta* **2006,** *70*, 2-6.
129. Santora, B. P.; Gagne, M. R.; Moloy, K. G.; Radu, N. S. *Macromolecules* **2001,** *34*, 658-661.
130. Huang, X.; Zhang, S.; Schultz, G. A.; Henion, J. *Anal. Chem.* **2002,** *74*, 2336-2344.
131. Peters, E. C.; Petro, M.; Svec, F.; Frechet, J. M. J. *Anal. Chem.* **1997,** *69*, 3646-3649.
132. Peters, E. C.; Petro, M.; Svec, F.; Frechet, J. M. J. *Anal. Chem.* **1998,** *70*, 2288-2295.
133. Peters, E. C.; Petro, M.; Svec, F.; Frechet, J. M. J. *Anal. Chem.* **1998,** *70*, 2296-2302.
134. Moravcova, D.; Jandera, P.; Urban, J.; Planeta, J. *J. Sep. Sci.* **2003,** *26*, 1005-1016.
135. Huo, Y.; Schoenmakers, P. J.; Kok, W. T. *J. Chromatogr. A* **2007,** *1175*, 81-88.
136. Canto-Mirapeix, A.; Herrero-Martinez, J. M.; Mongay-Fernandez, C.; Simo-Alfonso, E. F. *Electrophoresis* **2008,** *29*, 4399-4406.
137. Xie, S.; Svec, F.; Frechet, J. M. J. *J. Polym. Sci. Part A-Polym. Chem.* **1997,** *35*, 1013-1021.
138. Palm, A.; Novotny, M. V. *Anal. Chem.* **1997,** *69*, 4499-4507.
139. Sinitsyna, E. S.; Sergeeva, Y. N.; Vlakh, E. G.; Saprikina, N. N.; Tennikova, T. B. *React. Funct. Polym.* **2009,** *69*, 385-392.
140. Cooper, A. I.; Holmes, A. B. *Adv. Mater.* **1999,** *11*, 1270-1274.
141. Hebb, A. K.; Senoo, K.; Cooper, A. I. *Compos. Sci. Technol.* **2003,** *63*, 2379-2387.
142. Bakry, R.; Huck, C. W.; Bonn, G. K. *J. Chromatogr. Sci.* **2009,** *47*, 418-431.
143. Eeltink, S.; Herrero-Martinez, J. M.; Rozing, G. P.; Schoenmakers, P. J.; Kok, W. T. *Anal. Chem.* **2005,** *77*, 7342-7347.
144. Ueki, Y.; Umemura, T.; Iwashita, Y.; Odake, T.; Haraguchi, H.; Tsunoda, K. *J. Chromatogr. A* **2006,** *1106*, 106-111.
145. Urban, J.; Svec, F.; Frechet, J. M. J. *Anal. Chem.* **2010,** *82*, 1621-1623.

CHAPTER 2 POLY[HYDROXYETHYL ACRYLATE-CO-POLY(ETHYLENE GLYCOL) DIACRYLATE] MONOLITHIC COLUMN FOR EFFICIENT HYDROPHOBIC INTERACTION CHROMATOGRAPHY OF PROTEINS*

2.1 Introduction

HIC is a valuable technique for the separation and purification of proteins under non-denaturing conditions, which was pioneered by Porath et al.[1] and Hjertén.[2] Principles of HIC involve weak hydrophobic interaction of a protein with a moderately hydrophobic ligand distributed on the stationary phase matrix. This interaction is promoted through the use of a mobile phase containing high salt concentration, such as sodium sulfate, ammonium sulfate, or sodium citrate. The separation is usually achieved by first using an initial high salt concentration that enhances hydrophobic interaction by removing water from the vicinity of the protein surface, and then the retained proteins are eluted in order of increasing hydrophobicity either isocratically or, more generally, by a descending salt gradient that allows the proteins to rehydrate selectively. This is in sharp contrast to RPLC where organic solvents and acidic conditions are used for sample elution, which tends to promote protein denaturation. While both HIC and RPLC are based on hydrophobic interactions of solutes with the stationary phase to effect separation, HIC differs from RPLC mainly in three ways: ligand hydrophobicity, ligand density, and hydrophobicity of the column matrix. Compared to RPLC, HIC columns usually have ligands that are less hydrophobic and have lower ligand densities, and the polymeric matrix is relatively hydrophilic. Consequently, HIC is less denaturing and allows elution with entirely aqueous eluents rather than organic solvents.

A number of packing materials have been developed for HIC separation,[3-6] while

* This chapter was largely taken from: Li, Y.; Tolley, H. D.; Lee, M. L. *Anal. Chem.* **2009**, *81*, 9416-9424.

materials in the form of a continuous bed or monolith have been few. Application of monoliths as chromatographic phases was introduced in the 1990s.[7-9] As an alternative to packed columns, monolithic columns have received increasing interest because of advantages, such as low back pressure, fast mass transfer, and simple preparation. Excellent reviews have appeared describing the preparation of polymer monoliths and their applications in LC.[10-14] HIC applications of polymer monoliths are much less widespread than, for example, RPLC or IEC. Recently, Zhang et al. reported a poly(N-isopropylacrylamide)-grafted polymer monolith for HIC separation of proteins,[15] for which poly(N-isopropylacrylamide) was grafted onto a poly(chloromethylstyrene-divinylbenzene) macroporous monolith contained in a 100 mm × 4.6 mm I.D. stainless steel column using surface-initiated atom transfer radical polymerization. Baseline separation of six model proteins within 20 min was achieved using this grafted monolithic column. The chromatographic peaks tailed, which was probably caused by non-specific adsorption of proteins on the monolith. In 2006, Svec and co-workers prepared HIC monolithic capillary columns by single-step in situ polymerization of butyl methacrylate (BMA), hydroxyethyl methacrylate (HEMA), and 1,4-butanediol methacrylate.[16] BMA was used to provide the hydrophobic ligands, while HEMA was added to the polymerization mixture to achieve the desired stationary phase hydrophilicity and, hence, protein retention. Baseline separation of three proteins was achieved using a 20 min gradient from 2.0 to 0 M $(NH_4)_2SO_4$ in 10 mM phosphate buffer. However, the chromatographic peaks were broad and the peak capacity was low. While these and a few other studies[17,18] have been published on HIC monolithic columns, none to date have shown chromatographic performance as good as packed columns.[19]

An ideal stationary phase for protein separation by HIC should be inert, thus avoiding non-specific binding of proteins, and the proteins should interact only with the hydrophobic ligands present at relatively low concentration. Materials made of, or containing, polyethylene glycol (PEG) are well-known for their resistance to protein adsorption. Lee's group has reported several monoliths synthesized from PEG-functionalized monomers or crosslinkers for size-exclusion,[20,21] cation-exchange,[22-24] and anion-exchange[25] chromatography of peptides and proteins. It was clearly demonstrated that a monolith prepared from PEGMEA as monomer and PEGDA as crosslinker showed negligible non-specific adsorption of bovine serum albumin.[20] PEGDA has proven to be very useful as a crosslinker in suppressing nonspecific interaction for analysis of peptides and proteins. In this work, PEGDA was copolymerized with HEA to form monoliths for HIC of proteins, taking advantage of the moderately hydrophilic and biocompatible PEG-containing backbone for protein separation. Copolymer monoliths of HEA and diethylene glycol dimethacrylate (DEGDMA) have been reported,[26] and the authors found that an increase in HEA content in the monomer mixture resulted in monoliths with increased hydrophilic character. This tendency was also observed for HEA/PEGDA monoliths in this work. Although the HEA/PEGDA monolith was prepared with the original intention for use in hydrophilic-interaction chromatography (HILIC), it showed excellent performance for HIC of protein standards.

2.2 Experimental Section

2.2.1 Chemicals and Reagents

DMPA (99%), TPM (98%), HEA (96%), HEMA (≥99%), PEGDA (Mn ~ 258), and EDMA (98%) were purchased from Sigma-Aldrich (St. Louis, MO, USA). All of the

monomers were used without further purification. Protein standards (cytochrome *c* from bovine heart, myoglobin from equine skeletal muscle, ribonuclease A, type I-A, from bovine pancreas, lysozyme from chicken egg white, and α-chymotrypsinogen A, type II, from bovine pancreas) were obtained from Sigma-Aldrich. α-Chymotrypsin was obtained by activating α-chymotrypsinogen A. All porogenic solvents and chemicals for use in mobile-phase buffer preparation were HPLC or analytical reagent grade. Buffer solutions were prepared with HPLC water and filtered through a 0.22-μm membrane filter.

2.2.2 Polymer Monolith Preparation

UV-transparent fused-silica capillary tubing (75-μm i.d., 375-μm o.d., Polymicro Technologies, Phoenix, AZ) was treated with TPM to provide vinyl groups for anchoring of polymer monoliths following a procedure previously described.[23] The silanized capillary was sealed with rubber septa at both ends until it was used.

Monomer solution was prepared in 1-dram (4 mL) glass vials by admixing initiator, monomer, cross-linker, and porogens (see Table 2.1 for reagent compositions). The solution was vortexed instead of ultrasonicated because of the high volatility of ethyl ether, and was then kept in ice before it was introduced into the surface-silanized capillary. Usually, the polymer precursor was introduced into the capillary simply by capillary action; however, I found that this method formed an inhomogeneous section of monolith at the detection end of the column that was observed under a microscope to be approximately 1 cm in length. This was mainly caused by the high volatility of the methanol/ethyl ether porogen system. When using long-chain alcohols as porogens, such as decanol or dodecanol, this problem did not exist. To relieve this problem, helium gas pressure was used to fill the whole

Table 2.1. Compositions and Properties of Selected Monoliths Synthesized in this Study.

monolith	composition[a]										properties	
	HEA (g)	HEMA (g)	PEGDA (g)	EDMA (g)	methanol (g)	ethyl ether (g)	cyclohexanol (g)	2-octanol (g)	decanol (g)	dodecanol (g)	back pressure (MPa)[b]	morphology
A	0.32	/	0.44	/	0.80	0.80	/	/	/	/	0.869	similar to B, but microglobules less distinct
B	0.38	/	0.38	/	0.60	1.00	/	/	/	/	0.848	see Figure 2.2A
C	0.44	/	0.32	/	0.80	0.80	/	/	/	/	0.772	similar to B, but less homogeneous
D	0.44	/	/	0.32	/	/	0.50	0.70	/	/	∞	white solid material, methanol cannot be pushed through
E	0.44	/	/	0.32	/	/	0.20	1.0	/	/	1.57	conventional morphology, microglobule ~0.7 μm
F	0.44	/	/	0.32	/	/	0.20	/	1.0	/	2.93	similar to E, but larger microglobule clusters
G	0.44	/	/	0.32	/	/	0.20	/	/	1.0	-	backpressure keeps increasing, collapse occurs
H	/	0.44	/	0.32	/	/	0.60	0.60	/	/	-	white hard gel, center cracks
I	/	0.44	/	0.32	/	/	0.20	1.0	/	/	1.89	conventional morphology, microglobule ~0.5 μm, see Figure 2.2C
J	/	0.44	/	0.32	/	/	0.15	1.05	/	/	1.40	similar to I, but center less polymerized
K	/	0.44	/	0.32	/	/	0.20	/	1.0	/	0.938	conventional morphology, microglobule ~0.7 μm, larger microglobule clusters compared to I, see Figure 2.2D
L	/	0.44	/	0.32	/	/	0.20	/	/	1.0	1.28	similar to I, but larger microglobule clusters
M	/	0.44	/	0.32	/	/	/	1.2	/	/	0.538	conventional morphology, large throughpores, not homogeneous
N	/	0.44	0.32	/	/	/	0.40	/	0.80	/	3.26	conventional morphology, microglobule ~0.5 μm
O	/	0.44	0.32	/	/	/	0.40	/	/	0.80	3.30	similar to N, but center less polymerized

[a] All monoliths contain 0.0076 g DMPA. [b] For a 75 μm i.d. × 10 cm column with methanol at 0.1 μL/min flow rate.

capillary with precursor solution, and black tape was used to mask one end to form a detection window. Then the capillary was sealed with rubber septa at both ends and was placed on a copper plate which was freeze-mounted on ice in advance. The capillary together with the ice bath was placed directly under a PRX 1000-20 Exposure Unit UV lamp (TAMARACK Scientific, Corona, CA) for 3.5 min. The polymerization was very quick; within 2 min of UV exposure, a rigid monolith formed. A longer exposure time of 3.5 min was used to ensure complete conversion of the monomers. The ice bath was necessary to ensure that the section covered with the mask did not polymerize due to heating, and to prevent inhomogeneity that could be caused by irregular heating. By following the above procedure, the inhomogeneous end section was effectively reduced to less than 0.3 cm, and column preparation became highly repeatable and almost 100% successful. After the monolithic column was prepared, it was then flushed with methanol and water sequentially to remove porogens and unreacted monomers using an HPLC pump. The capillary was stored after filling with water or aqueous 10% methanol solution to avoid drying out the monolith.

Monolithic columns were characterized by scanning electron microscopy (SEM, FEI Philips XL30 ESEM FEG, Hillsboro, OR) at low vacuum, without coating with a conducting gold layer. SEM images of the monolith provided information concerning its morphology and pore structure.

2.2.3 Capillary Liquid Chromatography (CLC)

The CLC system used in all experiments was an UltiMate 3000 high pressure gradient LC system (Dionex, Bannockburn, IL) equipped with an FLM-3300 nano flow manager (1:1000 split ratio). The system was operated with Chromeleon software. A

section of 50-μm i.d. poly(vinyl alcohol)-coated fused-silica capillary was used as sample loop,[27] and the loop volume was calculated to be 200 nL. The two mobile phase components for gradient elution of proteins were 0.1 M phosphate buffer, pH 6.9 (buffer B), and 3.0 M ammonium sulfate in buffer B (buffer A). On-column detection was performed using a Crystal 100 variable wavelength UV–vis absorbance detector and Chrom Perfect software (Mountain View, CA) for data collection and treatment. UV absorbance was monitored at 214 nm. The test protein mixture contained 0.2 mg/mL each of cytochrome *c*, myoglobin, ribonuclease A and lysozyme, and 0.4 mg/mL of α-chymotrypsinogen A dissolved in the initial buffer. The chromatographic conditions are given in the figure captions. Chromatograms were transferred to Excel files and redrawn using Microcal Origin (Northampton, MA). Baseline drift caused by the salt gradient was subtracted from all chromatograms.

For measurement of the dynamic binding capacity (DBC) of the monolithic column, the sample loop was replaced with a 2-m long fused-silica capillary with 250-μm i.d. for frontal analysis. The monolithic column (4.5 cm long, 75-μm i.d.) was connected to the injector valve using a 10-cm long capillary with 30-μm i.d. (a length no shorter than 13 cm was needed from the pump to the detection window for the CLC system). One end of the capillary was connected to the injector valve and the other end was connected to the column using a True ZDV Union (Upchurch Scientific, Oak Harbor, WA). The monolithic column was first equilibrated with 67% buffer A (i.e., 2.0 M ammonium sulfate) at a flow rate of 0.3 μL/min, and then the large sample loop was loaded with a solution of 0.5 mg/mL lysozyme dissolved in 67% buffer A. Frontal analysis was started simply by switching the injector valve to the inject position. The volume of protein solution needed to saturate the

column was measured by observing the breakthrough curve which could be recorded directly by monitoring the UV absorbance. The large loop was installed at the sample loop position rather than in front of the column in order to eliminate the time needed for building the pressure and to minimize unwanted peaks caused by union connections.[25] A short column, low protein concentration, and 2.0 M salt concentration rather than 3.0 M were chosen to avoid protein denaturation or precipitation.

The recoveries of the model proteins were determined by a method similar to that described by Yang et al.[28] Specifically, a 23 cm long column was prepared and used for HIC separation of the proteins. The column was then cut down to 13 cm in length, and protein separation was carried out again using this shorter column. The proteins were eluted with a gradient of buffer A to B in 15 min at 0.3 μL/min flow-rate. The peak areas of the five proteins (myoglobin, ribonuclease A, lysozyme, α-chymotrypsin and α-chymotrypsinogen A) were obtained directly from the Chrom Perfect software. The protein peak areas obtained using the long column were compared with those obtained using the short column according to the following equation:

$$\text{Mass recovery} = \frac{A_{\text{p(long column)}}}{A_{\text{p(short column)}}} \times 100$$

2.3 Results and Discussion

2.3.1 Polymer Monolith Preparation

As described in detail in Chapter 1, once the monomer and crosslinker for a monolith preparation are selected, the porous properties of the monolith and its morphology are mainly a consequence of the porogen types, the ratio between porogens, the percentage of crosslinker monomer, and the ratio between the total monomers and porogens. Among

these factors, the selection of porogens and their ratio are considered to be the most important, since they do not change the chemical composition of the final polymer monolith. Methanol and ethyl ether have proven to be two effective porogenic solvents for synthesizing monoliths from PEG-based monomers.[20] Thus, methanol and ethyl ether were chosen as the starting porogen system. Weight percentages of 32.2% total monomers and 67.8% total porogens were chosen to ensure the rigidity of the resulting monolith, and the initiator concentration was 1% of the monomers. Figure 2.1 shows the flow resistance of HEA/PEGDA monoliths prepared with varying ratios of ethyl ether and methanol when the ratio between monomer and crosslinker was kept at 1:1. All resulting monoliths were rigid and contained through pores. The curve reveals that methanol and ethyl ether are good and poor solvents, respectively, for the HEA/PEGDA monomer system. This is consistent with the synthesis of poly(PEGDA) monoliths using methanol and ethyl ether as porogens at low temperature (note: methanol becomes a poor solvent for poly(PEGDA) monoliths when the precursor solution is at room temperature). Whether a solvent is good or poor mostly depends on its relative polarity compared to the growing polymer chain during polymerization. It is reasonable to conclude that the addition of HEA increases the polarity of the HEA/PEGDA copolymer compared to a polymer synthesized solely from PEGDA. Methanol is a relatively good solvent for the copolymer regardless of whether the solution is at room temperature or at lower temperature. However, the monolithic copolymer with the lowest resistance was prepared from a precursor solution composed of 43.8:56.2 wt ratio methanol/ethyl ether, and not 100% ethyl ether. This was also observed in the synthesis of poly(PEGDA) monoliths.

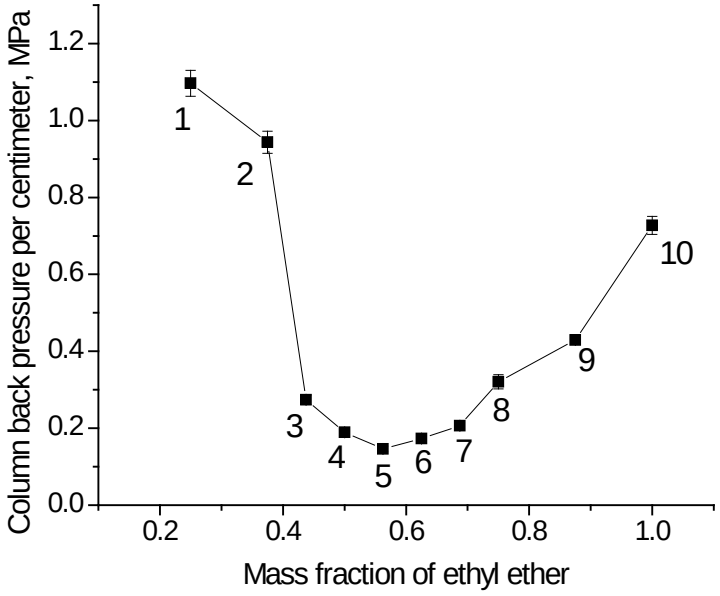

Figure 2.1. Effect of ethyl ether ratio on back pressure of poly(HEA-co-PEGDA) monoliths. Monolith composition: 0.38 g HEA, 0.38 g PEGDA, and 1.6 g total porogens (methanol and ethyl ether). The back pressure for each data point was averaged from two or three columns using methanol at 0.2 μL/min. The data points 1-10 in the graph represent (1) 0.4 g ethyl ether and 1.2 g methanol, (2) 0.6 g ethyl ether and 1.0 g methanol, (3) 0.7 g ethyl ether and 0.9 g methanol, (4) 0.8 g ethyl ether and 0.8 g methanol, (5) 0.9 g ethyl ether and 0.7 g methanol (6) 1.0 g ethyl ther and 0.6 g methanol, (7) 1.1 g ethyl ether and 0.5 g methanol, (8) 1.2 g ethyl ether and 0.4 g methanol, (9) 1.4 g ethyl ether and 0.2 g methanol and (10) 1.6 g ethyl ether.

SEM images of the monoliths represented by data points in Figure 2.1 were taken and compared. Figure 2.2A shows an electron micrograph of the HEA/PEGDA monolith synthesized from 32.5:67.5 wt ratio methanol/ethyl ether (data point 6 in Figure 2.1). As can be observed, the copolymer was homogeneous and attached firmly to the inside wall of the capillary. The morphology of this monolithic polymer was a cross between a fused microglobule structure and a conventional polymer monolithic structure. Microglobules were observed, however, they were not as discrete as those in conventional polymer monoliths. With an increase in methanol, the SEM images (see Figure 2.2B) showed that the monoliths were as homogeneous as (or even better than) that shown in Figure 2.2A, and the morphology approached the fused microglobule structure. When the ethyl ether concentration was increased, the microstructure was also more similar to fused microglobules, the backpressure increased, and the monolith was less homogeneous. In fact, voids were directly observed in SEM images of monoliths represented by data points 8, 9 and 10 (Figure 2.1). Theoretically, monoliths represented by data points from 1 to 7 (Figure 2.1) could all be used for chromatographic applications. However, the steep curve from data points 1 to 5 indicates that these compositions would be less suitable for control of the pore properties because even a small change in the porogen composition would lead to a large difference in porosity and flow resistance; hence, reproducibility would suffer. In contrast, the changes were much less pronounced for compositions near data point 6 (Figure 2.1). Therefore, the composition represented by data point 6 (i.e., 32.2% monomers composed of 50:50 wt ratio HEA/PEGDA, and 67.8% porogens composed of 37.5:62.5 methanol/ethyl ether) was chosen as the final composition for detailed study. Fortunately,

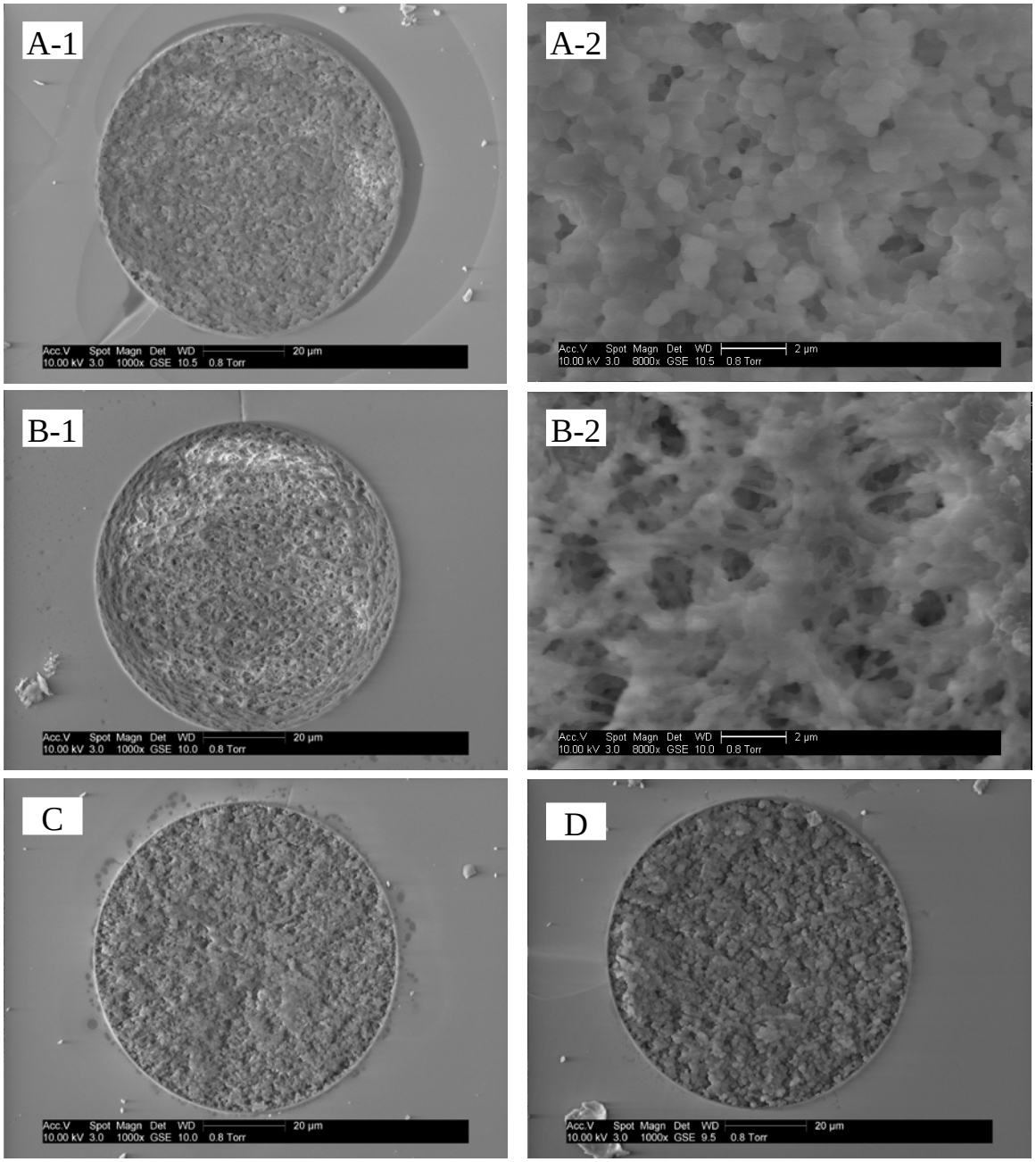

Figure 2.2. SEM micrographs of several synthesized monoliths. Monolith composition: (A) as B in Table 2.1, (B) 0.38 g HEA, 0.38 g PEGDA, 1.2 g methanol, 0.4 g ethyl ether (data point 1 in Figure 2.1), (C) as I in Table 2.1, (D) as K in Table 2.1. Scale bar: 20 and 2 µm, respectively.

both the low resistance to flow and high uniformity of this monolith were quite acceptable for chromatographic separations.

It is worth pointing out that water was also selected as one of the porogens for the HEA/PEGDA monolith at the start of this work. Appropriate combination of water, methanol and ethyl ether, or only water and ethyl ether could produce a homogeneous monolith similar to those shown in Figure 2.2, with similar pressure drop. For example, a 1:5:10 water/methanol/ethyl ether porogen system produce similar pressure drop and efficiency as an 8:8 methanol/ethyl ether system. However, by comparing bulk polymers in a glass vial, I found that with the addition of water, the HEA/PEGDA monolith was less rigid, which was further demonstrated by collapse of the monolith in a capillary after approximately 60 injections. This prompted me to improve the mechanical stability of the copolymer, which eventually led to the elimination of water from among the porogen candidates.

2.3.2 Porogen Selection

A wide variety of solvents or their mixtures could be potential porogenic solvents for monolith preparation; however, selection of appropriate porogens still must be primarily achieved by trial and error. With the intention to obtain data that could possibly lead to a rational porogen selection strategy, I also investigated the synthesis of HEA/EDMA, HEMA/EDMA and HEMA/PEGDA monoliths. For easy comparison, the polymerization mixtures contained 57.9% (0.44 g) monomer and 42.1% (0.32 g) crosslinker, and the ratio of monomers to porogens was kept at 0.63:1 (1.2 g total porogens), except for the water/methanol/ethyl ether porogen system which was 1.6 g total porogens. The initiator

concentration was 1% of the monomers, and 5 min UV light exposure time was used for all cases.

The most commonly used porogenic solvents were first evaluated in this study. Water, methanol, and ethyl ether, or any combination of the three, were found to be ineffective for monolith formation. With only ethyl ether, HEA/EDMA formed a cloud-like, white, soft polymer. If methanol or methanol and water were added, the resulting material became more like a rigid gel than a monolith. The combination of water and ethyl ether gave an immiscible HEA/EDMA solution. When low molecular weight alcohols, such as propyl alcohol and IPA (or their combination with ethyl ether) were tested, monoliths with very high backpressures were obtained, which indicates that very small throughpores were formed, or monoliths with inhomogeneous structures resulted. For example, polymerization of a precursor solution composed of 0.32 g EDMA, 0.44 g HEA, 0.55 g ethyl ether and 0.65 g IPA generated a monolith with a backpressure of 2100 psi at 0.1 μL/min flow rate for a 10 cm × 75 μm i.d. column. For HEMA/EDMA, a mixture of methanol and hexane was tested using an optimized ratio previously reported,[29] however, the resulting monolith had very large pores. For HEMA/PEGDA, water/methanol/ethyl ether or methanol/cyclohexanol porogen systems produced a translucent gel with milk white color and/or the monomer solution was hard to polymerize. Also, no polymerization was observed when using methanol with THF or hexane.

Long chain aliphatic alcohols have often been employed in monolith preparation when EDMA was used as crosslinker. I tested cyclohexanol with 2-octanol, decanol and dodecanol for all four monomer mixtures including HEA/PEGDA. We found that long chain alcohols were not suitable for throughpore generation for HEA/PEGDA; however, the

other three monomer mixtures yielded monoliths using appropriate compositions of the binary alcohol porogens. Table 2.1 lists a number of combinations used to produce monoliths D to O that possessed sufficient rigidity. SEM images were taken and back pressures were measured using methanol at 0.1 μL/min. Cyclohexanol was found to be a good solvent for all three mixtures. An increase in cyclohexanol percentage usually yielded a material like D or H in Table 2.1.

From the standpoint of chemical composition, the only difference between HEA/PEGDA and HEA/HEMA is that HEMA has one more methyl group than HEA. It is this additional methyl group that makes the properties of the growing polymer chain so different. It is possible that additional methyl groups make the polymer chain more hydrophobic, which has a significant effect on phase separation during polymerization and, consequently, pore formation. Therefore, alcohols with long alkyl chains are preferred as porogenic solvents. Of course, this statement is not completely correct because the reactivity of methacrylate and acrylate monomers is also different. I noticed that the lowest pressure drop was obtained with HEMA/EDMA (column K in Table 2.1). One of the possible reasons is that there are unreacted monomers in HEA/EDMA and HEMA/PEGDA mixtures, and these unreacted monomers make good solvents for the polymers, serving as microporogens.

2.3.3 Effect of Crosslinker Concentration on the Elution of Protein Standards

In a one-step in situ monolith synthesis protocol, the functional group is usually provided by the monomer and not the crosslinker. Varying the monomer concentration is a simple method to adjust the density of the functional group. In order to investigate the influence of HEA concentration on monolithic column properties, three columns were made

with mixtures containing 0.72:1, 1:1 or 1.37:1 HEA/PEGDA, identified as columns A, B and C, respectively, in Table 2.1. Protein standards were separated using each column, and their chromatograms are shown in Figure 2.3. In HIC, the primary effect of increasing the ligand density is enhanced protein retention. At first glance, it is interesting to see that with an increase in HEA concentration, the retention times of proteins were not increased; instead, they were eluted in shorter times. This turns out to be reasonable since the hydroxyethyl group provided by HEA is among the weakest hydrophobic ligands used for HIC. In fact, it is so weakly hydrophobic that it is relatively hydrophilic compared to PEGDA, which makes PEGDA not only a crosslinker, but also a functional monomer at the same time. Keeping the total monomers constant and decreasing the HEA content produced the same result as increasing the PEGDA concentration and, subsequently, the ligand density. Enhanced protein retention may have been caused by free ends of the PEGDA or by a more exposed backbone for interaction with the proteins. This observation encouraged me to prepare a poly(PEGDA) monolith for application in HIC. Figure 2.3D shows a separation using a monolithic column based solely on PEGDA. Protein standards had longer retention times and were eluted in sharper peaks compared to their separation in HEA/PEGDA monoliths.

Figure 2.3 reveals that cytochrome *c* has no retention on all three HEA/PEGDA columns. Because the 200 nL injection volume together with the system dead volume produced a long injection band, the eluted cytochrome *c* peak was flat rather than approximately Gaussian in shape. Furthermore, with 0.44 g HEA, the column was no longer hydrophobic enough to retain myoglobin under 3.0 M initial $(NH_4)_2SO_4$ concentration, and a distorted peak was observed. A small peak between cytochrome *c* and

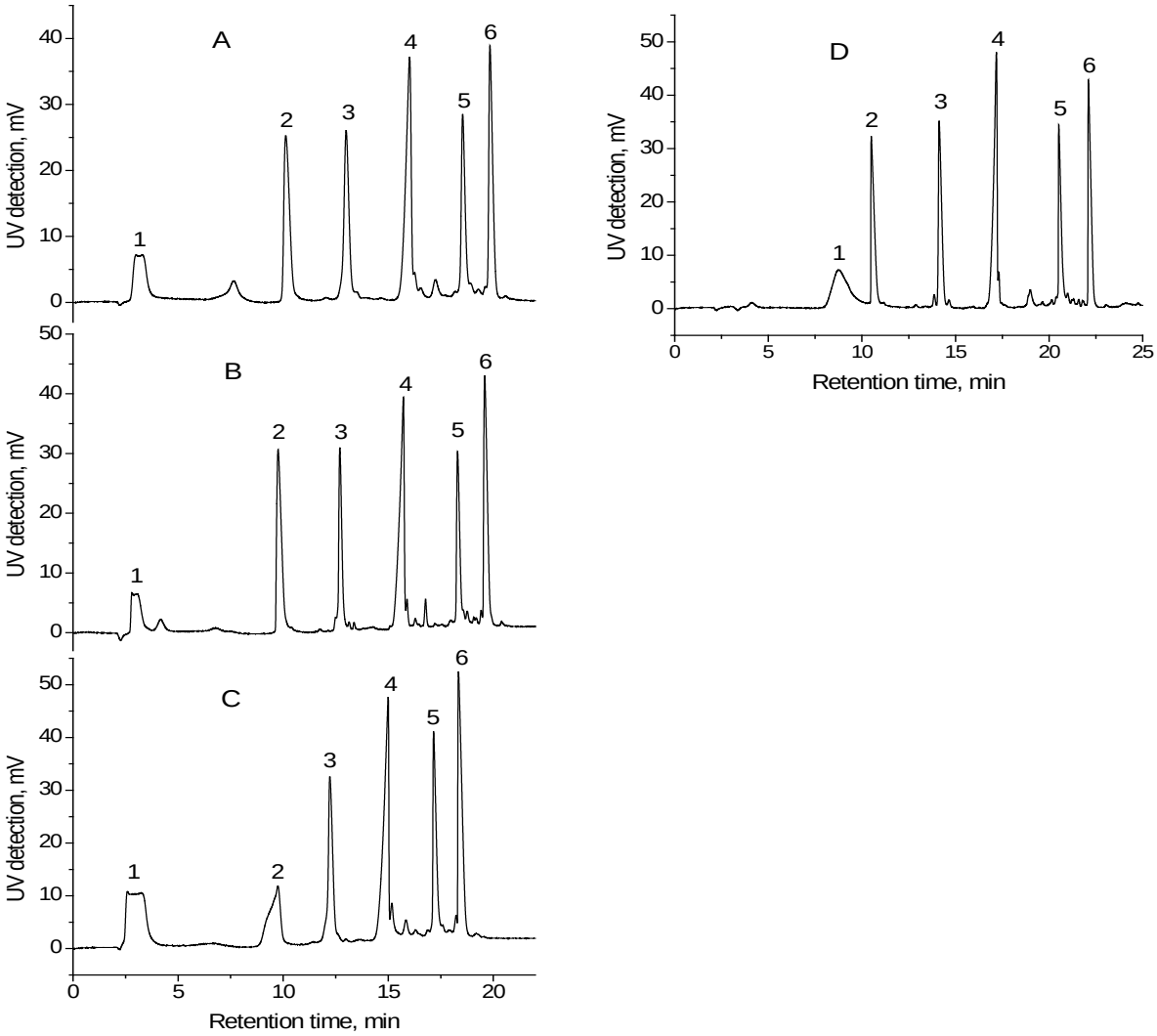

Figure 2.3. HIC of protein standards using monolithic columns prepared from varying amounts of cosslinker. Monolith composition: (A) as A in Table 2.1, (B) as B in Table 2.1, (C) as C in Table 2.1, (D) poly(PEGDA) monolith. Conditions: 16 cm × 75 μm i.d. monolithic columns; buffer A was buffer B plus 3.0 M $(NH_4)_2SO_4$, and buffer B was 0.1 M Na_2HPO_4 (pH 6.90); 1-min isocratic elution with 100% A, followed by a linear A-B gradient from 0% to 100% B in 20 min, and then isocratic elution with 100% B; 0.3 μL/min flow rate; on-column UV detection at 214 nm. Peak identifications: (1) cytochrome *c*, (2) myoglobin, (3) ribonuclease A, (4) lysozyme, (5) α-chymotrypsin and (6) α-chymotrypsinogen A.

myoglobin was periodically observed, which most probably originated from degradation of protein samples, such as oxidation/reduction of cytochrome *c*.

The reason why these three polymerization solutions were chosen to prepare columns is because they yielded monoliths with similar back pressures. I already pointed out that the addition of HEA increased the polarity of the HEA/PEGDA copolymer. The use of methanol in the porogen mixture led to a greater percentage of micropores when the HEA concentration was higher, and vice versa. At the same time, an increase or decrease in crosslinker to monomer ratio raised or reduced the pressure drop. Although an 8:8 wt ratio of methanol/ethyl ether yielded a monolith with much higher backpressure than a 6:10 wt ratio when the wt ratio of HEA to PEGDA was 1:1, it produced a column with similar flow resistance when the wt ratio of HEA to PEGDA was 1:1.37 because of the decrease in HEA. When the HEA to PEGDA ratio was increased to 1.37:1, the effect of methanol was mitigated by the decrease in crosslinker. Therefore, these three columns exhibited a similar pressure drop. Despite this, column B showed the best performance. SEM images of the three columns indicate that column B was more uniform than the other two. The binding capacity is another important property, which is discussed later.

2.3.4 Effect of Elution Gradient on the Elution of Protein Standards

The effect of gradient rate on protein retention and resolution were examined using column B. As shown in Figure 2.4, for all gradient rates, the proteins were eluted as sharp peaks, indicating that there was little non-specific protein adsorption when using this HEA/PEGDA monolith. The performance was comparable or superior to the performance of HIC packed columns.[3,5,6,19,30] Essentially, baseline separation was achieved even with a short gradient time of 5 min. In this case, the gradient volume corresponded to only 2.1

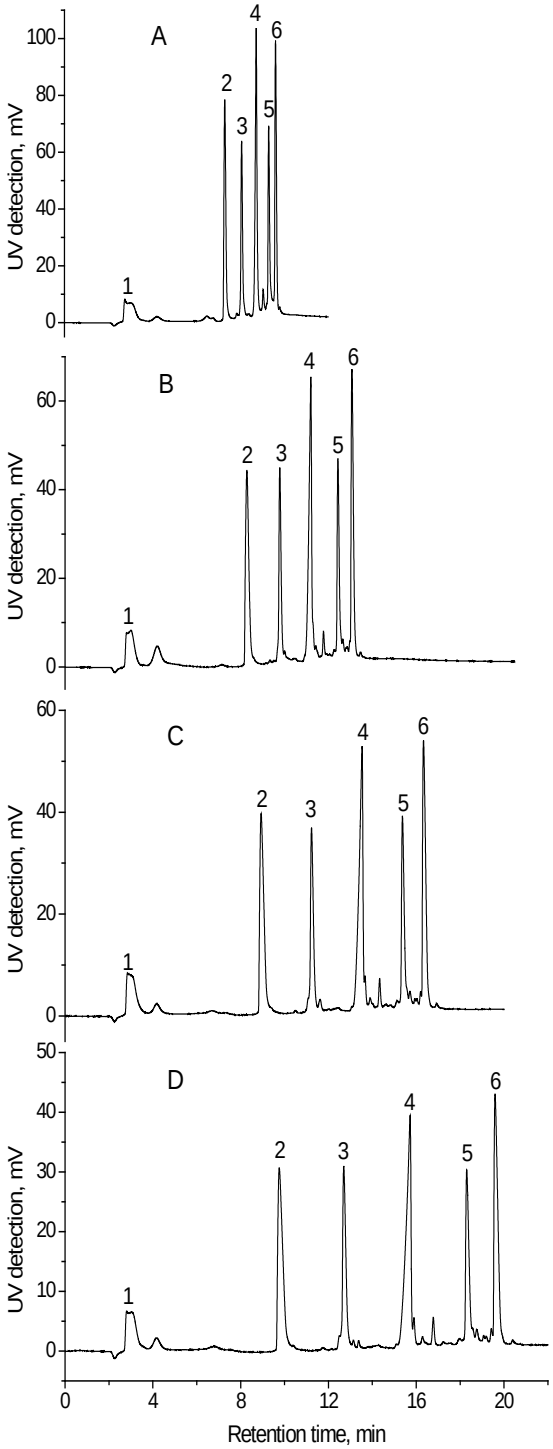

Figure 2.4. HIC of protein standards with different gradient rates of (A) 5 min, (B) 10 min, (C) 15 min, and (D) 20 min. Other conditions are the same as in Figure 2.3B.

column volumes, while the 10, 15, and 20 min gradients represented 4.2, 6.4 and 8.5 column volumes, respectively. Resolution values for ribonuclease A and lysozyme, and α-chymotrypsin and α-chymotrypsinogen A were calculated for each gradient rate and listed in Table 2.2. Peak capacities were calculated by dividing the gradient time by the average peak width of peaks 2 to 6.[31] The peak widths were obtained directly from integration using Chrom Perfect software. The results indicated that the shallower gradients afforded better resolution and higher peak capacity, with the greatest improvement arising from increasing the gradient time from 5 min to 10 min. As the gradient became more shallow, the degree of improvement became smaller.

The run-to-run reproducibility of the poly(HEA-*co*-PEGDA) column was quite good. For four runs carried out on separate days using conditions as in Figure 2.4D, the relative standard deviations (RSD) of the retention times of proteins 2 to 6 were 0.73, 0.77, 0.67, 0.25, and 0.17%, respectively. These data not only demonstrate good reproducibility, but they also indicate the stability of the monolithic column. Re-equilibration of the column was readily achieved with starting buffer; approximately 2 column volumes for approximately 6 min were sufficient. Column-to-column reproducibility was also measured, and RSD values (n = 3) of retention times for proteins 2 to 6 were 2.0, 0.87, 0.74, 0.88, and 1.1%, respectively.

2.3.5 Effect of Initial Salt Concentration on the Retention of Protein Standards

In HIC, selectivity and resolution can be modified by adjusting stationary phase variables such as ligand type or ligand density and/or by adjusting mobile-phase variables such as salt type and salt concentration. $(NH_4)_2SO_4$ has been the most commonly used salt for HIC because of its high solubility (4 M at 25 ^oC), lack of significant ultraviolet

Table 2.2. Resolution Values and Peak Capacities for Protein Standards Separated Using Different Gradient Times.

	gradient time (min)			
	5	10	15	20
resolution[a]	1.98	3.17	4.02	3.98
resolution[b]	3.99	6.11	7.38	8.21
peak capacity[c]	30	42	48	54

[a] Resolution of peaks 5 and 6, α-chymotrypsin and α-chymotrypsinogen A. [b] Resolution of peaks 3 and 4, ribonuclease A and lysozyme. [c] Peak capacity = time of gradient/average peak width.

absorbance or specific-ion effects, and moderate molal surface tension increment which plays a major role in HIC.[32] Thus, $(NH_4)_2SO_4$ was used for all chromatographic testing in this work. We investigated the effect of different initial $(NH_4)_2SO_4$ concentrations on retention of proteins. Chromatograms from initial salt concentrations of 2.8, 2.5 and 2.0 M are shown in Figure 2.5. Comparing the three elution patterns together with Figure 2.4D, we observed that the initial $(NH_4)_2SO_4$ concentration had a significant effect on the retention of proteins. Decreasing the concentration had a greater influence on retention of proteins with low hydrophobicity compared to proteins with high hydrophobicity. When the initial salt concentration was 2.8 M, it was not high enough to retain myoglobin, and severe fronting was observed. When the concentration was decreased to 2.0 M, myoglobin and ribonuclease A were both eluted unretained together with cytochrome *c*, and lysozyme began to show fronting.

Sample is typically dissolved in the initial buffer for injection in HIC. For the poly(HEA-*co*-PEGDA) monolithic column, 3.0 M initial $(NH_4)_2SO_4$ concentration was required to achieve effective separation. This high concentration tended to promote protein precipitation or denaturation. During the experiments, I observed that the six proteins dissolved in 3.0 M $(NH_4)_2SO_4$ precipitated or denatured to different degrees after 12 h when kept at room temperature, and a major peak just after the dead time (eluting at approximately 4.0 min) appeared. α-Chymotrypsin and α-chymotrypsinogen A were little affected, however.

2.3.6 Dynamic Binding Capacity (DBC) and Mass Recovery

Breakthrough curves in frontal chromatography provide valuable information with respect to the DBC of the separation medium. This is a very important characteristic for

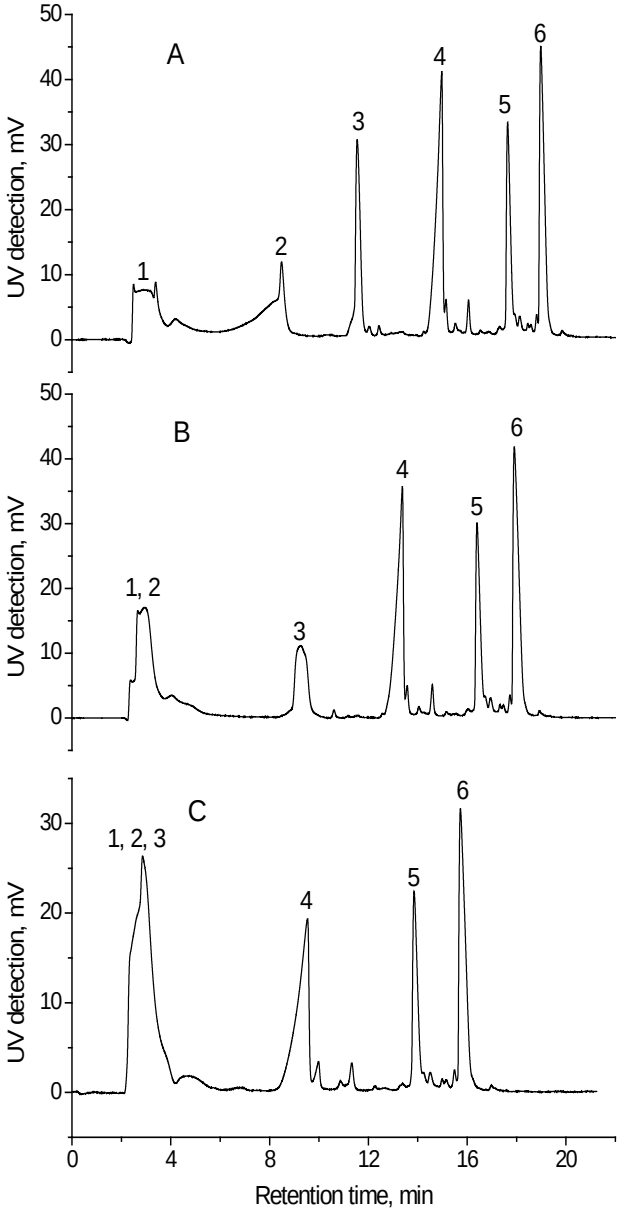

Figure 2.5. HIC of protein standards using different initial $(NH_4)_2SO_4$ concentrations of (A) 2.8 M, (B) 2.5 M, and (C) 2.0 M. Other conditions are the same as in Figure 2.3B.

large-scale separation. Figure 2.6 shows breakthrough curves for columns A and B monitored for lysozyme at a flow rate of 0.3 μL/min. Both curves are characterized by a sharp increase in baseline, indicating excellent mass transfer efficiency. The dynamic binding capacities for columns A and B were calculated to be 5.87 and 7.70 mg/mL of column volume, respectively. It should be mentioned that these capacities were obtained with 2.0 M $(NH_4)_2SO_4$. Figure 2.5D indicates that 2.0 M $(NH_4)_2SO_4$ was just high enough to retain lysozyme. If 3.0 M $(NH_4)_2SO_4$ was used to measure the capacity, the values would be much higher. To ensure the accuracy of the measurements and to avoid any precipitation or denaturation of the proteins, a lower salt concentration of 2.0 M $(NH_4)_2SO_4$ was used to obtain a conservative estimate of the high capacity of this poly(HEA-*co*-PEGDA) monolithic column.

Figure 2.3 already revealed that proteins have greater retention on column A composed of 0.44 g PEGDA and 0.32 g HEA than on column B composed of 0.38 g PEGDA and 0.38 g HEA. This is also reflected in the breakthrough curves in Figure 2.6. By comparing curves A and B, a gradual increase in baseline before the steep increase for curve B was observed, indicating that column B was less hydrophobic than column A. This led to early elution of lysozyme, which was manifested by fronting of the lysozyme peak as shown in Figure 2.5C. Since structural effects of the monolith would also contribute to the gradual increase in baseline, I also measured the breakthrough curves for α-chymotrypsinogen A dissolved in 2.0 M $(NH_4)_2SO_4$. A gradual increase before the steep increase was not observed for α-chymotrypsinogen A, indicating that lower hydrophobicity of column B was the main reason. Although column B was less hydrophobic, it provided a higher DBC than column A because of better homogeneity and larger surface area.

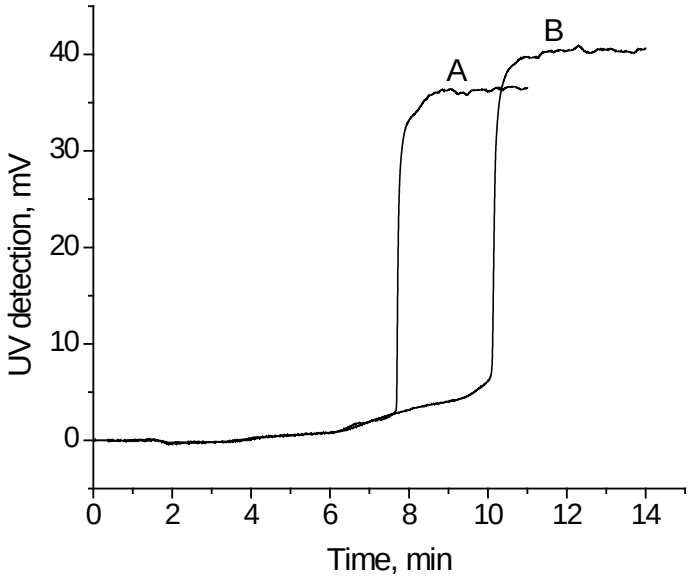

Figure 2.6. Breakthrough curves obtained by frontal analysis. Conditions: 4.5 cm × 75 µm i.d. monolithic column; curves A and B represent monoliths A and B in Table 2.1; sample: 0.5 mg/mL lysozyme dissolved in 67% buffer A/33% buffer B; 0.3 µL/min flow rate; UV detection at 214 nm.

To further evaluate the protein adsorption properties of the HEA/PEGDA monolith,a protein recovery experiment was performed as described in section 2.3.6. The recoveries of myoglobin, ribonuclease A, lysozyme, α-chymotrypsin and α-chymotrypsinogen A were 100%, 101%, 97%, 97% and 96%, repectively. The RSDs for recoveries of these five proteins from three parallel tests were 2.7%, 1.1%, 2.3%, 5.6% and 6.7%, respectively. These results showed that proteins were almost completely recovered from the poly(HEA-*co*-PEGDA) monolithic column.

2.3.7 Stability of the Poly(HEA-*co*-PEGDA) Monolithic Column

Permeability is a good index to reflect swelling or shrinking of the monolith. If a monolith swells, its throughpores will decrease in size, resulting in lower permeability, and vice versa. The permeability of the poly(HEA-*co*-PEGDA) monolithic column was determined by pumping acetonitrile, methanol, water, buffer B and buffer A through the column at different flow rates. As shown in Figure 2.7, linear relationships between back pressure and flow rate for all five solvents were observed, which clearly demonstrated that the monolith was mechanically stable. Moreover, the column back pressure was observed to reach a constant value at 1.0 μL/min flow rate using water, which corresponds to a linear flow rate of 31.4 cm/min. The porosity of this poly(HEA-*co*-PEGDA) monolithic column was roughly estimated to be 72% using inverse size-exclusion chromatography.

The permeability values for the poly(HEA-*co*-PEGDA) monolithic column were calculated from Darcy's law[33] and listed in Table 2.3. The results were similar when water, methanol or acetonitrile were passed through the column. This indicates that the monolith was quite stable, and shrank or swelled very little in different polarity solvents. The permeabilities in buffers A and B were both higher than in water. An obvious increase was

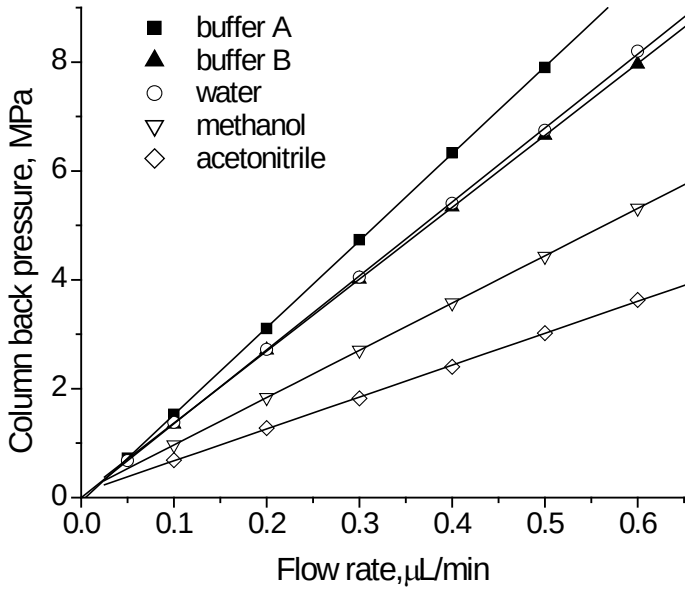

Figure 2.7. Effect of mobile phase flow rate on column back pressure. Buffers A and B are the same as in Figure 2.3. Conditions: 10 cm × 75 μm i.d. monolithic column; monolith composition as in Figure 2.3B.

observed with buffer A which contained 3.0 M $(NH_4)_2SO_4$. This salt-dependent permeability was also observed in previous work from Lee's group.[22] Although the monolith shrank a little in buffer A, it could be regenerated in less than 10 min at 0.3 μL/min flow rate. The polymer monolith remained stable over a period of one and a half months of investigation. Over 200 injections were carried out during this period.

2.4 Conclusions

Poly(HEA-*co*-PEGDA) monolithic columns for HIC were prepared by one-step in situ polymerization in capillary columns for using methanol and ethyl ether as porogens. It was interesting to find that the PEGDA crosslinker provided moderately hydrophobic sites to interact with proteins. An optimized monolithic column was used for HIC of proteins, and six proteins were separated within 20 min with high resolution using a 20 min elution gradient, resulting in a peak capacity of 54. Chromatographic performance measurements such as resolution, peak capacity and mass recovery were found to be comparable or superior to commercial packed columns. Mass recovery was found to be greater than 96%, indicating the biocompatibility of this monolith. Due to their easy preparation, good stability, and high reproducibility, poly(HEA-*co*-PEGDA) monolithic columns showed promise for applications such as protein purification and separation, and monitoring of protein denaturation.

A strategy for porogen selection for the synthesis of monoliths was found by systematic investigation of the copolymerization between HEMA, HEA, PEGDA and EDMA. A single methyl group made a large difference in the properties of the copolymers, for example between HEA/PEGDA and HEMA/PEGDA. Porogens suitable for formation of HEA/PEGDA monoliths were not effective for HEMA/PEGDA. Although an

Table 2.3. Permeabilities of the Poly(HEA-*co*-PEGDA) Monolithic Column for Different Mobile Phases.

mobile phase	relative polarity[a]	viscosity, η (mPa s)[b]	permeability, k ($\times 10^{-14}$m^2)[c]
buffer A	/	1.906	6.25
buffer B	/	0.935	3.71
water	1.000	0.890	3.43
methanol	0.762	0.544	3.28
acetonitrile	0.460	0.369	3.30

[a] Relative polarity data were from ref. 22. [b] Viscosity data were from online *CRC Handbook of Chemistry and Physics*. 89th ed.; CRC: Boca Raton, 2008-2009. [c] Peameability $k = \eta L u / \Delta p$, where η is the viscosity, L is the column length (10 cm in this case), u is the solvent linear velocity, and Δp is the column back pressure. The values for $u / \Delta p$ are based on Figure 2.7.

interrelation between the thermodynamic quality of the porogen and the pore formation process was already established for thermally initiated monoliths,[34,35] to date, the practical selection of porogen system still largely depends on experience and trial and error.

In this work, 3.0 M $(NH_4)_2SO_4$ was required to promote hydrophobic interaction due to the hydrophilic character of the HEA/PEGDA monolith. Future work should focus on improvement of ligand hydrophobicity and density. During this research, I found that monoliths synthesized from PEGDA also showed excellent performance in HIC of proteins. Poly(PEGDA) monoliths and their comparison with PEG-based dimethacrylate monoliths are described in Chapter 3.

2.5 References

1. Porath, J.; Sundberg, L.; Fornstedt, N.; Olsson, I. *Nature* **1973**, *245*, 465-466.
2. Hjertén, S. *J. Chromatogr. A* **1973**, *87*, 325-331.
3. Eriksson, K.O. In *Protein Purification: Principles, High Resolution Methods, and Application*; Janson, J. C.; Rydén, L.; VCH Publ., New York, **1989**, pp 207-226.
4. Queiroz, J. A.; Tomaz, C. T.; Cabral, J. M. S. *J. Biotech.* **2001**, *87*, 143-159.
5. Fexby, S.; Ihre, H.; Bülow, L.; Alstine, J. M. V. *J. Chromatogr. A* **2007**, *1161*, 234-241.
6. Gong, B.; Wang, L.; Wang, C.; Geng, X. *J. Chromatogr. A* **2004**, *1022*, 33-39.
7. Hjertén, S.; Liao, J.-L., Zhang, R. *J. Chromatogr. A* **1989**, *473*, 273-275.
8. Liao, J.-L.; Zhang, R.; Hjertén, S. *J. Chromatogr. A* **1991**, *586*, 21-26.
9. Svec, F.; Frechet, J. M. J. *Anal.Chem.* **1992**, *64*, 820-822.
10. Svec, F. *J. Sep. Sci.* **2004**, *27*, 747-766.
11. Svec, F. *J. Sep. Sci.* **2004**, *27*, 1419–1430.
12. Vlakh, E. G.; Tennikova, T. B. *J. Sep. Sci.* **2007**, *30*, 2801-2813.
13. Urban, J.; Jandera, P. *J. Sep. Sci.* **2008**, *31*, 2521-2540.
14. Vlakh, E. G.; Tennikova, T. B. *J. Chromatogr. A* **2009**, *1216*, 2637-2650.
15. Zhang, R.; Yang, G.; Xin, P.; Qi, L.; Chen, Y. *J. Chromatogr. A* **2009**, *1216*, 2404-2411.
16. Hemström, P.; Nordborg, A.; Irgum, K.; Svec, F.; Fréchet, J. M. J. *J. Sep. Sci.* 2**006**, *29*, 25-32.
17. Zeng, C.-M.; Liao, J.-L.; Nakazato, K.; Hjertén, S. *J. Chromatogr. A* **1996**, *753*, 227-234.

18. Xie, S.; Svec, F.; Fréchet, J. M. J. *J. Chromatogr. A* **1997**, *775*, 65-72.
19. Alpert, A. J. *J. Chromatogr. A* **1986**, *359*, 85-97.
20. Gu, B.; Armenta, J. M.; Lee, M. L. *J. Chromatogr. A* **2005**, *1079*, 382-391.
21. Li, Y.; Tolley, H. D.; Lee, M. L. *Anal. Chem.* **2009**, *81*, 4406–4413.
22. Gu, B.; Chen, Z.; Thulin, C. D.; Lee, M. L. *Anal. Chem.* **2006,** *78*, 3509-3518.
23. Gu, B.; Li, Y.; Lee, M. L. *Anal. Chem.* **2007**, *79*, 5848-5855.
24. Chen, X.; Tolley, H. D.; Lee, M. L. *J. Sep. Sci.* **2009**, *32*, 2565-2573.
25. Li, Y.; Gu, B.; Tolley, H. D.; Lee, M. L. *J. Chromatogr. A* **2009**, *1216*, 5525-5532.
26. Beiler, B.; Vincze, Á.; Svec, F.; Sáfrány, Á. *Polymer* **2007**, *48*, 3033-3040.
27. Clarke, N. J.; Tomlinson, A. J.; Schomburg, G.; Naylor, S. *Anal. Chem.* **1997**, *69*, 2786–2792.
28. Yang, Y.-B.; Harrison, K.; Kindsvater, J. *J. Chromatogr. A* **1996**, *723*, 1-10.
29. Yu, C.; Xu, M.; Svec, F.; Fréchet, J. M. J. *J. Polym. Sci., Part A: Poly. Chem.* **2002**, *40*, 755-769.
30. To, B. C. S.; Lenhoff, A. M. *J. Chromatogr. A* **2008**, *1205*, 46-59.
31. Neue, U. D. *J. Chromatogr. A* **2005**, *1079*, 153-161.
32. Melander, W. R.; Corradini, D.; Horváth, C. *J. Chromatogr. A* **1984**, *317*, 67-85.
33. Gusev, I.; Huang, X.; Horváth, C. *J. Chromatogr. A* **1999**, *855*, 273-290.
34. Viklund, C.; Svec, F.; Fréchet, J. M. J.; Irgum, K. *Chem. Mater.* **1996**, *8*, 744-750.
35. Svec, F.; Fréchet, J. M. J. *Chem. Mater.* **1995**, *7*, 707-715.

CHAPTER 3 MONOLITHS FROM POLY(ETHYLENE GLYCOL) DIACRYLATE AND DIMETHACRYLATE FOR CAPILLARY HYDROPHOBIC INTERACTION CHROMATOGRAPHY OF PROTEINS*

3.1 Introduction

Monolithic columns for LC were introduced approximately two decades ago and have been applied in most of the LC separation modes. Organic polymer monoliths were first introduced by Hjertén et al.[1] and Svec et al.[2,3] in the beginning of the 1990s, and are now represented by abundant chemistries and preparation methods. In a monolithic column, the microglobular skeleton is interconnected to form a continuous porous stationary phase that is absent of structural void volumes that are sometimes present in packed columns. Furthermore, mass transfer resistance in and out of the stationary phase support is less in monolithic stationary phases compared to packed columns because the diameters of the microglobules are typically less than for spherical particles, and there are more pores through which the mobile phase can flow. Mass transfer is facilitated by convection, which reduces the time required for mass transfer between the mobile and stationary phases. This difference in hydrodynamics allows high permeability and fast mass transfer. In spite of the favorable properties of monoliths, there is still work that must be done to improve their performance. One of the major concerns is column-to-column reproducibility,[4] which is more difficult to achieve with monolithic columns compared to packed columns because preparation of the stationary phase and "packing" of the column occur at the same time. The precise precursor solution composition and polymerization conditions greatly influence the resulting monolith.

* This chapter was largely taken from: Li, Y.; Tolley, H. D.; Lee, M. L. *J. Chromatogr. A* **2010**, *1217*, 4934-4945.

The desired monolithic stationary phase selectivity can be incorporated through direct polymerization of functionalized monomers or through surface modification of pre-formed monolithic matrices. Since there is initially only one phase in the polymerization solution, the range of monomers that can be used is much broader than for classical suspension polymerization. However, one disadvantage of direct polymerization is that optimized polymerization conditions for one system cannot be transferred directly to another, and further experimentation is needed to re-optimize the polymerization. Despite this inconvenience, direct polymerization of monomers provides the simplest and most convenient approach for preparation of functionalized monoliths. For example, Gu et al. designed and synthesized a series of monoliths for strong cation exchange chromatography of peptides and proteins by direct copolymerization of different sulfonic acid-functionalized monomers and a crosslinker, PEGDA (M_n = 258).[5-7]

One of the most widely used functional group types for post modification of the monolith surface is the epoxy group as in glycidyl methacrylate.[8] For example, poly(GMA-*co*-EDMA) monoliths are easily post-modified.[3,9-11] Surface modification enables independent optimization of the synthesis of the monolith and its surface chemistry. Thus, it is possible to prepare a variety of functionalized monoliths from a single "universal" monolith. However, surface modification also has its limitations. For example, the monolith network must be stable (i.e., no excessive shrinking or swelling, and no detachment from the column wall) during modification, even if harsh conditions such as high temperature and non-polar solvents are used. If photografting is performed, UV transparent molds are required, and one dimension of the monolith must be shallow enough for effective initiation.

Regardless of which method is used to obtain the desired surface functionality, a monomer is required either to provide the functional groups directly or to provide reactive sites for subsequent modification. In conventional monolith design, the desired group is provided by the monomer, and the crosslinker usually serves to ensure rigidity. A nontraditional approach to synthesize monoliths involves the use of only a crosslinker as monomer, i.e., a single-monomer system. Monolithic materials synthesized solely from crosslinkers have been reported for diacrylate,[12,13] dimethacrylate,[13] divinylbenzene,[14,15] N,N-methylenebis(acrylamide),[16] 1,2-bis(p-vinylphenyl)ethane,[17,18] and tetrakis(4-vinylbenzyl)silane.[19,20] Although chemistries for single-monomer systems are not as rich as those for two- or three-monomer systems, optimization of the monolith polymerization is much easier, and reproducibility of column preparation increases. Furthermore, the monoliths are more rigid due to their highly crosslinked structures. It has also been reported that a higher crosslinker concentration produces monoliths with greater surface areas.[21,22] A recently reported hypercrosslinked monolithic poly(styrene-co-vinylbenzyl chloride-co-divinylbenzene) capillary column exhibited a surface area of 663 m^2/g.[23]

In this work, I describe monoliths prepared solely from PEGDA or PEGDMA monomers containing different lengths of ethylene glycol chains. The monoliths were designed for HIC of proteins, with the linked alkyl end-groups providing hydrophobic interaction sites and the PEG groups providing a mildly hydrophilic matrix. Porous polymer monoliths prepared from PEGDA-based crosslinking monomers have been previously reported using water or aqueous PEG solutions as porogenic solvents, and their hydrophilicities were evaluated by measuring the contact angle of water.[13] However, no chromatographic results were reported. Another study of monoliths prepared from a

PEGDA oligomer (Mn = 700 g/mol) reported the use of ethanol and poly(propylene oxide).[12] Scanning electron micrographs indicated that the pores were more representative of enclosed pores than through-pores.

3.2 Experimental

3.2.1 Chemicals and Reagents

DMPA (99%), TPM (98%), PEGDA (M_n = 258, 302, 575, and 700), and PEGDMA (M_n = 286, 330, and 550) were purchased from Sigma-Aldrich (St Louis, MO, USA). Protein standards used for HIC (cytochrome *c* from bovine heart, myoglobin from equine skeletal muscle, ribonuclease A, type I-A, from bovine pancreas, lysozyme from chicken egg white, α-chymotrypsin, type II, from bovine pancreas, and α-chymotrypsinogen A, type II, from bovine pancreas) and two types of trypsin inhibitors [Type I-S from glycine max (soybean), product No. T9003, lot 128K7253; and trypsin inhibitor from glycine max (soybean), product No. T6522, lot 106K7034] were purchased from Sigma-Aldrich. Proteins and peptides used for SEC (thyroglobulin from porcine thyroid gland, trypsin inhibitor from glycine max, angiotensin I human acetate salt hydrate, and leucine enkephalin acetate salt hydrate) were also purchased from Sigma-Aldrich. All porogenic solvents and chemicals for use in mobile phase buffer preparation were HPLC or analytical reagent grade. Buffer solutions were prepared with HPLC water and filtered through a 0.22-μm membrane filter.

3.2.2 Polymer Monolith Preparation

Before filling with the precursor solution, UV-transparent fused-silica capillary tubing (75-μm and 250-μm i.d., 375-μm o.d., Polymicro Technologies, Phoenix, AZ) was

treated with TPM according to a procedure previously described in order to covalently attach the polymer to the capillary wall.[6] The two ends of the capillary were sealed with rubber septa until further use. Monomer solutions were prepared in 1-dram (4 mL) glass vials by admixing initiator (DMPA), monomer (PEGDA or PEGDMA), and porogen solvents (methanol/ethyl ether or cyclohexanol/decanol) (see Tables 3.1 and 3.2 for reagent compositions). The solution was vortexed and then degassed by sonicating for 5 min if cyclohexanol/decanol was used as porogen. If methanol/ethyl ether was used, the solution was vortexed only to avoid excessive evaporation of the volatile porogens. A section of the silanized capillary was cut and filled with the precursor solution using helium gas pressure. One end of the capillary was left empty to form a detection window when cyclohexanol/decanol was used as porogens, or masked using black tape if methanol/ethyl ether was used. After filling with the solution, the capillary was sealed with rubber septa at both ends and was placed directly under a PRX 1000-20 Exposure Unit UV lamp (TAMARACK Scientific, Corona, CA) for 3.5 min. Polymerization at lower temperature (~ 0 ^{o}C) was achieved by placing the capillary on a copper plate which was freeze-mounted on ice in advance. After the monolithic column was prepared, it was then flushed with methanol and water sequentially using an HPLC pump to remove porogens and unreacted monomers. Monolithic columns were characterized by SEM (FEI Philips XL30 ESEM FEG, Hillsboro, OR) without coating with a conducting gold layer.

3.2.3 Capillary Liquid Chromatography (CLC)

The CLC system was described in Chapter 2. Briefly, an UltiMate 3000 high pressure gradient LC system (Dionex, Sunnyvale, CA) equipped with an FLM-3300 nano

Table 3.1. Compositions and Performance Measurements for Poly(PEGDA$_{258}$) Monoliths.

	composition[a]			retention time (min) / peak width at half-height (min)[d]			
monolith	methanol (g / wt.%)[b]	ethyl ether (g / wt.%)	back pressure, (MPa)[c]	myoglobin	ribonuclease A	lysozyme	peak capacity[e]
1	1.60 / 67.8	0 / 0	7.47	12.62±0.03 / 0.140±0.004	15.56±0.04 / 0.161±0.004	17.52±0.05 / 0.187±0.003	54
2	1.40 / 59.3	0.20 / 8.47	7.09	12.65±0.01 / 0.188±0.003	15.60±0.06 / 0.230±0.002	17.53±0.05 / 0.231±0.001	40
3	1.20 / 50.8	0.40 / 16.9	6.14	12.47±0.04 / 0.187±0.004	15.39±0.04 / 0.221±0.004	17.45±0.07 / 0.234±0.001	41
4	1.00 / 42.4	0.60 / 25.4	4.34	12.59±0.18 / 0.135±0.004	15.40±0.14 / 0.155±0.004	17.36±0.13 / 0.179±0.006	56
5	0.80 / 33.9	0.80 / 33.9	3.42	12.41±0.10 / 0.188±0.014	15.38±0.04 / 0.196±0.008	17.43±0.01/ 0.199±0.004	45
6-1	0.60 / 25.4	1.00 / 42.4	3.12	12.53±0.06 / 0.169±0.010	15.41±0.05 / 0.178±0.007	17.49±0.04 / 0.182±0.003	50
6-2	0.60 / 25.4	1.00 / 42.4	1.50	12.63±0.13 / 0.160±0.004	15.59±0.04 / 0.181±0.006	17.65±0.07 / 0.189±0.008	49
7	0.40 / 16.9	1.20 / 50.8	3.32	12.75±0.06 / 0.204±0.017	15.45±0.05 / 0.186±0.003	17.53±0.01 / 0.210±0.005	44
8	0 / 0	1.60 / 67.8	4.85	12.84±0.06 / 0.186±0.020	15.65±0.04 / 0.162±0.009	17.63±0.06 / 0.162±0.009	51

[a] All monoliths contained 0.0076 g DMPA and 0.76 g PEGDA 258, and were exposed to UV light for 3.5 min; 6-2 was polymerized at room temperature, and all others at approximately 0 ^{O}C. [b] wt.% related to total polymerization mixture. [c] 16 cm × 75 µm i.d. column with water at 0.2 µL/min flow rate. Data are average of measurements from two or three columns, RSD was within 10%, and in most case, less than 6.0%. [d] Proteins were eluted with 1 min isocratic elution with 100% A, followed by a 15 min linear gradient from A to B, at 0.2 µL/min flow rate. Data were based on three measurements. [e] Peak capacity = time of gradient/average peak width.

Table 3.2. Compositions of the Monolithic Columns.

monolith	composition[a]					polymerization condition[c]
	monomer (g / wt.%)[b]	methanol (g / wt.%)	ethyl ether (g / wt.%)	cyclohexanol (g / wt.%)	decanol (g / wt.%)	
PEGDA 302	0.76 / 32.2	1.60 / 67.8	/	/	/	UV 3.5 min on ice
PEGDA 575	0.76 / 32.2	0.20 / 8.47	1.40 / 59.3	/	/	UV 3.5 min on ice
PEGDA 700	0.76 / 25.7	/	2.20 / 74.3	/	/	UV 3.5 min at RT
PEGDMA 286	0.76 / 20.2	/	/	1.90 / 50.5	1.10 / 29.3	UV 3.5 min at RT
PEGDMA 330	0.76 / 32.2	/	/	1.60 / 67.8	/	UV 3.5 min at RT
PEGDMA 550	0.76 / 32.2	/	/	0.80 / 33.9	0.80 / 33.9	UV 3.5 min at RT

[a] All monoliths contained 0.0076 g DMPA. [b] wt.% related to total polymerization mixture. [c] "At RT" means monoliths were prepared at room temperature, and "on ice" means the capillaries were placed on ice during polymerization.

flow manager (1:1000 split ratio) was used in all experiments. The system was operated with Chromeleon software. A 10.2-cm long 50-μm i.d. poly(vinyl alcohol)-coated capillary was used as sample loop, and the loop volume was calculated to be 200 nL. The two mobile phase components for gradient elution of proteins in HIC were 0.1 M phosphate buffer (i.e., 1.5:1 v/v 0.1 M Na_2HPO_4/0.1 M NaH_2PO_4, pH 6.9 (buffer B), and 3.0 M ammonium sulfate in buffer B (buffer A). The mobile phase used for SEC was 20 mM phosphate buffer (i.e., 1.5:1 v/v 20 mM Na_2HPO_4/20 mM NaH_2PO_4, pH 6.9) plus 0.15 M sodium chloride. On-column detection was performed using a Crystal 100 variable wavelength UV–vis absorbance detector and Chrom Perfect software (Mountain View, CA) for data collection and treatment. UV absorbance was monitored at 214 nm.

A mixture of protein standards containing 0.2 mg/mL each of cytochrome *c*, myoglobin, ribonuclease A, lysozyme, α-chymotrypsin and α-chymotrypsinogen A was prepared in the initial buffer for HIC. For Figure 3.4, α-chymotrypsin was activated from 0.4 mg/mL α-chymotrypsinogen A; therefore, to distinguish it from α-chymotrypsin standard, it is referred to as neo-chymotrypsin. The concentration of the two trypsin inhibitors in Figure 3.5 were 0.5 mg/mL dissolved in the initial buffer. A compound mixture containing 0.5 mg/mL each of thyroglobulin and trypsin inhibitor, 0.25 mg/mL each of angiotensin I and leucine enkephalin, and 0.10 mg/mL of thiourea was prepared in the mobile phase for SEC. The chromatographic conditions are given in the figure captions. Chromatograms were transferred to an Excel file and redrawn using Microcal Origin (Northampton, MA). Baseline drift caused by the salt gradient was subtracted from all chromatograms.

3.2.4 Dynamic Binding Capacity (DBC), Mass Recovery and Permeability

The DBC of monolithic column 6-2 in Table 3.1 and columns in Table 3.2 was measured following a procedure described in Chapter 2. Specifically, measurements were carried out with a 6-cm long monolithic column at flow rates of 0.1 or 0.3 μL/min. The monolithic column was equilibrated with 67% buffer A (i.e., 2.0 M ammonium sulfate), and then loaded with 0.5 mg/mL lysozyme dissolved in 67% buffer A.

The recoveries of three model proteins (myoglobin, ribonuclease A, and lysozyme) from column 6-2 in Table 3.1 were determined by a method described in Chapter 2. Specifically, HIC separation of proteins was carried out with a 28-cm long column, the column was then cut down to 14 cm in length, and protein separation was carried out again using this short column. The proteins were eluted with a gradient of buffer A to B in 15 min at 0.3 μL/min flow rate. The mass recoveries were calculated by dividing the protein peak areas obtained using the long column with those obtained using the short column.

The Darcy's law permeability of a porous medium is a measure of its capacity to transmit a solvent driven by an imposed pressure drop. The equation to calculate the permeability is $k = \eta L u / \Delta p$, where η is the solvent viscosity, L is the column length, u is the solvent linear velocity, and Δp is the column back pressure. The specific permeability of the column was determined by forcing acetonitrile, methanol, water, buffer B and buffer A through a 10-cm long monolithic column at flow rates from 0.1 to 0.5 μL/min. The values for $u / \Delta p$ were determined from the slopes of the Δp versus u plots. Permeability was then determined to evaluate the stability of poly(PEGDA) monoliths.

3.3 Results and Discussion

3.3.1 Effect of Porogens and Porogen Ratios

With only one monomer in the precursor solution, porogen selection and composition optimization are easier than with conventional two-monomer systems. Since methanol and ethyl ether have proven to be effective porogenic solvents for PEG-containing acrylate monolith synthesis,[25] they were chosen as porogens for poly(PEGDA) monolith synthesis, while cyclohexanol and decanol were chosen as porogens for preparation of poly(PEGDMA) monoliths, since they are two of the most frequently used porogenic solvents when EDMA is used as crosslinker. The ratio of monomer to total porogens was set at 32.2:67.8 wt.% for consistency when investigating the effect of porogen ratio on back pressure (e.g., Figure 3.1). This ratio was also the optimized value for most of the monoliths (except for PEGDMA 286 and PEGDA 700) since it provided rigidity and, at the same time, acceptable low back pressure. The initiator concentration was 1% of the monomer concentration.

Figure 3.1 shows the column back pressures for monoliths synthesized with varying ratios of the two porogen combinations: methanol/ethyl ether and cyclohexanol/decanol. All data points in Figure 3.1 represent rigid monoliths that contain through-pores. Ethyl ether and decanol were relatively poor solvents for PEGDA and PEGDMA monoliths, respectively, which was reflected by the lower back pressures obtained when using those two solvents. SEM images also show larger through-pores or voids when the monoliths were synthesized using ethyl ether or decanol than when using methanol or cyclohexanol. For PEGDA 258 and PEGDA 302 in Figure 3.1A, all tested combinations of methanol and

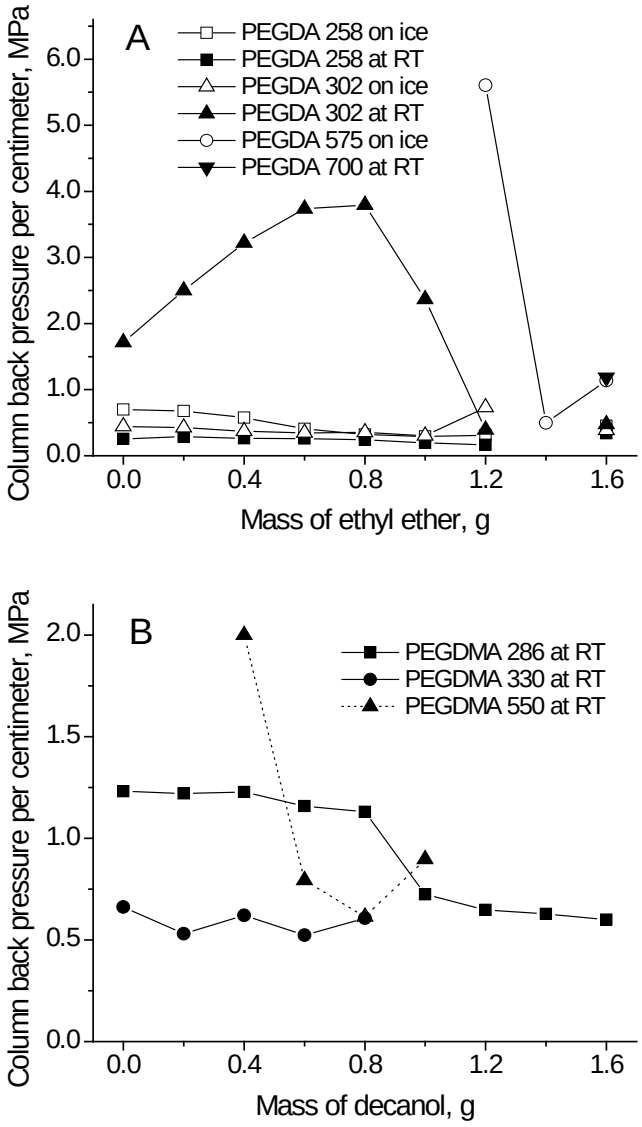

Figure 3.1. Effect of porogen ratio and reaction temperature on back pressure of (A) poly(PEGDA) and (B) poly(PEGDMA) monoliths. Monolith composition: 0.0076 g DMPA, 0.76 g monomer and 1.6 g total porogens (methanol/ethyl ether for PEGDA and cyclohexanol/decanol for PEGDMA). "At RT" means monoliths were prepared at room temperature, and "on ice" means the capillaries were placed on ice during polymerization. The back pressure for each data point was averaged from two or three columns using water at 0.3 μL/min (RSD ≤ 10%; in most cases, less than 7.0%).

ethyl ether formed rigid monoliths, except when the mass of ethyl ether was 1.4 g (59.3 wt.%). At this point, the resultant polymers were either soft or only partially polymerized in small segments within the capillary, likely caused by an immiscible phase in the initial stages of polymerization. For PEGDA 575, an ethyl ether mass less than 1.2 g (50.8 wt.%) produced a transparent gel or polymer with extremely small pores. For PEGDA 700, the combination of 0.2 g (8.47 wt.%) methanol and 1.4 g (59.3 wt.%) ethyl ether formed a polymer with extremely small pores, and the addition of more methanol yielded a gel. These results indicate that an increase in ethylene glycol units makes methanol a better solvent for the growing polymer chains during polymerization. The same tendency was also observed for PEGDMA (Figure 3.1B). A longer PEG chain in PEGDMA made decanol a poorer solvent for monolith formation. For example, all combinations of cyclohexanol and decanol yielded rigid monoliths for PEGDMA 286; however, for PEGDMA 330 and 550, when decanol was 1.0 g (42.4 wt.%) or more, the resulting polymer was easily compressible and/or non-homogeneous. The polymerization rates and properties of the monoliths were also affected by the molar concentrations of acrylate or methacrylate groups in the monomers. Since the same weight of monomer was used for all tested monoliths (Figure 3.1), the molar concentrations of polymerizing groups in the polymerization mixture were lower for crosslinkers with the higher molecular weights. This affects phase separation and, consequently, the pore properties of the monoliths.

Studies also demonstrated that methanol/ethyl ether was not effective for PEGDMA monolith formation, and cyclohexanol/decanol was not suitable for PEGDA monoliths. The resulting structures were either soft polymers, or gels, or polymers with extremely small pores. Another observation worth mentioning is that it was much more difficult to push

cyclohexanol/decanol out of the monoliths than methanol/ethyl ether because cyclohexanol/decanol is more viscous. For example, although the back pressure of a 16-cm long PEGDMA 286 monolith in Table 3.2 was 6.03 MPa using methanol at 0.3 μL/min, the pressure was as high as 21.14 MPa even at 0.05 μL/min when trying to push the porogens out using methanol. However, the pressure to remove methanol/ethyl ether was usually not higher than the intrinsic monolith back pressure. This offers the potential advantage of using less viscous porogenic solvents such as methanol/ethyl ether when monoliths are incorporated in micro-chip LC. Washing at higher temperature should help to remove the porogens at lower pressure, since the viscosity is lower at higher temperature.

3.3.2 Effect of Polymerization Temperature

UV-initiated polymerization is typically performed at room temperature; thus, temperature has not generally been used as an effective way to control pore sizes in UV-initiated polymerization as it has been in thermal-initiated polymerization.[22,26] When monoliths were prepared within a specific section of the channel in microfluidic devices, lower temperature (approximately 0 ^{o}C) was sometimes used to avoid polymerization in other areas due to heating.[27] The effect of temperature on UV initiated polymerization of monoliths has been described in recent papers.[28,29] In this work, I conducted polymerizations at room temperature and at approximately 0 ^{o}C to investigate the effect of low temperature on UV-initiated polymerization, as well as to control the high volatility of methanol/ethyl ether. While temperature has only limited effect on the rate of photo-polymerization, it significantly affects the polymer solution properties, thus affecting phase separation during polymerization. To determine the appropriate polymerization time, exposure times of 3.5 and 5 min to UV light were tested. The resulting monoliths exhibited

the same column back pressure, indicating that 3.5 min exposure time was adequate both at room temperature and at approximately 0 ^{o}C.

For the PEGDMA monolith series, those prepared at approximately 0 ^{o}C had a much higher back pressure (2 ~ 4 times higher) than those prepared at room temperature, and it was also more difficult to remove the porogens after polymerization. Therefore, the lower temperature was not investigated in detail for the dimethacrylate monomers. The effect of polymerization temperature for PEGDA monoliths is shown in Figure 3.1A. For PEGDA 258, monoliths prepared at approximately 0 ^{o}C had higher back pressures than those prepared at room temperature, while for PEGDA 302 and 575, polymerization at room temperature produced monoliths that had higher back pressures than at approximately 0 ^{o}C. For example, when the porogen composition was 0.4 g (16.9 wt.%) methanol and 1.2 g (50.8 wt.%) ethyl ether, polymerization of PEGDA 575 at room temperature formed a polymer with very small pores (pressure drop greater than 4.07 MPa/cm using water at 0.1 μL/min). Lower temperature was not tested for PEGDA 700 because it formed a wax at 4 ^{o}C.

The effect of temperature has been well explained for thermal-initiated polymerization.[22] At higher reaction temperature, the free-radical initiator creates a larger number of free radicals, which forms a larger number of growing nuclei and microglobules of small size. When these small microglobules interconnect to form a monolith, smaller pores are generated, resulting in a higher pressure drop. Although the decomposition of initiator mostly depends on the intensity of UV light in photo-polymerization, polymerization of PEGDA 302 and 575 at room temperature produced monoliths with lower permeability compared to polymerization at 0 ^{o}C. Furthermore, higher temperature

enhances the dissolution ability of a solvent since the mixing of a polymer with a solvent is an endothermic process in most cases. Therefore, the nuclei tend to accumulate to a higher molecular weight before phase separation occurs. Thus, both the microglobules and the voids between them would be larger, and the resulting monoliths would have higher permeability. Although this effect was not observed for thermal-initiated polymerization when the reaction temperatures were in the range of 50 to 80 ^{o}C,[22] it was obvious when the reaction temperatures were lower, such as for PEGDA 258 and all of the PEGDMA monoliths in this study. Figure 3.1A also reveals that the pressure drops of monolithic columns prepared at the two temperatures exhibited a greater difference when methanol was used than ethyl ether for both PEGDA 258 and PEGDA 302 monoliths. This can be readily explained since ethyl ether was a poor solvent compared to methanol. The temperature effects on nucleation rate and on solvency were partially compromised by the effect of a poor solvent on phase separation that occurs during polymerization.

SEM is a useful tool to study the structure and morphology of monoliths directly. SEM images of monoliths represented by each data point in Figure 3.1 were taken and compared. Most of the monoliths possessed conventional interconnected-microglobule morphology such as shown in Figures 3.2A, 3.2B and 3.2E. Monoliths with lower permeability contained smaller microglobules and/or more compact microglobule clusters (smaller through-pores) than monoliths with higher permeabilities. Examples of PEGDA 258 monoliths are shown in Figures 3.2A and 3.2B which represent monoliths 6-1 and 6-2 in Table 3.1 prepared at approximately 0 ^{o}C and room temperature, respectively. However, for PEGDA 302, the morphology differences were greater for monoliths prepared at different temperatures as shown in Figures 3.2E and 3.2F. At approximately 0 ^{o}C, a

conventional polymer monolithic structure (i.e., interconnected microglobules) was observed, while at room temperature, the microglobules became less distinct, and the structure approached a fused morphology. The higher the back pressure, the less distinct the microglobules were. For example, for a PEGDA 302 monolith prepared at room temperature with 0.8 g (33.9 wt.%) methanol and 0.8 g (33.9 wt.%) ethyl ether as porogens (Figure 3.2F), the microglobule structure almost disappeared. I predicted that this structure had a larger surface area and more mesopores, so I tested these monoliths for SEC. Figure 3.3 shows a separation of proteins and peptides using a monolith as shown in Figure 3.2F prepared in a 250-µm i.d. capillary. Five compounds were separated under isocratic elution conditions using a PEGDA 302 monolith prepared at room temperature, while the corresponding monolith prepared at approximately 0 ^{o}C provided much worse results. Since separation in SEC is based on differential exclusion of particles from the pores, the above results demonstrate that PEGDA 302 monoliths prepared at room temperature contain more mesopores and greater surface area.

3.3.3 Poly(PEGDA$_{258}$) Monoliths

PEGDA 258 was chosen to investigate the effect of porogen ratio on chromatographic performance, since it offered the best chromatographic performance, as will be discussed later. Table 3.1 lists monoliths prepared with varying ratios of methanol and ethyl ether, along with their back pressures and chromatographic performance measurements. All of the compositions listed in Table 3.1 formed rigid monoliths with through-pores. Table 3.1 reveals that the three test proteins had similar retention on all listed monoliths, which is reasonable since only one monomer was involved in the polymerization. Usually, any variation in porogen ratio changes the properties of the

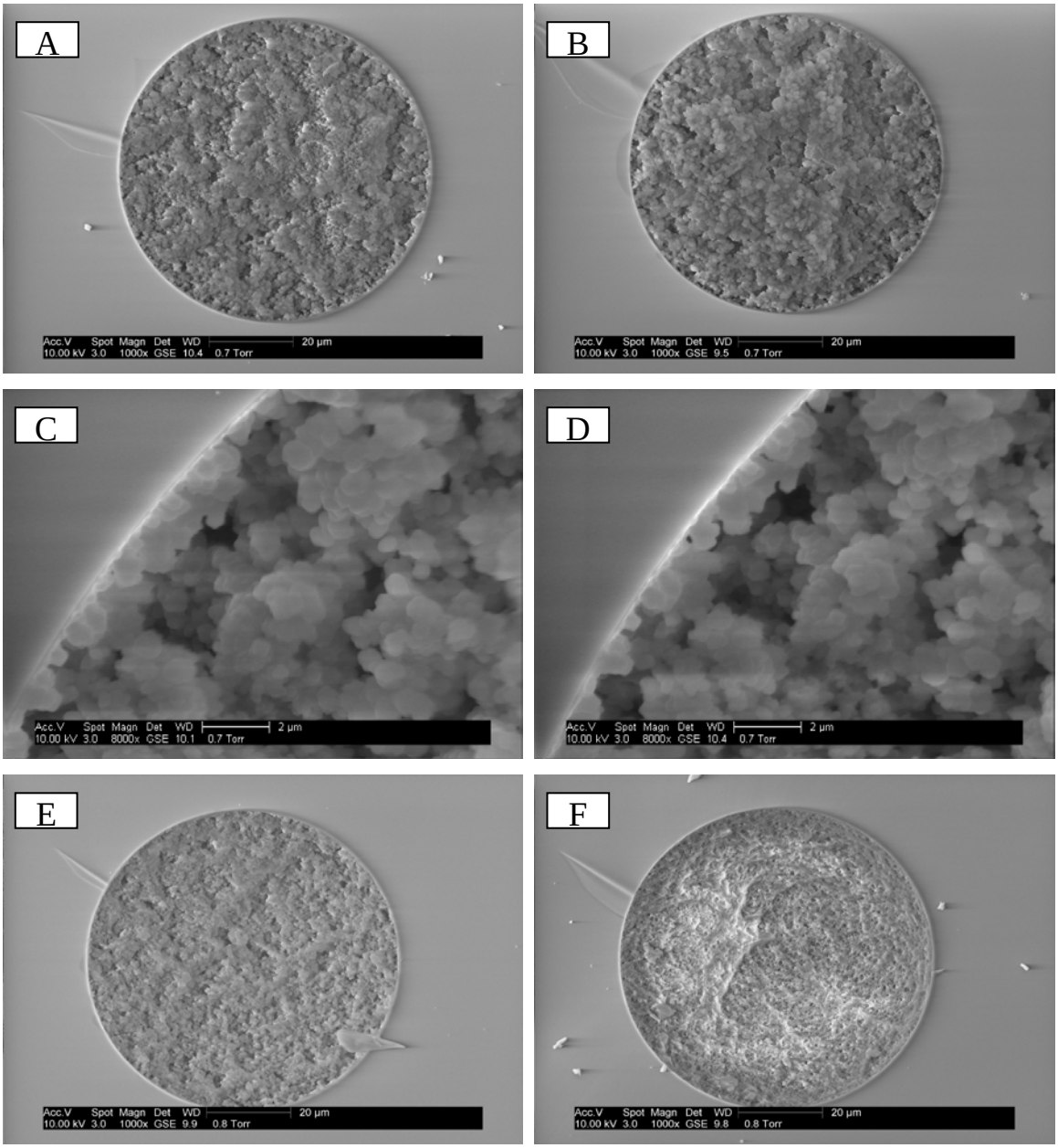

Figure 3.2. SEM images of selected monoliths. (A) Monolith 6-1 in Table 3.1, (B) monolith 6-2 in Table 3.1, (C) monolith 6-1 in Table 3.1 at higher magnification kept continuously wet with water, (D) monolith 6-1 in Table 3.1 at higher magnification after allowing to dry for two weeks, (E) PEGDA 302 monolith prepared at approximately 0 ^{o}C (precursor composition: 0.76 g monomer, 0.8 g methanol, and 0.8 g ethyl ether), (F) PEGDA 302 monolith prepared at room temperature (precursor composition same as E).

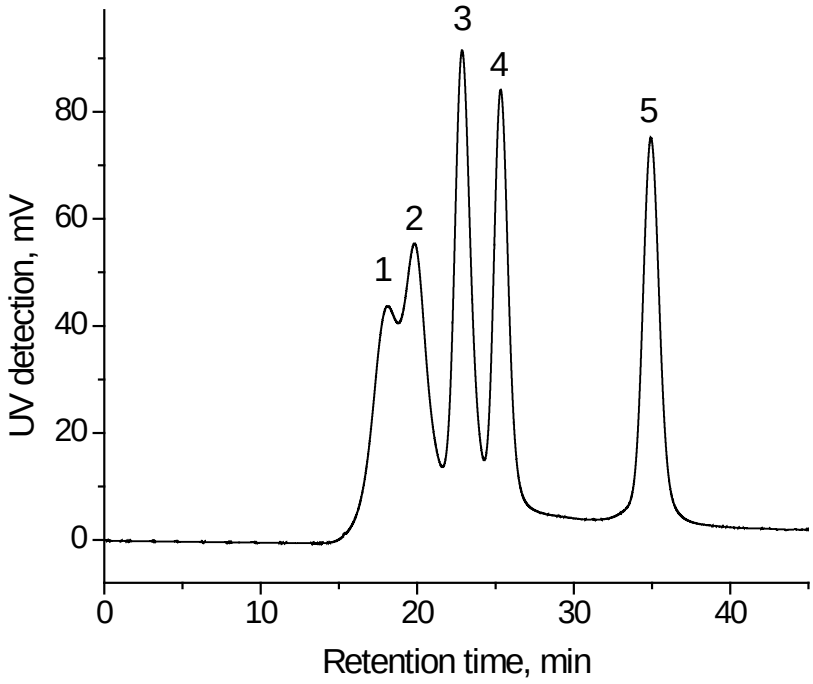

Figure 3.3. SEC of proteins and peptides using PEGDA 302 monolith. Monolith precursor composition: 0.76 g PEGDA 302, 0.8 g methanol, and 0.8 g ethyl ether. The monolith was prepared at room temperature. Conditions: 16 cm × 250 µm i.d. monolithic column; mobile phase was 20 mM phosphate buffer (pH 6.90); isocratic elution at 0.3 µL/min flow rate; on-column UV detection at 214 nm. Peak identifications: (1) thyroglobulin, (2) soybean trypsin inhibitor, (3) angiotensin I, (4) enkephalin, (5) thiourea.

porogen system, which may consequently affect the individual monomer conversions or the surface properties of the monoliths. Thus, the chemical compositions of the monoliths may change by changing the porogen ratio, even if the monomers are kept the same. However, for a one-monomer system, this problem does not exist because the chemical composition stays the same, even if the monomer conversion is different. Table 3.1 also shows that all listed monoliths gave comparable peak widths and peak capacities, which is a result of their rigid and homogeneous morphologies. Homogeneity was also verified from SEM images of the monoliths.

Optimization of a monolith involves producing the best chromatographic performance as possible and as low flow resistance as possible. Although the monoliths listed in Table 3.1 had comparable performances, they displayed quite different back pressures from one another. When polymerization was performed at approximately 0 ^{o}C, the lowest back pressure was observed when the ratio of methanol to ethyl ether was approximately 0.6:1.0 (monolith 6-1 in Table 3.1). Therefore, column 6-1 was chosen as the optimized monolith for detailed study due to its low flow resistance, good chromatographic performance and high column reproducibility.

Six protein standards were separated using column 6-1 in Table 3.1. Figure 3.4 shows separations using 5, 10, 15 and 20 min gradients from 0% to 100% B at 0.3 μL/min, which correspond to 2.1, 4.2, 6.4 and 8.5 column volumes, respectively. For all gradients, the proteins were separated from each other and eluted as sharp peaks with little noticeable tailing, indicating that non-specific protein adsorption was minimal when using this poly(PEGDA$_{258}$) monolith. Resolution values for ribonuclease A and lysozyme, and neo-chymotrypsin and α-chymotrypsinogen A were calculated for each gradient and listed in

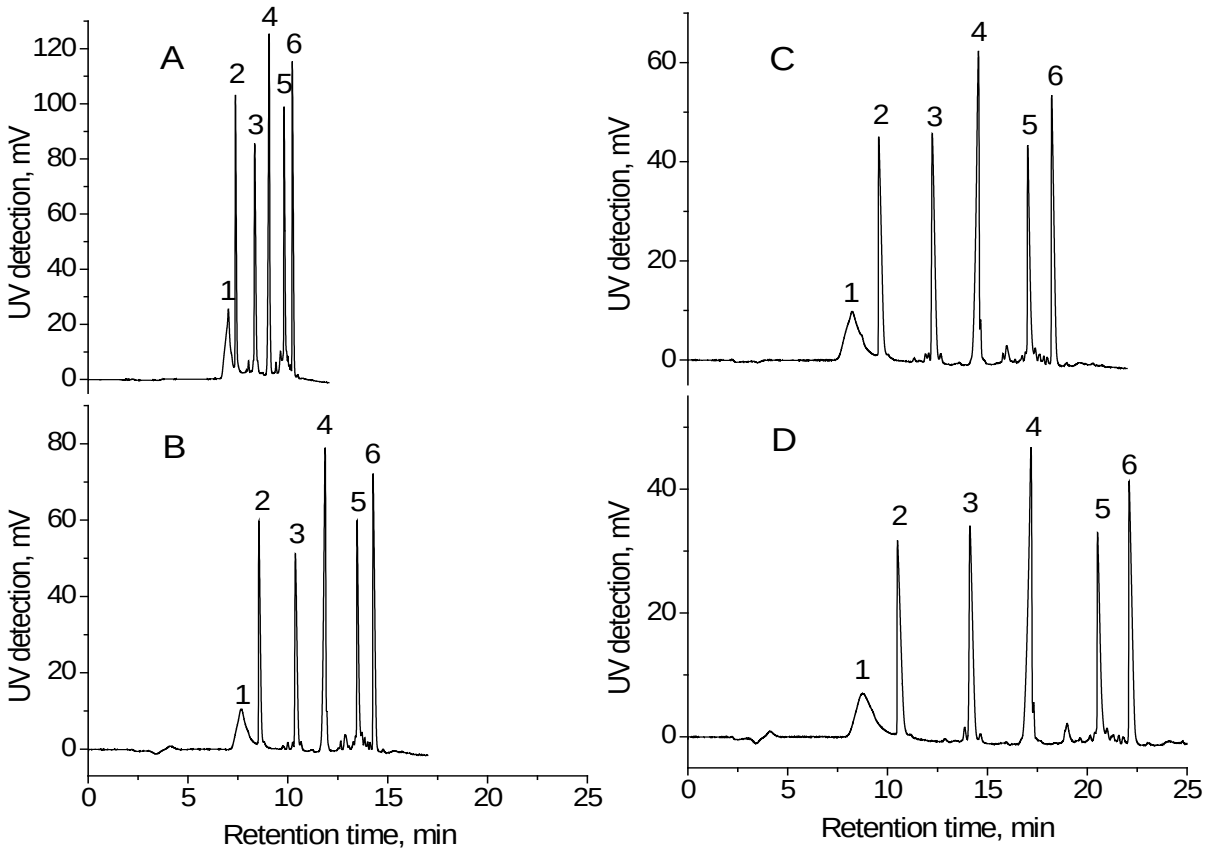

Figure 3.4. HIC of protein standards using monolith 6-1 in Table 3.1 with gradient rates of (A) 5 min, (B) 10 min, (C) 15 min, and (D) 20 min. Conditions: 16 cm × 75 µm i.d. monolithic column; buffer A was buffer B plus 3.0 M $(NH_4)_2SO_4$, and buffer B was 0.1 M phosphate buffer (pH 6.90); 1-min isocratic elution with 100% A, followed by a linear A-B gradient from 0% to 100% B, and then isocratic elution with 100% B; 0.3 µL/min flow rate; on-column UV detection at 214 nm. Peak identifications: (1) cytochrome *c*, (2) myoglobin, (3) ribonuclease A, (4) lysozyme, (5) neo-chymotrypsin, (6) α-chymotrypsinogen A.

Table 3.3. Peak capacities were calculated by dividing the gradient time by the average peak width of peaks 2 to 6.[30] The peak widths were obtained directly from integration using Chrom Perfect software. Table 3.3 reveals that the shallower gradients afforded better resolution and higher peak capacity, with the greatest improvement arising when increasing the gradient time from 5 min to 10 min, which is similar to the results observed for the poly(HEA-*co*-PEGDA) monolithic column described in Chapter 2. At the same time, the resolution and peak capacity for each gradient were better than the corresponding values for the poly(HEA-*co*-PEGDA) monolithic column. The improvements resulted primarily from improved selectivity and narrower peak widths. This is because monoliths prepared solely from PEGDA 258 provided more hydrophobic interaction sites and were more homogeneous than HEA/PEGDA monoliths. Compared to other reported monolithic columns for HIC of proteins,[31-34] this poly($PEGDA_{258}$) monolith was superior, and the performance was comparable or better than the performance of HIC packed columns.[35-37]

To further demonstrate the excellent performance of this poly($PEGDA_{258}$) monolithic column, two commercial trypsin inhibitor samples from Sigma-Aldrich were separated. According to the manufacturer, the two samples were chromatographically purified; however, the samples were rather crude as shown in Figure 3.5, containing three or more major components. Trypsin inhibitor (product number T9003) was previously separated using tandem columns packed with materials of different hydrophobicities in order to save HIC separation time, because the trypsin inhibitor sample was found to contain impurities differing widely in hydrophobicity.[38] In my work, all components were eluted from a single column in reasonable time with better resolution, demonstrating the resolving power of this HIC monolithic column.

Table 3.3. Resolution Values and Peak Capacities for Protein Standards Separated Using Different Gradient Times.

	gradient time (min)			
	5	10	15	20
resolution[a]	2.57	3.99	4.84	5.77
resolution[b]	4.22	6.73	7.69	8.62
peak capacity[c]	31	48	53	62

[a] Resolution of peaks 5 and 6, neo-chymotrypsin and α-chymotrypsinogen A. [b] Resolution of peaks 3 and 4, ribonuclease A and lysozyme. [c] Peak capacity = time of gradient/average peak width.

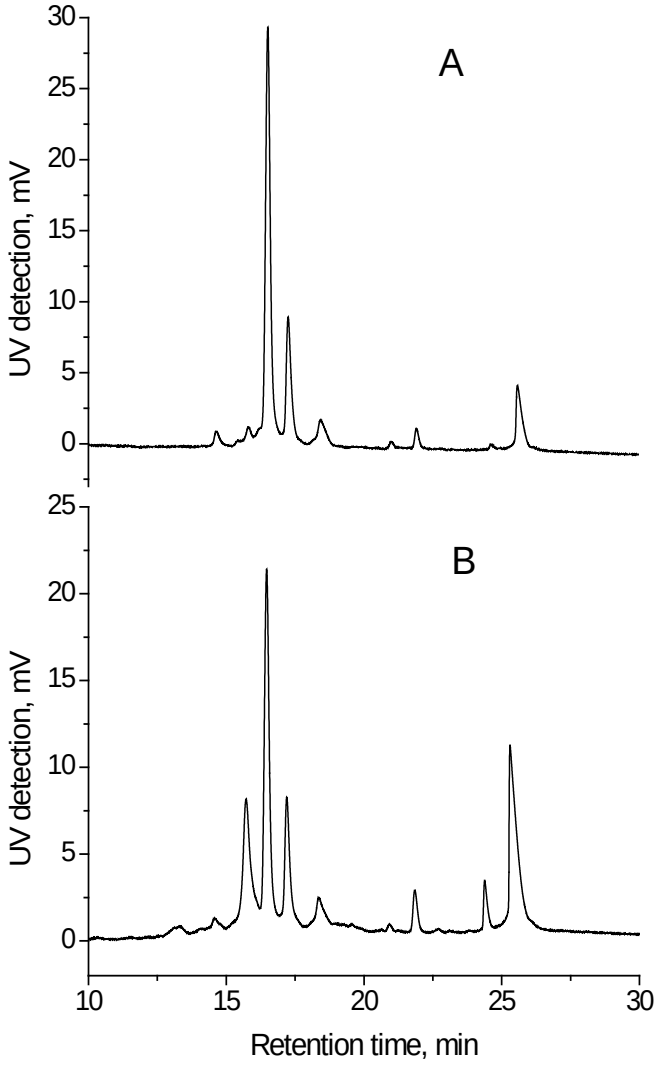

Figure 3.5. HIC of two commercial trypsin inhibitor samples. Panels A and B represent samples with product nos. T9003 and T6522, respectively. Conditions: 1-min isocratic elution with 67% A, followed by a linear A-B gradient from 33% to 100% B in 20 min, and then isocratic elution with 100% B; other conditions are the same as in Figure 3.4D.

3.3.4 Poly(PEGDA) and Poly(PEGDMA) Monoliths

Table 3.2 shows selected monoliths synthesized from PEGDA and PEGDMA with varying lengths of ethylene glycol chains. The listed monoliths were homogeneous (based on their SEM images), rigid, and had acceptably low back pressures. In Table 3.2, it can be seen that the weights of total porogens and monomer were 3.0 g (79.8 wt.%) and 0.76 g (20.2 wt.%) for the PEGDMA 286 monolith, which represents a high ratio of porogens to monomer. However, the resulting monolith was still rigid and mechanically stable due to its highly crosslinked structure, which is one advantage of using one monomer, i.e., it is possible to optimize monoliths with lower flow resistance by increasing the porogen volume.

For easy comparison, the same six standard proteins were used to evaluate the six monolithic columns listed in Table 3.2 for HIC. Chromatograms are shown in Figure 3.6. By comparing the PEGDMA monoliths to corresponding PEGDA monoliths (i.e., PEGDMA 286 to PEGDA 258, and PEGDMA 330 to PEGDA 302), it was observed that proteins had slightly greater retention on the PEGDMA monoliths compared to the PEGDA monoliths, which was due to a slight increase in hydrophobicity due to the extra methyl groups in the alkyl end-groups of the PEGDMA monomer. However, with an increase in ethylene glycol chain length, this extra methyl group effect became negligible. There are two possible explanations for this: (1) PEGDA 575 monoliths have a larger surface area than PEGDMA 550 monoliths and (2) PEGDMA 550 monoliths have more linked alkyl end-groups buried within the monolith structure. Regardless of which is more important, both result in a lower density of alkyl functionality in the PEGDMA 550 monoliths. Decreased density of alkyl functionality can also explain the decreased retention times of

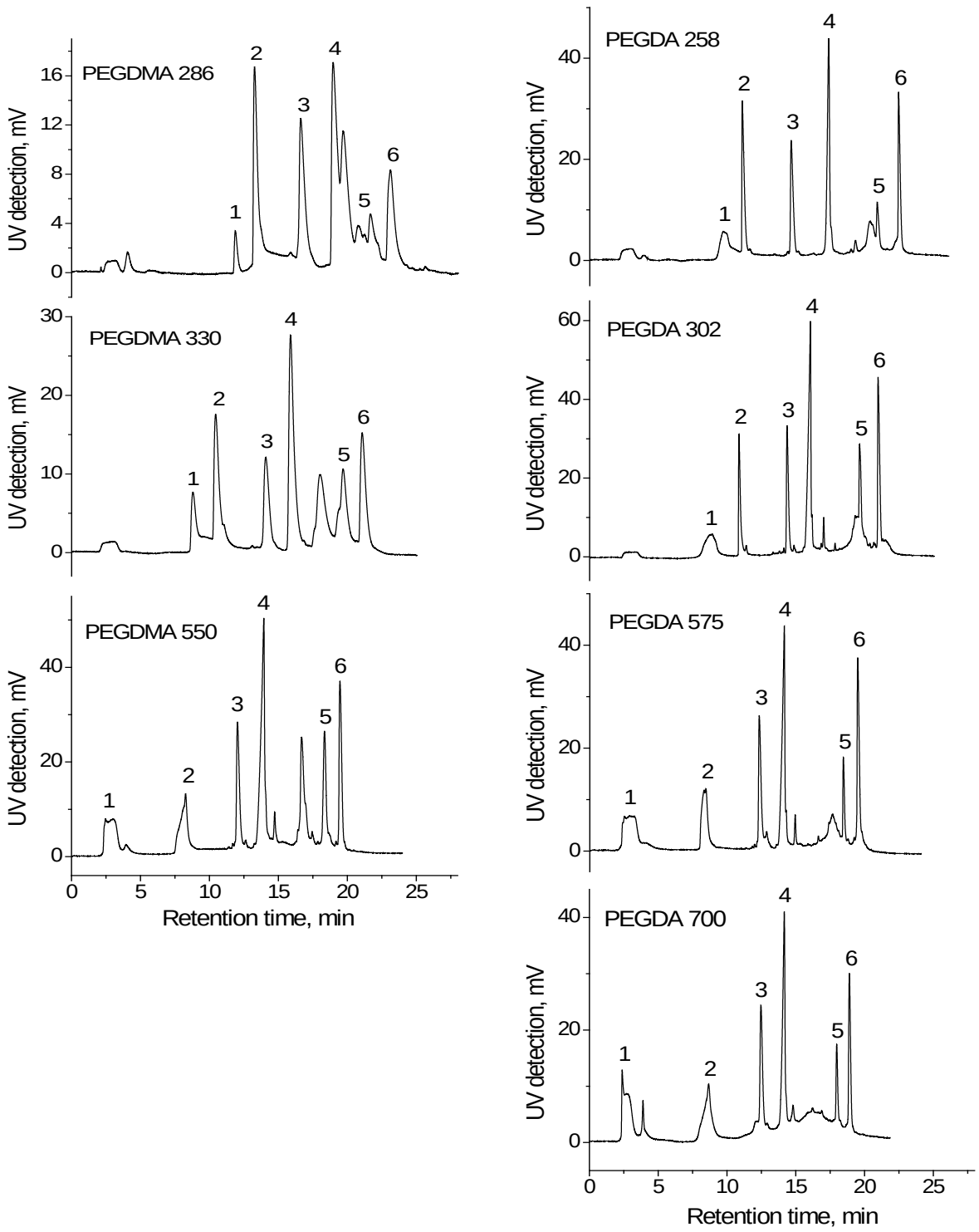

Figure 3.6. HIC of protein standards using monolith 6-1 in Table 3.1 and monoliths in Table 3.2. Conditions and peak identifications are the same as in Figure 3.4D.

proteins when using monoliths synthesized from monomers with increasing ethylene glycol chain length, i.e., longer ethylene glycol chain in the monomer, resulted in lower density of the linked alkyl end-groups in the monolithic polymer. When the ethylene glycol chain length increased from PEGDA 575 to PEGDA 700, the retention times were not significantly affected, which was probably due to the smaller difference in the density of alkyl linking groups.

In Figure 3.6, it was also observed that monoliths made from PEGDA offered better separations and higher peak capacities than monoliths made from PEGDMA. Tailing was easily observed when using PEGDMA 286 and PEGDMA 330 monoliths, and peaks were broad compared to PEGDA 258 and PEGDA 302 monoliths. When monoliths prepared from PEGDMA 550 were used for separation, the peak shapes improved considerably. These results indicate that peak tailing and broadening are not caused by the hydrophobicity of the functional alkyl linking groups themselves, but by their high density. The extra methyl groups in PEGDMA monomers made the alkyl linking groups larger in size, blocking the mildly hydrophilic matrix provided by the PEG chains. Usually in HIC stationary phases, mildly hydrophobic ligands are incorporated in a hydrophilic matrix, e.g., cross-linked agarose or hydrophilic polymeric matrix; and the ligand density in the HIC stationary phase is usually 10-100 times lower than in reversed-phase packing materials.[39] The protein binding capacities of the HIC adsorbents increase with increased degree of substitution of immobilized ligand. At a sufficiently high degree of ligand substitution, the apparent binding capacity of the adsorbent remains constant (i.e., a plateau is reached), but the strength of the interaction increases.[40] Solutes bound under such circumstances are difficult to elute due to multi-point attachment,[41] which is the main reason for peak

broadening and tailing observed for poly(PEGDMA$_{286}$) and poly(PEGDMA$_{330}$) monolithic columns. By comparing the performances of the columns in Figure 3.6, I concluded that the PEGDA 258 monolithic column represented the best results with regard to peak capacity, resolution and peak shape.

The elution profiles of α-chymotrypsin were also different for PEGDA and PEGDMA monoliths. For the PEGDMA monolithic columns, the unlabeled peak before neo-chymotrypsin (peak 5 in Figure 3.6) was eluted as a sharper and better resolved peak compared to separation on the PEGDA monoliths. I also observed that neo-chymotrypsin was present in α-chymotrypsin and α-chymotrypsinogen A samples, and more neo-chymotrypsin was activated from α-chymotrypsinogen A with time. Cytochrome *c* was eluted as peak 1 followed by a broad tailing peak which overlapped with peak 2 on PEGDMA 286 and 330 monoliths. This was probably caused by oxidation/reduction of cytochrome *c*. The small bump that was observed at the dead time was caused by the slight difference in absorbance between the mobile phase and the buffer used to dissolve the samples. When cytochrome *c* was not retained and eluted at the dead time, this peak was broad and flat because of the large injection volume (i.e., 200 nL) together with the system dead volume. The distorted peaks for less hydrophobic proteins in some chromatograms were caused by incomplete retention under the conditions used.

3.3.5 Reproducibility

Column-to-column reproducibility was measured for selected monolithic columns in this study. The RSD values based on retention times of retained proteins were all within 2.2%, and in most cases, less than 1.2%. The RSD values based on peak areas were larger (within 9.5%; in most cases, less than 7.0%) than those based on retention times since slight

changes in sample preparation and injection also contributed to the deviation. As an example, for poly($PEGDA_{258}$) monolithic columns, the RSD values (n = 3) of retention times for proteins 2 to 6 were 0.81, 0.68, 0.64, 0.58, and 0.91%, respectively; and the RSD values based on peak areas for proteins 2 to 4 were 6.6, 4.5, and 2.1%, respectively. The high reproducibility in column preparation was mainly a result of single-monomer polymerization.

The run-to-run reproducibility of these monolithic columns was also good. For any selected three runs carried out using any column prepared during the study, the RSD values of the retention times for proteins 2 to 6 were all within 1.5%. In most cases, the RSD was less than 1.0%. The RSD values based on peak areas were less than 9.0%, and in most cases, less than 6.0%. These data not only demonstrate good reproducibility, but they also indicate the stability of these monolithic columns. Re-equilibration of each column was readily achieved by flushing with 2~4 column volumes of initial buffer.

3.3.6 Stability of Proteins in High Salt Concentration

Compared to the extremely hydrophobic stationary phase and harsh mobile phase conditions (organic solvents and low pH) used in reversed-phase chromatography (RPC), the less hydrophobic stationary phase and aqueous solvents used in HIC lead to less tendency to denature proteins. In spite of the fact that HIC is conducted using mild conditions with the intention of maintaining proteins in their native conformations, such changes can still occur in certain situations.[42] A poly($PEGDA_{258}$) monolithic column was used to investigate the stability of proteins. Myoglobin is often used to demonstrate solvent and/or stationary phase effects on tertiary structure due to the presence of a non-covalently bound heme group. In my experiments, I did not observe any noticeable denaturation of

myoglobin or other protein standards, regardless of whether the 28-cm long column was used for mass recovery measurements or the protein analytes were kept on the column for 20 min before they were eluted. These results indicate that neither the poly($PEGDA_{258}$) monolith nor the starting solvent containing 3.0 M $(NH_4)_2SO_4$ induced denaturation of the protein standards.

The initial salt concentration used in HIC generally ranges from 1 to 3 M. A decrease in initial salt concentration results in earlier elution of proteins. When 2.8 M $(NH_4)_2SO_4$ was used as initial concentration for the poly($PEGDA_{258}$) monolithic column, cytochrome *c* was eluted unretained and myoglobin began to show fronting. When the initial salt concentration was decreased to 2.0 M $(NH_4)_2SO_4$, cytochrome *c*, myoglobin and ribonuclease A were all eluted unretained. Therefore, an initial salt concentration of 3.0 M $(NH_4)_2SO_4$ was required to promote hydrophobic interaction between the analytes and stationary phase for all six proteins. Since the sample is typically dissolved in the initial buffer, it is important to be aware of the effect of this high salt concentration on protein conformation. To evaluate how long protein conformation can be preserved when dissolved in 3.0 M $(NH_4)_2SO_4$, a protein standard solution was freshly prepared and kept on ice in a Styrofoam box with a cover. HIC was carried out every 6 or 12 h for a total of 48 h using the poly($PEGDA_{258}$) monolithic column. Selected chromatograms are shown in Figure 3.7. By comparing chromatograms obtained at 0, 12, 24 and 48 h, it was observed that cytochrome *c*, myoglobin and ribonuclease A remained unaffected, indicating that they were stable for at least 48 h. On the other hand, α-chymotrypsinogen A was activated to neo-chymotrypsin with time, which was reflected in a reduction in α-chymotrypsinogen A peak and a simultaneous increase in neo-chymotrypsin peak. These results demonstrate that

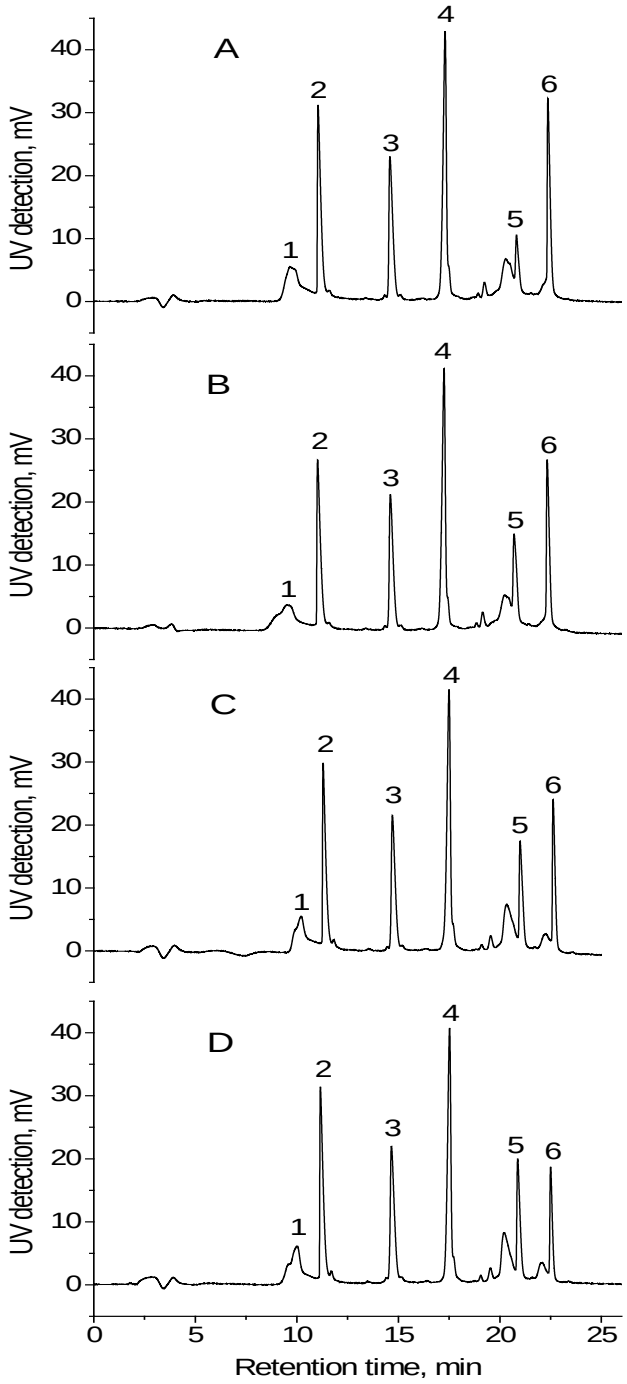

Figure 3.7. HIC of protein standards dissolved in 3.0 M $(NH_4)_2SO_4$ after storing on ice for (A) 0 h, (B) 12 h, (C) 24 h, and (D) 48 h. Other conditions and peak identifications are the same as in Figure 3.4D.

although protein standards were observed to precipitate, denature or decompose in 3.0 M $(NH_4)_2SO_4$ when kept at room temperature (see Chapter 2), they remained quite stable when kept on ice.

3.3.7 Stability of the Monolithic Columns

Monoliths synthesized from PEG-containing acrylates or methacrylates are usually preserved wet, filled with buffer.[5,7] Even vacuum drying during SEM imaging caused cracks around the circumference of the monolith due to shrinking.[5] To determine if PEGDA and PEGDMA monoliths can be dried, columns used for the separations in Figure 3.6 were flushed with water and stored in a hood at room temperature for at least one month without sealing the ends. Then the columns were rehydrated and HIC separations of protein standards were performed again. Chromatograms obtained after the columns were dried and then rehydrated are shown in Figure 3.8. For the PEGDMA 286 monolith, the back pressure after rehydration was less than half of the original value, and the performance also worsened, indicating that the monolith could not be recovered after drying. This is mainly because a large ratio of porogens to monomer was used during synthesis, making the monolith less rigid (note: when a composition of 1.6 g total porogen/0.76 g monomer was used to prepare the PEGDMA 286 monolith, the back pressure was the same before and after it was dried). At the same time, the PEGDA 700 monolith was found to be compressible after rehydration. However, this lack of stability is more likely caused by the long ethylene glycol chain in the monomer than by the higher ratio of porogens used, since monoliths prepared using lower ratios of porogens were also compressible after drying. For all other monoliths, the retention times and elution profiles of the components were almost identical to those in Figure 3.6, indicating that these monolithic columns can be dried and

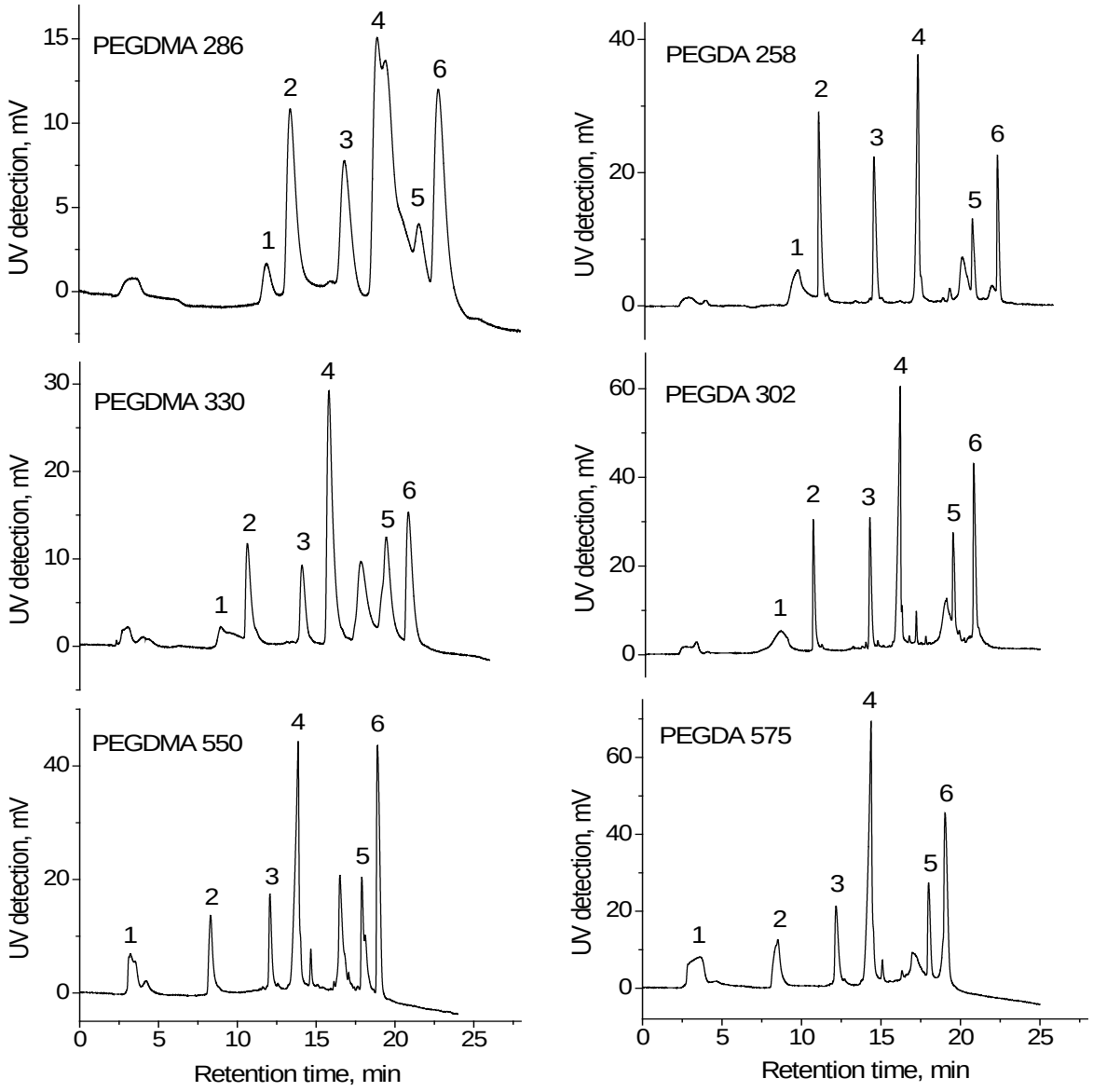

Figure 3.8. HIC of protein standards using monolithic columns used in Figure 3.6 after allowing them to dry for one month. Conditions and peak identifications are the same as in Figure 3.4D.

stored without any noticeable change in chromatographic properties. SEM images were also taken before and after the monoliths were dried. Specifically, small sections of capillary column (~ 0.7 cm) were cut and fixed on stubs using conductive tape, SEM images were taken, the capillary sections were stored at room temperature for two weeks and then the SEM images were taken again. As an example, images of a PEGDA 258 monolith before and after drying are shown in Figures 3.2C and 3.2D. The two images are almost the same, and no cracks or shrinkage were observed. The high rigidity and excellent mechanical stability are due to the highly crosslinked network of the monoliths synthesized from single monomers as well as their covalent attachment to the capillary wall.

Permeability was also determined to further evaluate the stability of each monolith. For plots of back pressure versus flow rate, acetonitrile, methanol, water, buffer B and buffer A were pumped through a 10-cm long monolithic column at flow rates from 0.1 to 0.5 µL/min. Linear relationships between back pressure and flow rate for all five solvents clearly demonstrated the mechanical stability of each monolith. The calculated permeabilities based on the slopes of back pressure versus flow rate are listed in Table 3.4. For all monolithic columns, the results were similar for all five solvents, indicating that all monoliths shrank or swelled very little in solvents of different polarities. Salt-dependent permeability observed previously for PEG-containing monoliths was also observed for several monoliths listed in Table 3.4,[5,24] supporting the general rule that the longer the monomer chain, the more apparent the effect. Among these columns, the PEGDA 258 monolithic column could be regenerated within 10 min at 0.3 µL/min flow rate, and it remained stable over a period of two and a half months of investigation. Over 100 injections were carried out during this period.

Table 3.4. Permeabilities of Monolithic Columns Using Different Mobile Phases.

mobile phase			permeability, k ($\times 10^{-14}$ m^2)[c]						
	relative polarity[a]	viscosity, η (mPa s)[b]	PEGDA 258	PEGDA 302	PEGDA 575	PEGDA 700	PEGDMA 286	PEGDMA 330	PEGDMA5 50
buffer A	/	1.906	4.44	2.58	2.74	3.61	3.32	2.12	3.77
buffer B	/	0.935	4.14	2.20	1.54	1.56	3.31	1.96	2.33
water	1.000	0.890	4.44	2.23	1.52	1.55	3.46	1.95	2.36
methanol	0.762	0.544	3.28	2.05	2.07	2.23	2.64	1.51	2.56
acetonitrile	0.460	0.369	2.69	1.53	1.50	1.61	2.23	1.12	1.81

[a] Relative polarity data were from ref. 5. [b] Viscosity data were from online *CRC Handbook of Chemistry and Physics*., 89th ed.; CRC: Boca Raton, 2008-2009. [c] $k = \eta L u / \Delta p$, where η is the viscosity, L is the column length (10 cm in this case), u is the solvent linear velocity, and Δp is the column back pressure. The values for $u / \Delta p$ are based on plots of back pressure versus flow rate.

3.3.8 DBC and Mass Recovery

Breakthrough curves provide valuable information about mass transfer efficiency and DBC of the separation medium. One advantage of monolithic columns compared to packed columns is their excellent mass transfer characteristics, leading to sharp breakthrough curves that are independent of the flow rate within a broad range.[43] Figure 3.9 shows results of frontal analysis using each monolithic column. For the PEGDA 258 monolith, the breakthrough curves for lysozyme obtained at flow rates of 0.1 and 0.3 μL/min are almost identical, and the fronts are both very sharp (Figure 3.9A). This indicates that mass transfer was very fast, and that adsorption was not mass transfer limited. The breakthrough times were 17.10, 17.15 and 17.16 min at 0.3 μL/min flow rate, and 51.06 min at 0.1 μL/min flow rate. A total binding capacity for lysozyme dissolved in 2.0 M $(NH_4)_2SO_4$ was calculated to be 9.68 mg/mL of column volume with 0.37% RSD for the four measurements.

Figure 3.9B shows breakthrough curves for other monoliths. The breakthrough curve for the PEGDA 302 monolith was as sharp as for the PEGDA 258 monolith. Monoliths synthesized from PEGDA 575, as well as from PEGDA 700 (data not shown), were not hydrophobic enough to retain lysozyme under the measurement conditions, showing a gradually increasing curve rather than a steep breakthrough curve. The PEGDMA 550 monolith could not retain lysozyme completely, reflected by an increasing gradient before the sharp increase. The curve for the PEGDMA 330 monolith was not as steep as others, probably due to less homogeneous morphology, which might also contribute to the peak broadening shown in Figure 3.6. PEGDMA 286 gave the highest DBC value, which was consistent with the chromatograms. The gradual increase following

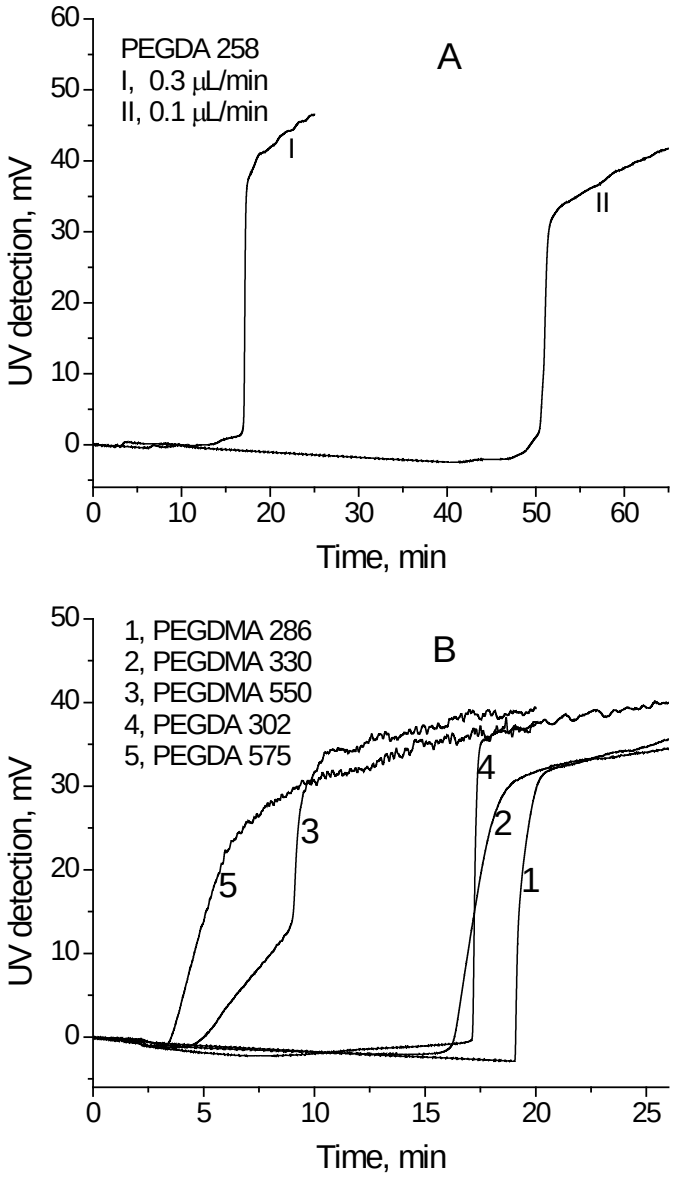

Figure 3.9. Breakthrough curves obtained by fontal analysis for (A) PEGDA 258 monolith at flow rates of 0.3 µL/min (curve I) and 0.1 µL/min (curve II), and (B) other monoliths at flow rates of 0.3 µL/min. Conditions: 6.0 cm × 75 µm i.d. monolithic column 6-1 in Table 3.1 and monolithic columns in Table 3.2; 0.5 mg/mL lysozyme dissolved in 67% buffer A/33% buffer B; UV detection at 214 nm.

the steep increase was mainly caused by the continuous adsorption of proteins in the high salt concentration. The binding capacities for lysozyme dissolved in 2.0 M $(NH_4)_2SO_4$ were calculated to be 11.09, 10.04, 5.15, and 9.72 mg/mL of column volume for PEGDMA 286, 330, 550 and PEGDA 302 monoliths, respectively. The DBC values were based on three measurements, and the RSD values were 1.0, 0.86, 0.75 and 0.54%, respectively. The high binding capacities most probably resulted from the large surface areas of these monoliths.

High mass recovery is an essential requirement for high performance protein separations. Protein recovery experiments were performed for poly($PEGDA_{258}$) monolithic columns as described in section 3.2.4. The recoveries for myoglobin, ribonuclease A and lysozyme were 96%, 92% and 90%, respectively, for a 14-cm long monolithic column. As demonstrated previously,[24,33] higher recoveries were achieved for less hydrophobic proteins. RSD values for recoveries of these three proteins in three parallel tests were 3.9%, 1.6% and 3.2%, respectively. These results indicate high recovery of proteins from the poly($PEGDA_{258}$) monolithic column.

3.4 Conclusions

Two series of rigid monoliths were synthesized solely from PEGDA or PEGDMA containing different ethylene glycol chain lengths by one-step UV-initiated polymerization. Methanol/ethyl ether and cyclohexanol/decanol were used as bi-porogen mixtures for the PEGDA and PEGDMA monoliths, respectively. Effects of PEG chain length, bi-porogen ratio and reaction temperature on monolith morphology and back pressure were investigated. For PEGDA 258 and PEGDA 302, most combinations of methanol and ethyl ether were effective in forming monoliths, while for diacrylates containing longer chain lengths (i.e., PEGDA 575 and PEGDA 700), polymerization became more sensitive to the

bi-porogen ratio. A similar tendency was also observed for PEGDMA monomers. Protein standards were used to characterize each column, and the poly($PEGDA_{258}$) monolithic column was found to provide the best performance with respect to peak capacity, resolution and peak shape in the HIC mode. The poly($PEGDA_{258}$) monolithic column was also used to separate two commercial trypsin inhibitor samples, which contained more than three major components, demonstrating the resolving power of this column. Although 3.0 M $(NH_4)_2SO_4$ was required to retain several test proteins on the column, it was non-denaturing to the proteins; a solution of protein standards proved to be stable for at least 48 h when kept on ice. Most monolithic columns in this study could be stored dry, which is convenient for intermittent use. Other characteristics such as resolution, peak capacity, binding capacity, mass recovery and permeability were all found to be excellent for this poly($PEGDA_{258}$) monolithic column.

The overall hydrophobicity of an HIC stationary phase is determined by both ligand hydrophobicity and ligand density. This work reveals that a hydrophilic matrix is important for an HIC stationary phase to avoid multi-point attachment of solutes which results in peak tailing due to difficulty in eluting the solutes. Investigation of a series of monoliths synthesized from monomers with different lengths of PEG spacers also provides a way to control the functionality density in single-monomer synthesis, namely, through control of the spacer length.

In photo-initiated polymerization, reaction temperature is often neglected. Investigation of the effect of reaction temperature by polymerizing monoliths at approximately 0 ^{o}C and room temperature in this work demonstrated that temperature affects the nucleation rate and solvent properties, and subsequently affects the monolith

properties, similar to thermal-initiated polymerization. These results suggest that in order to improve reproducibility, reaction temperature should also be considered in UV-initiated monolith preparation.

This work demonstrates several advantages with respect to monolith synthesis using a single-monomer system compared to conventional two-monomer systems, including: (1) optimization of polymerization solution components is straightforward and monoliths are usually more homogeneous; (2) a change in porogen ratio does not affect the chemical composition of the resulting monolith, making column preparation more reproducible; and (3) a highly crosslinked network results in higher rigidity and better mechanical stability, as well as higher surface area. The single-monomer synthetic approach improves column-to-column reproducibility in monolith preparation.

3.5 References

1. Hjerten, S.; Liao, J. L.; Zhang, R. *J. Chromatogr.* **1998**, *473*, 273-275.
2. Tennikova, T. B.; Bleha, M.; Svec, F.; Almazova, T. V.; Belenkii, B. G. *J. Chromatogr.* **1991**, *555*, 97-107.
3. Svec, F.; Frechet, J. M. J. *Anal. Chem.* **1992**, *64*, 820-822.
4. Svec, F.; Huber, C.G. *Anal. Chem.* **2006**, *78*, 2100-2107.
5. Gu, B.; Chen, Z.; Thulin, C. D.; Lee, M. L. *Anal. Chem.* **2006**, *78*, 3509-3518.
6. Gu, B.; Li, Y.; Lee, M. L. *Anal. Chem.* **2007**, *79*, 5848-5855.
7. Chen, X.; Tolley, H. D.; Lee, M. L. *J. Sep. Sci.* **2009**, *32*, 2565-2573.
8. Vlakh, E. G.; Tennikova, T. B.; *J. Sep. Sci.* **2007**, *30*, 2801-2813.
9. Ueki, Y., Umemura, T.; Li, J.; Odake, T.; Tsunoda, K. *Anal. Chem.* **2004**, *76*, 7007-7012.
10. Viklund, C.; Svec, F.; Frechet, J. M. J.; Irgum, K. *Biotechnol. Progr.* **1997**, *13*, 597-600.
11. Peters, E. C.; Svec, F.; Frechet, J. M. J. *Adv. Mater.* **1997**, *9*, 630-633.
12. Wu, Z.; Frederic, K. J.; Talarico, M.; De Keel, D. *Can. J. Chem. Eng.* **2009**, *87*, 579-583.
13. Kubo, T.; Kimura, N.; Hosoya, K., Kaya, K. *J. Polym. Sci. Part A-Polym. Chem.* **2007**, *45*, 3811-3817.

14. Kanamori, K.; Nakanishi, K.; Hanada, T. *Adv. Mater.* **2006**, *18*, 2407-2411.
15. Hasegawa, J.; Kanamori, K.; Nakanishi, K.; Hanada, T.; Yamago, S. *Macromolecules* **2009**, *42*, 1270-1277.
16. Hasegawa, J.; Kanamori, K.; Nakanishi, K.; Hanada, T.; Yamago, S. Macromol. *Rapid Commun.* **2009**, *30*, 986-990.
17. Greiderer, A.; Ligon, S. C.; Huck, C. W.; Bonn, G. K. *J. Sep. Sci.* **2009**, *32*, 2510-2520.
18. Greiderer, A.; Trojer, L.; Huck, C. W.; Bonn, G. K. *J. Chromatogr. A* **2009**, *1216*, 7747-7754.
19. Lubbad, S. H.; Buchmeiser, M. R. *J. Sep. Sci.* **2009**, *32*, 2521-2529.
20. Lubbad, S. H.; Buchmeiser, M. R. *J. Chromatogr. A* **2010**, *1217*, 3223-3230.
21. Santora, B. P.; Gagne, M. R.; Moloy, K. G.; Radu, N. S. *Macromolecules* **2001**, *34*, 658-661.
22. Viklund, C.; Svec, F.; Frechet, J. M. J.; Irgum, K. *Chem. Mater.* **1996**, *8*, 744-750.
23. Urban, J.; Svec, F.; Frechet, J. M. J. *Anal. Chem.* **2010**, *82*, 1621-1623.
24. Li, Y.; Tolley, H. D.; Lee, M. L. *Anal. Chem.* **2009**, *81*, 9416-9424.
25. Gu, B.; Armenta, J. M.; Lee, M. L. *J. Chromatogr. A* **2005**, *1079*, 382-391.
26. Svec, F.; Frechet, J. M. J. *Chem. Mater.* **1995**, *7*, 707-715.
27. Yang, W.; Sun, X.; Wang, H.; Woolley, A. T. *Anal. Chem.* **2009**, *81*, 8230-8235.
28. Szumski, M.; Buszewski, B. *J. Sep. Sci.* **2009**, *32*, 2574-2581.
29. Hirano, T.; Kitagawa, S.; Ohtani, H. *Anal. Sci.* **2009**, *25*, 1107-1113.
30. Neue, U. D. *J. Chromatogr. A* **2005**, *1079*, 153-161.
31. Zhang, R.; Yang,G.; Xin, P.; Qi, L.; Chen,Y. *J. Chromatogr. A* **2009**, *1216*, 2404-2411.
32. Hemstrom, P.; Nordborg, A.; Irgum, K.; Svec, F.; Frechet, J. M. J. *J. Sep. Sci.* **2006**, *29*, 25-32.
33. Zeng, C.-M.; Liao, J.-L.; Nakazato, K.; Hjerten, S. *J. Chromatogr. A* **1996**, *753*, 227-234.
34. Xie, S.; Svec, F.; Frechet, J. M. J. *J. Chromatogr. A* **1997**, *775*, 65-72.
35. Alpert, A. J. *J. Chromatogr.* **1986**, *359*, 85-97.
36. Gong, B.; Wang, L.; Wang, C.; Geng, X.; *J. Chromatogr. A* **2004**, *1022*, 33-39.
37. Fexby, S.; Ihre, H.; Buelow, L.; Van Alstine, J. A. *J. Chromatogr. A* **2007**, *1161*, 234-241.
38. Kato, Y.; Nakatani, S.; Nakamura, K.; Kitamura, T.; Moriyama, H.; Hasegawa, M.; Sasaki, H. *J. Chromatogr. A* **2003**, *986*, 83-88.
39. Goheen, S. C.; Engelhorn, S. C. *J. Chromatogr.* **1984**, *317*, 55-65.
40. Maisano, F.; Belew, M.; Porath, J. *J. Chromatogr.* **1985**, *321*, 305-317.
41. Jennissen, H. P. J. *Chromatogr.* **1978**, *159*, 71-83.
42. Wu, S.; Figueroa, A.; Karger, B. L. *J. Chromatogr.* **1986**, *371*, 3-27.
43. Wang, Q.; Svec, F.; Frechet, J. M. J. *Anal. Chem.* **1993**, *65*, 2243-2248.

CHAPTER 4 PREPARATION OF MONOLITHS FROM SINGLE CROSSLINKING MONOMERS FOR REVERSED-PHASE CAPILLARY CHROMATOGRAPHY OF SMALL MOLECULES

4.1 Introduction

In order to obtain high column efficiency in high performance liquid chromatography (HPLC), the exchange of solute molecules (i.e., mass transfer) between the mobile and stationary phases should be fast and frequent. This requires the diffusion distance in the stationary phase to be small and the accessible stationary phase surface area to be large. A logical way to satisfy these requirements in particulate packed columns has been to decrease the particle size, since column efficiency is directly proportional to the particle diameter according to the van Deemter equation.[1] However, as the particle size decreases, the permeability of the packed bed decreases proportionally. The pressure drop of a perfectly packed column is inversely proportional to the square of the particle diameter. UHPLC pumps are now available, which makes it possible to achieve fast and high-resolution separations by utilizing sub-micron particles in packed columns;[2,3] however, further reduction in particle size is practically limited by the resulting backpressure and, consequently, enhancement of the column performance by simply reducing particle size is not practical.

Monolithic materials are continuous, porous structures characterized by mesopores and macropores. In terms of chromatography, a major advantage of monolithic columns is the ability to control and optimize separately the average sizes of the macropores or throughpores and the interconnected porous skeleton, which can be related to the particle diameter in packed columns.[4] Compared to packed columns, monolithic columns do not have structural void volumes due to poor packing, and the microglobular skeleton is highly

interconnected. This leads to more pores through which the mobile phase can flow. Therefore, most of the porous bed becomes available to the mobile phase, and mass transfer is facilitated by convective flow instead of pore diffusion. This difference in hydrodynamics allows high permeability and fast mass transfer. Since monoliths for LC were introduced approximately two decades ago, they have been applied in most of the LC separation modes. Excellent reviews have appeared that describe the preparation of monoliths and their applications in LC.[4-11]

Current monolithic LC columns can be divided into two major categories based on the nature of the material from which they are made, i.e., silica monoliths and organic polymer monoliths. Typical silica monoliths feature high surface areas (i.e., 300 m^2/g) which result from the significant volume of mesopores and micropores in the skeletal structure. These monoliths functionalized with octyl- or octadecyl- groups are well suited for rapid separation of small molecules.[12,13] Compared to silica-based monoliths, organic polymer-based monoliths are characterized by a wide variety of monomer chemistries and more simple preparation, as well as smaller surface areas (i.e., 20-30 m^2/g) due to their typically monomodal macropore distribution. Polymer monolithic stationary phases have attracted particular attention with regard to the separation of high-molecular-weight molecules such as proteins and nucleic acids,[14-16] since their highly porous structures devoid of small mesopores make them suitable for fast mass transfer of large molecules. In contrast, efficient separation of small molecules on polymer monoliths has been relatively unsuccessful because of low surface area. Following recent reports of methacrylate monoliths for the separation of small molecules,[17-19] several new approaches were recently explored to prepare polymer monoliths with larger surface areas, including termination of

polymerization reactions at an early stage,[20] copolymerization of different alkyl dimethacrylates with stearyl methacrylate,[21] and preparation of monoliths with hypercrosslinked structures which increase surface area.[22] Besides these approaches, there is another straightforward way to obtain highly crosslinked monolithic structures, i.e., by using a high concentration of crosslinking monomer.

A conventional polymerization mixture for monolith preparation contains initiator, functional monomer, crosslinking monomer and porogen or porogen mixture. Although the presence of crosslinker usually serves to ensure mechanical stability of the monolith, variation in the nature and concentration also influences the chemistry and morphology of the resulting monolith. It has been reported that a higher crosslinker concentration produces monoliths with greater surface areas.[23,24] The upper limit of crosslinker to monomer ratio is 100%, which is a single-monomer system. Chapter 3 demonstrated advantages with respect to monolith synthesis using a single-monomer system, including straightforward optimization of the polymerization solution, improved column-to-column reproducibility, better mechanical stability and higher surface area due to the highly crosslinked network.[25] Monolithic columns synthesized from tetra(ethylene glycol) diacryate were able to separate proteins and peptides in the size-exclusion mode, indicating the presence of a significant number of mesopores. Monoliths prepared from TVBS[26,27] and from BVPE[28,29] were effective in RPLC of small molecules as well as large biomolecules.

In this work, I describe monoliths prepared solely from four crosslinking monomers, i.e., BADMA, BAEDA (EO/phenol = 2 or 4) and PDAM. The structures of the four monomers are shown in Figure 4.1. As an extension of Chapter 2, porogen selection was discussed with the intention of obtaining data that could possibly lead to a rational porogen

selection strategy. The optimized monoliths were applied for RPLC of small molecules such as alkylbenzenes and alkyl parabens.

4.2 Experimental Section

4.2.1 Chemicals and Reagents

DMPA (99%), TPM (98%), BADMA, BAEDA (EO/phenol = 2 or 4), PDAM, poly(ethylene glycol)-*block*-poly(propylene glycol)-*block*-poly(ethylene glycol) (EPE-2800, Mn = ~ 2800), and poly(propylene glycol)-*block*-poly(ethylene glycol)-*block*-poly(propylene glycol) (PEP-2700, Mn = ~ 2700) were purchased from Sigma-Aldrich (St Louis, MO, USA). Propylbenzene, butylbenzene, pentylbenzene and uracil were also obtained from Sigma-Aldrich. Benzene and ethylbenzene were purchased from Fisher Scientific (Pittsburgh, PA, USA). Toluene was purchased from Mallinckrodt (Phillipsburg, NJ, USA). Methyl paraben, ethyl paraben, propyl paraben and butyl paraben were purchased from Fluka (Buchs, Switzerland). All porogenic solvents and chemicals for monolith and mobile phase buffer preparations were HPLC or analytical reagent grade, and were used as received. Buffer solutions were prepared with HPLC water, and filtered through a 0.22-μm membrane filter.

4.2.2 Polymer Monolith Preparation

Before filling with precursor solution, UV-transparent fused-silica capillary tubing (75-μm i.d., 375-μm o.d., Polymicro Technologies, Phoenix, AZ) was treated with TPM in order to covalently attach the polymer to the capillary wall. The treatment was taken from procedures developed by Vidič et al.[30] and Courtois et al.[31] and can be briefly summarized as: (1) washing step, in which a 5-m-long capillary was rinsed sequentially with ethanol and

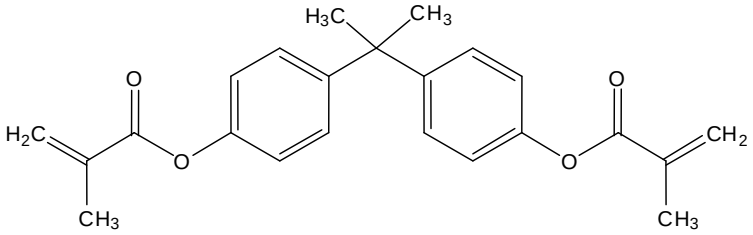

Bisphenol A dimethacrylate (BADMA)

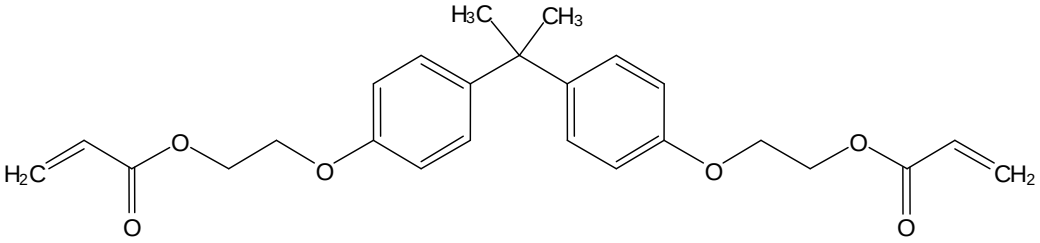

Bisphenol A ethoxylate diacrylate (BAEDA, EO/phenol = 2 or 4)

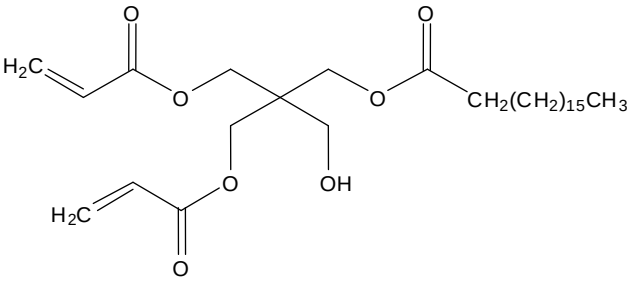

Pentaerythritol diacrylate monostearate (PDAM)

Figure 4.1. Chemical structures of monomers.

water to remove any impurities, (2) etching step, in which the capillary was filled with 1 M aqueous NaOH and heated to 120 ^{o}C for 3 h in a GC oven, (3) leaching step, in which the capillary was rinsed with water again, filled with 1 M HCl and heated to 110 ^{o}C for 3 h, (4) drying step, in which the capillary was rinsed with water and ethanol, and then dried at 120 ^{o}C for 1 h with a stream of nitrogen gas, (5) silanization step, in which the surface-activated capillary was filled with 15% (v/v) TPM in dry toluene at 35 ^{o}C overnight, and (6) drying step, in which the capillary was washed with toluene and acetone sequentially and then dried under a nitrogen gas purge at room temperature overnight. After treatment, the two ends of the capillary were sealed with rubber septa until synthesis of the monolith was started.

Monomer solutions were prepared in 1-dram (4 mL) glass vials by admixing initiator (DMPA), monomer, and porogen solvents (see Tables 4.1 and 4.2 for reagent compositions). The solution was vortexed and then degassed by sonicating for 3 min if nonvolatile solvents were used as porogens. If volatile reagents such as THF were used, the solution was vortexed and then sonicated for a few seconds to avoid excessive evaporation. A section of the silanized capillary was cut and filled with precursor solution using helium gas pressure. One end of the capillary was left empty for UV detection. After filling with solution, the capillary was sealed with rubber septa at both ends and placed directly under a PRX 1000-20 Exposure Unit UV lamp (390 ± 15 nm, 1000 W, TAMARACK Scientific, Corona, CA). Since bisphenol groups were contained in the monomers, which could absorb UV light, the polymerization time was investigated. Monoliths obtained after exposing with UV light for 3 and 5 min were found to have similar backpressures and morphology (based on SEM images), indicating that the reaction was finished within 3 min. A polymerization

Table 4.1. Compositions and Permeabilities of Selected Monoliths.

Monolith	Composition[a] (g/wt.%)[b]					Permeability (× 10^{-14} m^2)[c]		
	Monomer	Dimethyl formamide	Dodecanol	Tetrahydrofuran	Decanol	Acetonitrile	Methanol	Water
BAEDA-4	0.60/27.3	/	/	0.65/29.5	0.95/43.2	0.81	1.63	3.84
BAEDA-2	0.60/27.3	/	/	0.70/31.2	0.90/40.9	1.02	1.64	2.18
BADMA (1)	0.20/21.7	0.26/28.3	0.46/50.0	/	/	1.43	1.48	3.32
BADMA (2)	0.20/21.7	0.235/25.5	/	/	0.485/52.7	1.57	1.64	5.13

[a] All monoliths contained 1 wt% DMPA to monomer. [b] wt.% related to total polymerization mixture. [c] $k = \eta L u / \Delta p$, where η is the viscosity, L is the column length (15 cm in this case), u is the solvent linear velocity, and Δp is the column back pressure. The values for $u / \Delta p$ are based on plots of back pressure versus flow rate.

Table 4.2. Compositions and Permeabilities of Poly(PDAM) Monoliths.

Monolith	Composition[a] (g/wt.%)[b]					Permeability ($\times 10^{-14}$ m^2)[c]		
	PDAM	Tetrahydrofuran	Isopropyl alcohol	PEP-2700	EPE-2800	Acetonitrile	Methanol	Water
1	0.22/27.8	0.21/26.6	0.18/22.8	0.18/22.8	/	2.04	2.29	4.97
2	0.22/27.8	0.21/26.6	0.21/26.6	0.15/19.0	/	3.13	3.90	9.21
3	0.22/21.8	0.21/26.6	0.18/22.8	/	0.18/22.8	2.10	2.48	5.69
4	0.22/21.8	0.25/31.6	0.16/20.3	0.16/20.3	/	2.83	3.47	6.54

[a] All monoliths contained 1 wt% DMPA to monomer. [b] wt.% related to total polymerization mixture. [c] Permeabilities were calculated as in Table 4.1.

time of 4 min was selected for all monoliths to ensure complete conversion of the monomers. After the monolithic column was prepared, it was then flushed with methanol or acetonitrile and water sequentially using an HPLC pump to remove porogens and unreacted monomers.

SEM was used to provide direct visual images of the monolith surface structures using an FEI Philips XL30 ESEM FEG (Hillsboro, OR) without coating with a conducting gold layer.

4.2.3 Capillary Liquid Chromatography (CLC)

The CLC system was similar to that described in Chapter 2. Briefly, an UltiMate 3000 high pressure gradient LC system (Dionex, Sunnyvale, CA) equipped with an FLM-3300 nano flow manager (1:1000 split ratio) was used in all experiments. The system was operated with Chromeleon software. A 9-cm long 30-μm i.d. fused silica capillary was used as sample loop, and the injection volume was determined by manually controlling the injection time. The two mobile phase components for gradient elution of alkyl benzenes and alkyl parabens in RPLC were water (mobile phase A) and 90% acetonitrile in water (mobile phase B). The gradient delay time was approximately 2.4 min at 0.3 μL/min. On-column detection was performed using a Crystal 100 variable wavelength UV–vis absorbance detector. Chrom Perfect software (Mountain View, CA) was used for data collection and treatment. UV absorbance was monitored at 214 nm.

4.3 Results and Discussion

4.3.1 Preparation of Polymer Monoliths

There are two main concerns when designing a monolith for LC application, i.e., tuning the porous structure to allow the mobile phase to percolate through the monolithic bed at a reasonable pressure drop, and tailoring the surface chemistry to obtain the desired chromatographic selectivity. The porous structure is influenced by several variables, including initiator nature and concentration, total monomer to porogen ratio, monomer to crosslinker ratio, porogen nature and ratio of porogens if more than one porogen is used. The desired surface chemistry can be incorporated through direct polymerization of functionalized monomers or through surface modification of pre-formed monolithic matrices.

The most important factors that affect synthesis of the desired porous structure of a polymer monolith are the selection of porogen and proportions of monomer(s) and porogen(s). The solvents used as porogens for a poly(styrene-divinylbenzene) monolith were chosen as a reference for bisphenol A-containing monomers;[23,24] thus, a binary porogen system of toluene with dodecanol and THF with decanol were evaluated as starting point. The appropriate combinations of toluene with dodecanol or decanol formed rigid poly(BADMA) monoliths with toluene as a good solvent and a long-chain aliphatic alcohol as a poor solvent. However, the porosities of the resulting monoliths were found to be very sensitive to the porogen ratio. For example, a polymerization mixture containing 0.20 g BADMA, 0.42 g toluene and 0.30 g decanol formed monoliths that exhibited no back pressure; when the porogen compositions were changed to 0.44 g toluene and 0.28 g decanol, the monolithic column had a back pressure of 1.25 MPa/cm (182 psi/cm) at 0.3

μL/min using methanol and was observed in SEM images to shrink and detach from the capillary wall upon drying. These results led to the elimination of toluene from among the good porogen candidates. At the same time, the results also indicated that aromatic monomers and/or porogenic solvents could also be used for monolith synthesis in UV-initiated polymerization, although it is generally believed that the monolith precursor solution should not absorb UV light to any significant degree.[5] However, larger dimension molds or UV lamps with lower intensity were not investigated in this work.

Toluene was then replaced by THF as the good solvent. Figure 4.2 shows the relationship of column back pressure for BAEDA-2, BAEDA-4 and BADMA monoliths as a function of varying ratio of the two porogens. The ratio of monomer to total porogens was set at 27.3:72.7 by weight for BAEDA-2 and BAEDA-4 monoliths for evaluation of consistency, rigidity and column pressure drop. For BADMA monoliths, the monomer concentration was reduced a little more, and weight percentages of 21.7% monomer and 78.3% total porogens were adopted for all porogen system studies. All data points in Figure 4.2 represent rigid monoliths that contain through-pores. As indicated in Figure 4.2A, THF and decanol were effective in forming rigid monoliths from BAEDA-2 and BAEDA-4 with THF as good solvent and decanol as poor solvent. Actually, the two monomers were not soluble in decanol at room temperature. Similar to what was observed in previous work from Lee's group,[16,25] the lowest back pressure was obtained by combining the two porogens. For both monomers, when THF was less than 0.40 g (18.2 wt.%), the precursor solution became immiscible, while a higher THF concentration (higher than the right two data points in Figure 4.2A) produced polymers with extremely small pores or transparent gels. Figure 4.3 shows SEM images of selected BAEDA-2 monoliths. Monoliths with lower

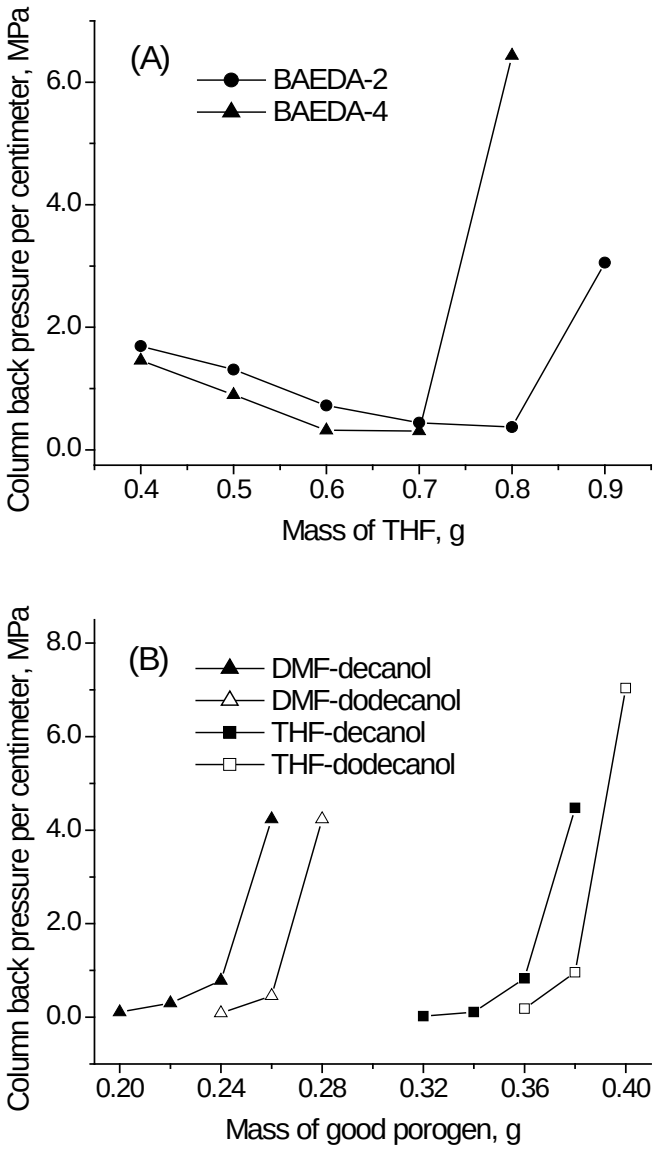

Figure 4.2. Effect of porogen nature and porogen ratio on back pressure of (A) poly(BAEDA-2) and poly(BAEDA-4) monoliths and, (B) poly(BADMA) monoliths. Monolith composition: (A) 0.006 g DMPA, 0.6 g monomer and 1.6 g total porogens (THF and decanol), and (B) 0.002 g DMPA, 0.2 g BADMA and 0.72 g total porogens. The back pressure for each data point was averaged from two or three columns using methanol at 0.3 μL/min (RSD ≤ 11%; in most cases, less than 7.0%).

back pressure contained larger microglobules and microglobule clusters (Figure 4.3B), while monoliths that exhibited higher back pressure were composed of microglobules that were much smaller in size (Figures 4.3A and 4.3C). The finer structure resulting from 0.90 g (40.9 wt.%) THF can be readily explained by later phase separation during polymerization because of the presence of a higher ratio of good solvent; however, the exact reason was not clear about why further decrease in the THF concentration also produced monoliths with finer structure. BAEDA-4 monoliths shown in Figure 4.4 had a different morphology than BAEDA-2 monoliths. Distinct microglobules were not observed; instead, the monolith resembled a fused skeletal structure. All BAEDA-4 monoliths represented by data points in Figure 4.2 featured similar morphologies as shown in Figure 4.4; however, they were different in porosity. With higher concentration of THF, the throughpores were smaller in size and the monoliths became less porous, resulting in lower permeability. The bright areas in Figure 4.4 were caused by charging during acquisition of SEM images.

THF with decanol or dodecanol were also suitable porogens for forming rigid BADMA monoliths. However, the pressure drop was much more sensitive to the ratio of the two porogens compared to the BAEDA-2 and BAEDA-4 monoliths. Since THF is highly volatile, the reproducibility of column preparation was not acceptable. Therefore, I investigated other nonvolatile solvents to replace THF as the good porogen, and DMF was found to be effective. Although variation in DMF concentration also influenced the column back pressure of the resulting monoliths (Figure 4.2B), using DMF significantly improved column reproducibility. The morphology of BADMA monoliths was similar to BAEDA-2 monoliths (Figure 4.5). With more concentrated good porogenic solvent, the resulting

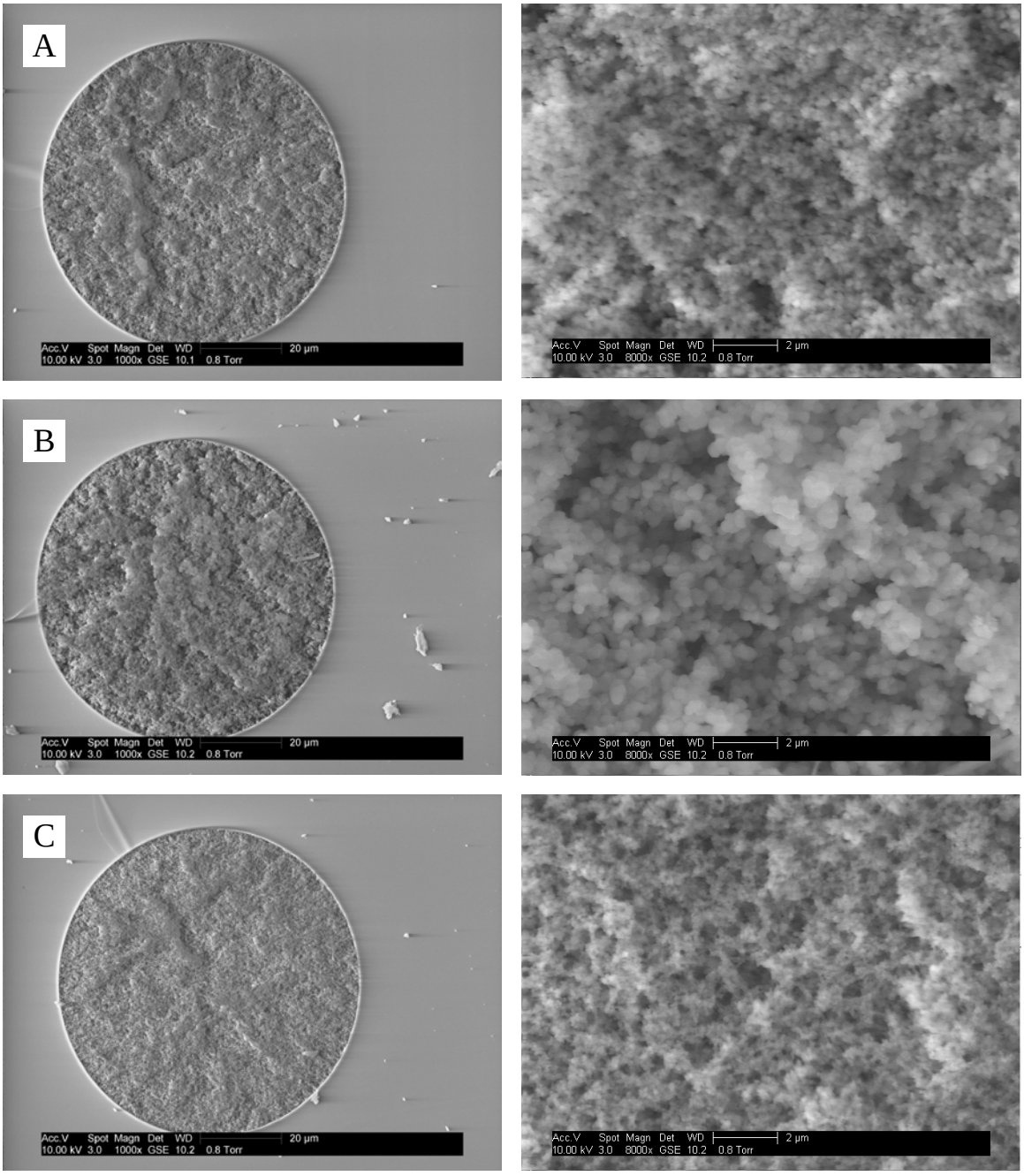

Figure 4.3. SEM images of BAEDA-2 monoliths. (A) 0.60 g BAEDA-2, 0.40 g THF, and 1.20 g decanol, (B) 0.60 g BAEDA-2, 0.70 g THF, and 0.90 g decanol (monolith BAEDA-2 in Table 4.1), and (C) 0.60 g BAEDA-2, 0.90 g THF, and 0.70 g decanol. The images on the right are taken from images on the left at a higher magnification.

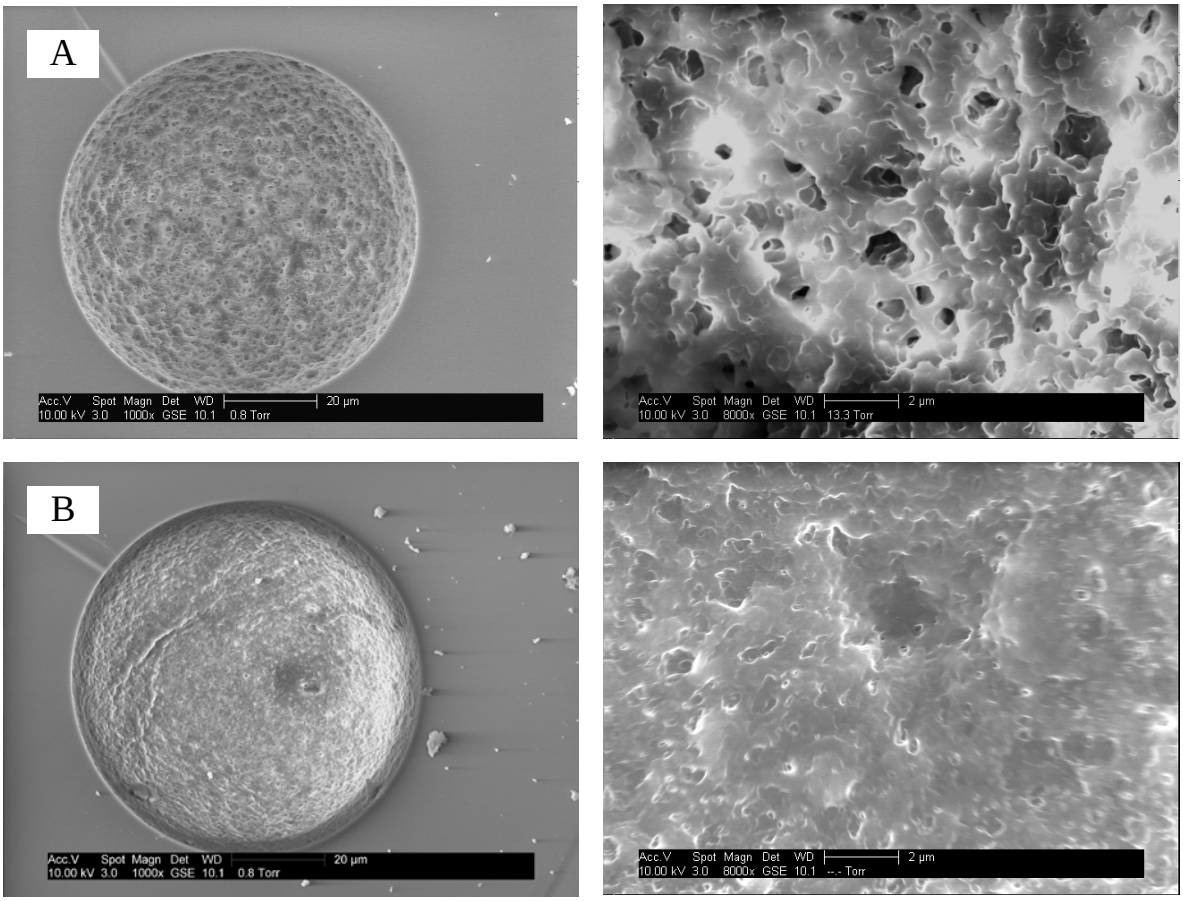

Figure 4.4. SEM images of BAEDA-4 monoliths. (A) 0.60 g BAEDA-4, 0.65 g THF, and 0.95 g decanol (monolith BAEDA-4 in Table 4.1), and (B) 0.60 g BAEDA-4, 0.80 g THF, and 0.80 g decanol.

monoliths exhibited higher back pressure, since both microglobules and microglobule clusters, as well as throughpores, became smaller in size. This tendency was observed for all four binary porogen systems indicated in Figure 4.2B. It was also observed that monoliths with comparable pressure drops shared similar morphology based on their SEM images. It is worth mentioning that the monolith shown in Figure 4.5A was highly permeable and may be useful in applications requiring fast separation.

The selection of suitable porogenic solvents to form a rigid PDAM monolith proved to be challenging. PDAM was used as a single monomer to synthesize a monolith for CEC,[32] and as a crosslinking monomer to copolymerize with a low concentration of 2-sulphoethyl methacrylate (SEMA) for mixed-mode reversed-phase and IEC.[33] In both studies, a ternary porogenic solvent made of cyclohexanol or pentanol, ethylene glycol and water was employed to produce pores. The optimized polymerization composition reported in the former paper,[32] which contained 30 wt.% PDAM, 55.5 wt.% cyclohexanol, 12.0 wt.% ethylene glycol and 2.5 wt.% water, were evaluated in this study, and the resulting polymer was more like a gel than a porous monolith. It was also found in the later study[33] that a small amount of EDMA had to be added to the mixture to improve the mechanical stability of the poly(PDAM) or poly(PDAM-co-SEMA) monoliths, making these monoliths suitable for applications in CLC. Thanks to fast column preparation using UV-initiated polymerization, we were able to test different solvents within a reasonable time period. However, all tested often-used solvents or their combinations, including hexane, toluene, THF, ethyl ether, DMF, ethylene glycol, PEG (Mn = 200 or 400), methanol, IPA, and long chain alcohols such as decanol or dodecanol, were not effective in forming rigid PDAM monoliths. Most of them produced either gel or immiscible mixtures with PDAM, which

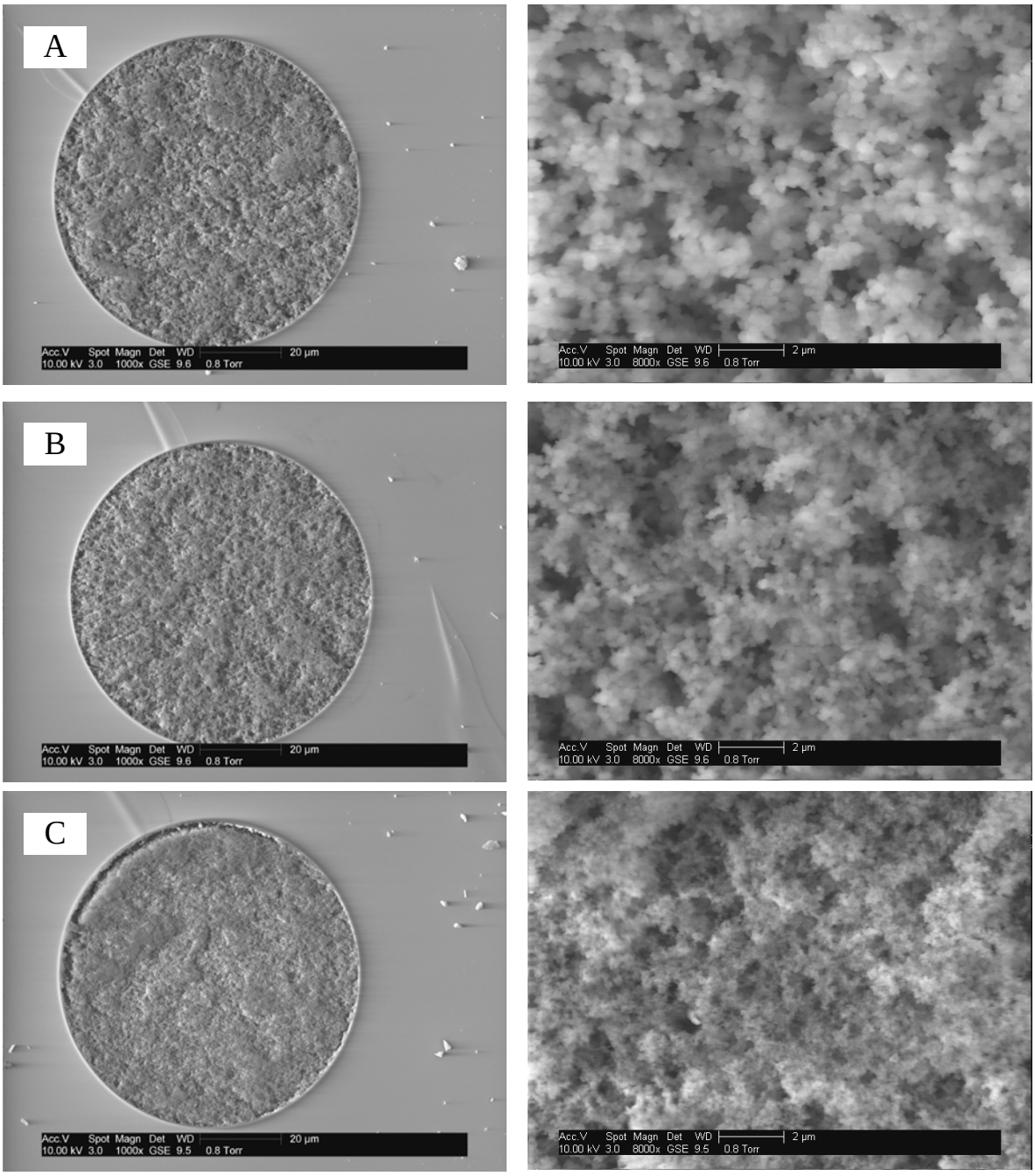

Figure 4.5. SEM images of BADMA monoliths. (A) 0.20 g BADMA, 0.24 g DMF, and 0.48 g dodecanol, (B) 0.20 g BADMA, 0.26 g DMF, and 0.46 g dodecanol (monolith BADMA (1) in Table 4.1), and (C) 0.20 g BADMA, 0.26 g DMF, and 0.46 g decanol.

meant that they were either too good or too poor as solvents. This is mainly because PDAM has a unique molecular structure which contains both highly hydrophobic long-chain alkyl and hydrophilic hydroxyl groups.

Considering that the structure of the PDAM monomer is similar to a surfactant, it was predicted that some nonionic surfactants might be potential porogen candidates. Thus, triblock copolymers with different molecular weights were tried. Poly(alkylene oxide) block copolymers and alkyl poly(ethylene oxide) oligomeric surfactants have been reported to form highly ordered mesoporous silica structures.[34] Lee's group also synthesized monoliths that exhibited an enhanced fraction of mesopores by using triblock poly(ethylene oxide)-poly(propylene oxide)-poly(ethylene oxide) (PEO-PPO-PEO) or PPO-PEO-PPO copolymers.[35] Although combinations of a triblock copolymer with a good solvent such as THF were also not effective in forming rigid monoliths, it was found that the resulting polymer had a slightly white color rather than being totally transparent. This might indicate that the polymer contained extremely small pores, and the triblock copolymer porogens were intermediate between a good solvent such as THF and a poor solvent such as IPA. By combining appropriate ratios of these three solvents, PDAM was able to form rigid monoliths. Several PDAM monoliths are listed in Table 4.2, and their SEM images are shown in Figure 4.6. As can be observed, the PDAM monoliths exhibited the conventional morphology of polymer monoliths. PEP-2700 and EPE-2800 produced similar monolith structure and porosity as shown in Figure 4.6A, while the monoliths became more porous and the microglobules were slightly larger in size with higher concentration of IPA (Figure 4.6B). An increase in THF from 0.21 to 0.25 g (from 26.6 to 31.6 wt.%) did not produce a less porous structure. Instead, the resulting monoliths had higher permeability.

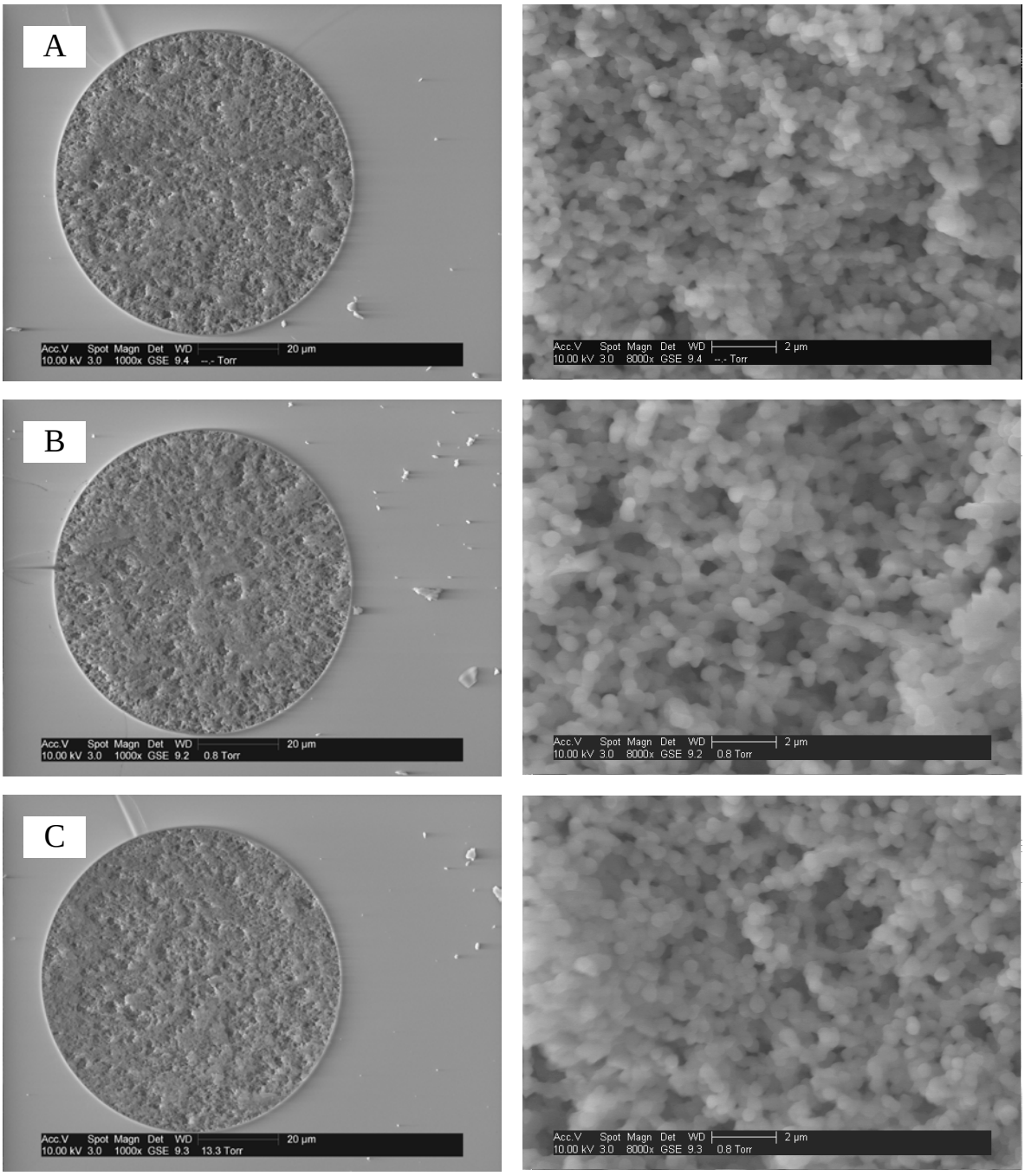

Figure 4.6. SEM images of PDAM monoliths. (A) as monolith (1) in Table 4.2, (B) as monolith (2) in Table 4.2, and (C) as monolith (4) in Table 4.2.

4.3.2 Porogen Selection

Once the monomers are selected to design a monolithic stationary phase, the critical step remaining is to find an appropriate porogenic solvent or solvent combination to form rigid monoliths with throughpores that enable the flow of mobile phase at a reasonable pressure drop. Although modern monolith techniques have been studied for two decades, to date, there are still no generally-accepted theories for porogen selection. Dipole moment or polarity is one solvent property that is considered when selecting porogenic solvents. In the work conducted by Courtois et al,[36] it was predicted that porogens that exhibit high dipole moment values were likely to produce monoliths with small pore diameter for the monomer system containing glycidyl methacrylate, triethylene glycol dimethacrylate and trimethylol-propane trimethacrylate. Similar results were found in my previous work. When I prepared poly(hydroxyethyl acrylate-*co*-triethylene glycol diacrylate) monoliths (Chapter 2), the replacement of methanol with water resulted in monoliths with lower permeability. Another solvent property that was proposed as a guideline for porogen selection is the solubility parameter (δ) for monomers and solvents.[21] Solubility is an often-used guideline for selecting the appropriate solvents for preparing macroporous copolymer beads.[37] If the solvent has a similar δ value as the monomer, the solvent can be considered to be a good solvent, while the solvent is a poor solvent for the monomer if there is a large difference between the two δ values.

BADMA was chosen as an example monomer to study in detail. Polarity was first used as a guideline to select the porogens as usual. It was found that BADMA formed a soft or hard transparent gel after polymerization when dissolved in toluene, THF, DMF or DMSO, indicating these were good solvents for BADMA. They were able to form rigid

macroporous monoliths when combined with decanol or dodecanol. To produce monoliths with similar permeability, the required weight amounts of these four solvents were: toluene>THF>DMF>DMSO. The polarity index values for these solvents are DMSO>DMF>THF>toluene (i.e., 7.2, 6.4, 4.0 and 2.4, respectively). These results agreed with the prediction that more polar solvents are likely to produce smaller pores. This is clearly demonstrated in Figure 4.2B; less DMF was needed than THF to produce monoliths with similar back pressure. It was also observed that the column back pressure was more sensitive to the porogen ratios when DMF or THF was combined with dodecanol than with decanol. This was because the polarities between the two good solvents and dodecanol were more different than decanol. However, similar curves for DMF-decanol and THF-decanol (or DMF-dodecanol and THF-dodecanol) were observed, indicating that solvent polarity is not the only property that determines the porogen effect. Other often-used solvents, including ethyl ether, acetonitrile, IPA, methanol and cyclohexanol, were also evaluated for BADMA monolith synthesis. White soft polymers were obtained after polymerization using ethyl ether and acetonitrile as solvents, which indicated that they could potentially be poor. However, they were not able to form rigid monoliths when combined with DMF (Note: combinations with the other three good solvents were not tested). Furthermore, the polarity index of ethyl ether (i.e., 2.8) is close to toluene, and that of acetonitrile (i.e., 5.8) is also between THF and DMF, but they formed totally different polymer morphologies. BADMA was not soluble in methanol, IPA, cyclohexanol, decanol or dodecanol at room temperature. Despite this observation, only decanol and dodecanol were able to form rigid porous monoliths when combined with DMF.

The solubility parameter (δ) was also investigated in this study. The δ values for toluene, THF, DMF and DMSO are 18.3, 18.5, 24.7, and 26.4 $MPa^{1/2}$ respectively (SI Hildebrand values from Barton, *Handbook of Solubility Parameters*, CRC Press, 1983). Although the values vary from 18.3 to 26.4, these solvents could all be good solvents for BADMA. For comparison, the δ values for acetonitrile, ethyl ether, cyclohexanol and methanol are 23.8, 15.4, 22.4 and 29.7 respectively. Both acetonitrile and cyclohexanol have δ values that are close to DMF, but they exhibited totally different porogen effects in BADMA polymerization. Thus, similar to polarity, the solubility parameter is not the only property that contributes to the porogen effect in monolith synthesis. Compared to polarity, the solubility parameter is less often used when selecting porogens, which is probably because it is more difficult to obtain solubility parameter data. Researchers still prefer to look for appropriate porogenic solvents based on their experience and published work from others. In the case of PDAM, it was more difficult to find the proper solvents to form rigid monoliths if only polarity or solubility of the solvents was considered.

4.3.3 Separation of Small Molecules

Compared to the number of reports of the successful separation of large-molecular-weight compounds using organic polymer monoliths, only a handful have been successful for small molecules due to the general lack of mesopores in polymer monoliths. Monoliths synthesized from single crosslinking monomers in this study provided excellent separation of small molecules such as alkyl benzenes and alkyl parabens. This was because smaller microglobules were formed during polymerization, leading to more mesopores and larger surface areas.

Figure 4.7 shows the gradient elution of uracil, benzene, toluene, ethylbenzene, propylbenzene, butylbenzene and pentylbenzene using the monolithic columns listed in Table 4.1. The flow rate was 0.3 μL/min and the gradient was 40% - 100 % B in 10 min. As can be seen in Figure 4.7, all peaks have high symmetries and narrow peak widths at half peak height ranging between 8.2 and 3.7 s for alkyl benzenes. BAEDA-4 monoliths showed greater retention for alkyl benzenes than BAEDA-2 monoliths, which was very likely caused by dipole-dipole interactions between the solutes and the BAEDA-4 monolithic stationary phases. The longer chain length of the BAEDA-4 molecule may also contribute to greater retention, which causes the bisphenol functionalities to stick out and enable better interaction with solutes. BADMA monoliths synthesized using the four binary porogen systems indicated in Figure 4.2B with similar permeability had almost identical chromatographic performance for the separation of alkyl benzenes. The results from monoliths using THF as good porogen were not shown in this report, since the reproducibility of column preparation was not satisfactory. This demonstrates that changes in porogen composition do not affect the surface chemistry in single-monomer synthesis approach.[25] All of the BADMA monoliths retained alkyl benzenes more than BAEDA-2 and BAEDA-4 monoliths, and the resolution was also better. BADMA monolithic columns also exhibited better resolution of alkyl parabens as shown in Figure 4.8. In contrast to chromatograms of alkyl benzenes, alkyl parabens were retained more on BAEDA-4 monoliths compared to BADMA monoliths, indicating that dipole-dipole interaction was the dominating factor that affected retention.

Figure 4.9 shows the elution of alkyl benzenes using PDAM monolithic columns with different gradients and flow rates. The six compounds were eluted within 8 min with

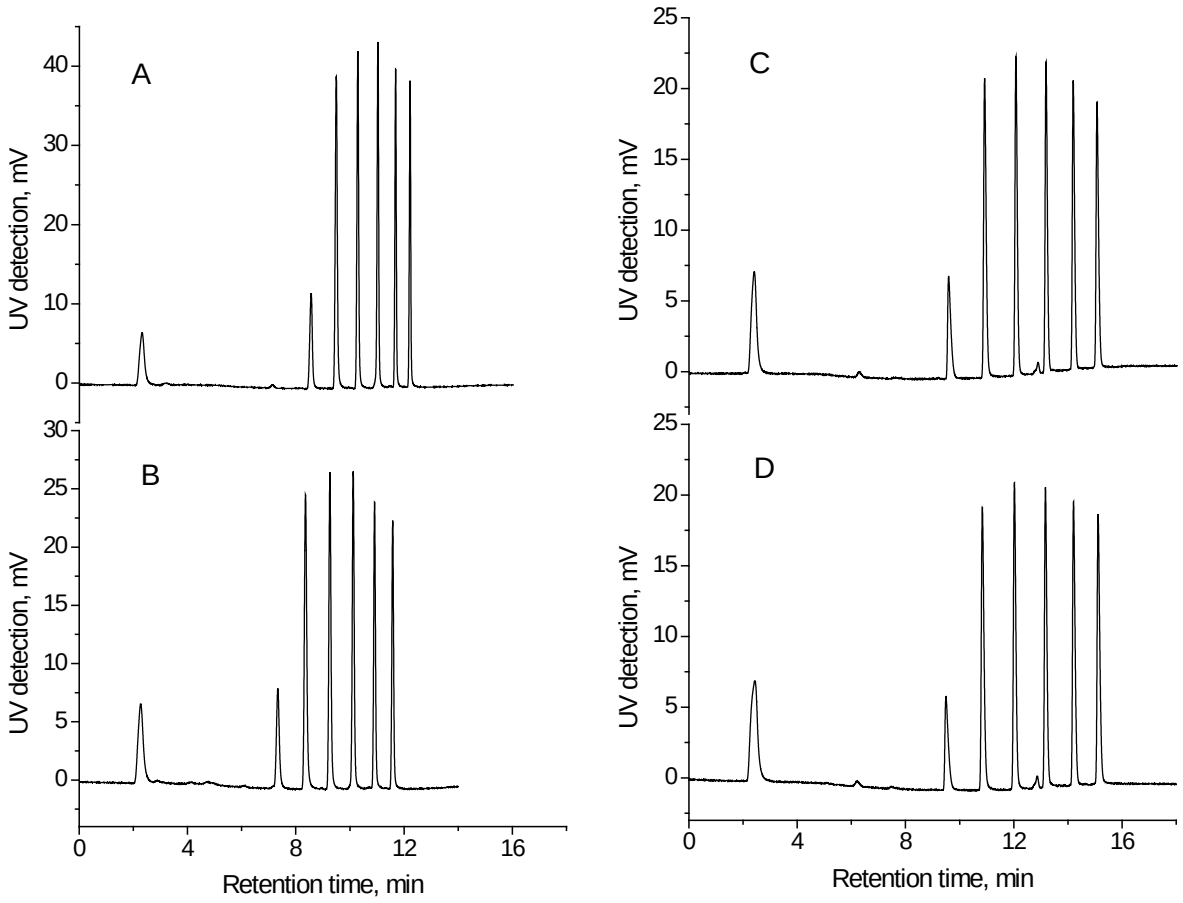

Figure 4.7. Separations of alkyl benzenes using monolithic columns (A) BAEDA-4, (B) DAEDA-2, (C) BADMA (1), and (D) BADMA (2) in Table 4.1. Conditions: 16 cm × 75 µm i.d. monolithic column; mobile phase A was water, and buffer B was 90% acetonitrile in water; linear A-B gradient from 40% to 100% B in 10 min, and then isocratic elution with 100% B; 0.3 µL/min flow rate; on-column UV detection at 214 nm. Peak identifications: uracil, benzene, methylbenzene, ethylbenzene, propylbenzene, butylbenzene and pentylenzene in order of elution.

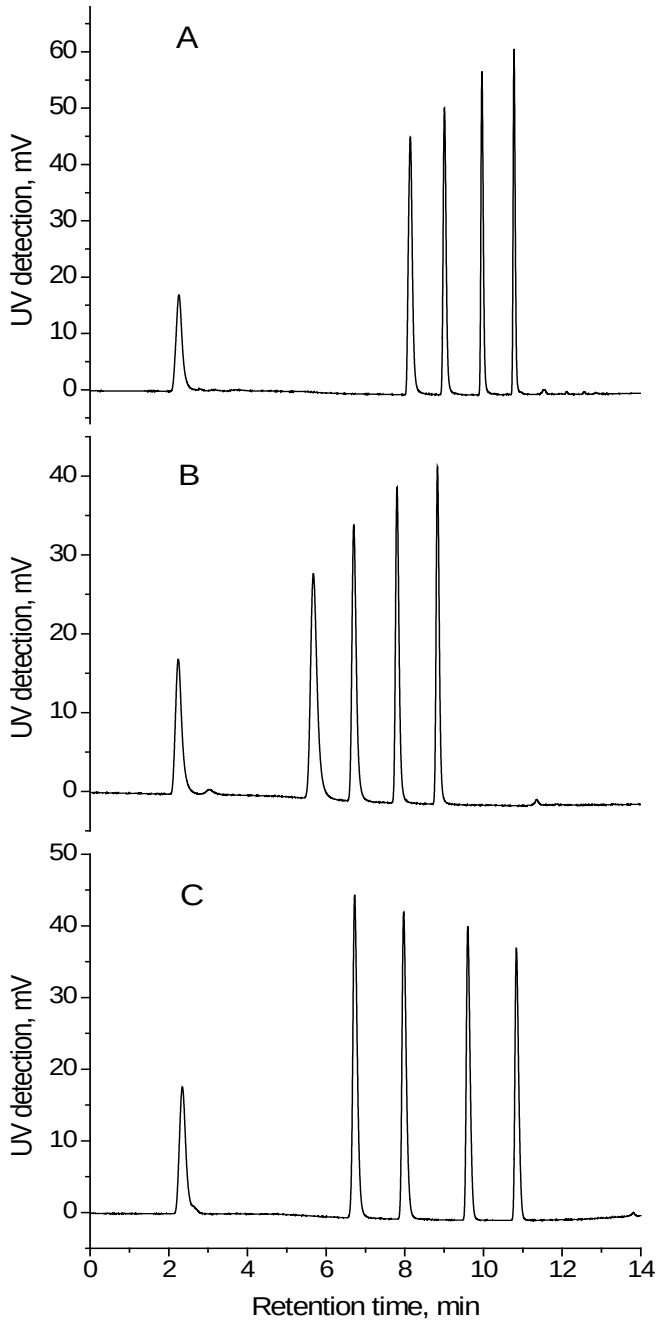

Figure 4.8. Separations of alkyl parabens using monolithic columns (A) BAEDA-4, (B) DAEDA-2, and (C) BADMA (1) in Table 4.1. Conditions: linear A-B gradient from 30% to 100% B in 10 min, and then isocratic elution with 100% B; other conditions are the same as in Figure 4.7. Peak identifications: uracil, methyl paraben, ethyl paraben, propyl paraben and butyl paraben, in order of elution.

high resolution using a 5 min gradient from 40% - 100% B in 10 min and a flow rate of 0.6 uL/min. As expected, a shallower gradient required longer elution time and, at the same time, provided better resolution. For example, the resolution of butylbenzene and pentylbenzene was 4.28 and 5.40 in Figures 4.9A and 4.9B, respectively. Compared with BADMA monolithic columns, the alkyl benzenes were separated better from each other on PADM monolithic columns. Since the column pressure drop can be higher, it should be possible to improve the column efficiency of PADM monolithic columns by further optimizing the precursor composition. Separations of alkyl parabens using PDAM monolithic columns are shown in Figure 4.10. The PDAM monolith showed less retention for alkyl parabens than the BADMA monolith due to the hydroxyl group in PDAM. However, a higher aqueous content in the mobile phase was not appropriate for the separation since peaks with shoulders were observed due to the hydrophobic character of the alkyl parabens.

The plate numbers of all monolithic columns listed in Tables 4.1 and 4.2 were between 20,000 and 30,000 plates/m measured using uracil at 0.1 uL/min (i.e., 0.38 mm/s), which was the optimized flow rate for the BAEDA-4 monolithic column based on the van Deemter curve shown in Figure 4.11. The performance of these columns was comparable to or better than the performance of previously reported polymer monoliths.[21,26,28,38] If retained compounds such as ethylbenzene or propylbenzene were used to measure the efficiency, the plate values would be higher. Since the injection volume was found to have a large influence on the measurement of efficiency (i.e., the loop volume together with the dead volume was estimated to be larger than 170 nL), a smaller volume was injected by manually switching the injector valve. The lower number of column plates obtained using

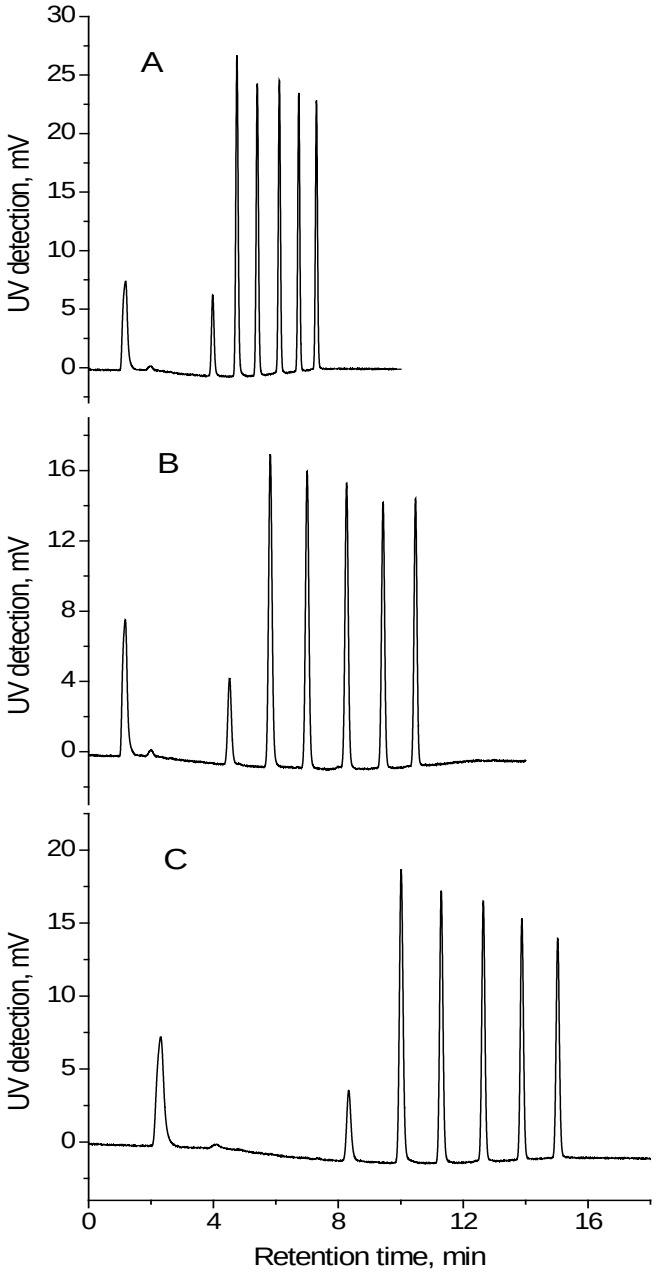

Figure 4.9. Separations of alkyl benzenes using poly(PDAM) monolithic column (2) in Table 4.2 for panels (A) and (B), and column (1) in Table 4.2 for panel (C). Conditions: linear A-B gradient from 40% to 100% B in (A) 5 min, 0.6 µL/min flow rate, (B) 10 min, 0.6 µL/min flow rate, and (C) 10 min, 0.3 µL/min flow rate; other conditions are the same as in Figure 4.7.

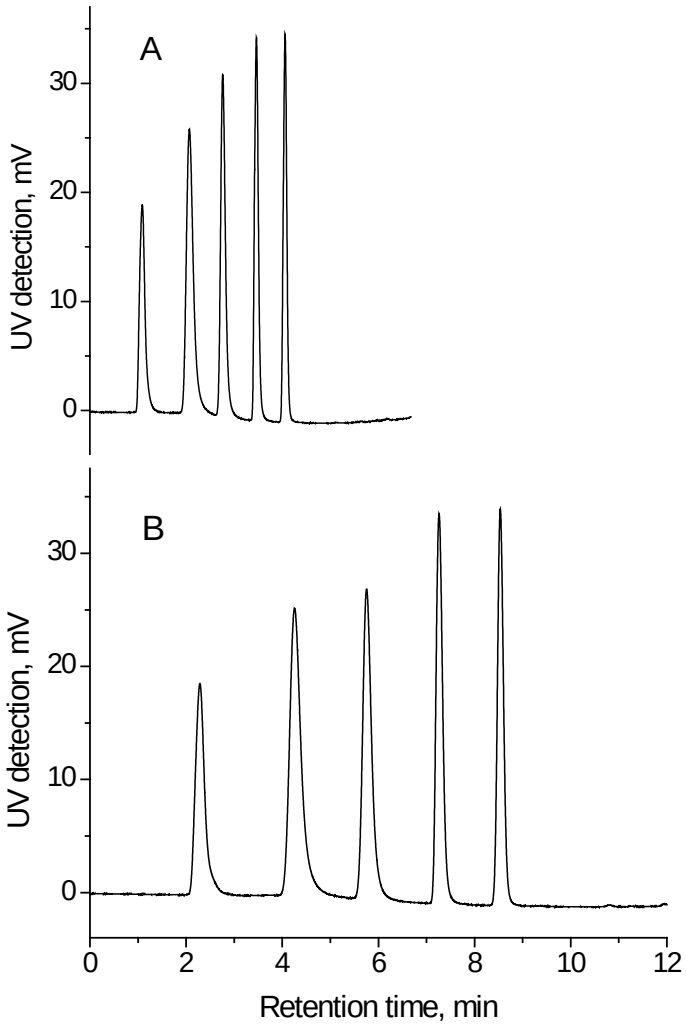

Figure 4.10. Separations of alkyl parabens using poly(PDAM) monolithic column 2 in Table 4.2 for panel A, and column 4 in Table 4.2 for panel B. Conditions: linear A-B gradient from 30% to 100% B in (A) 5 min, 0.6 µL/min flow rate, and (B) 10 min, 0.3 µL/min flow rate; other conditions are the same as in Figure 4.8.

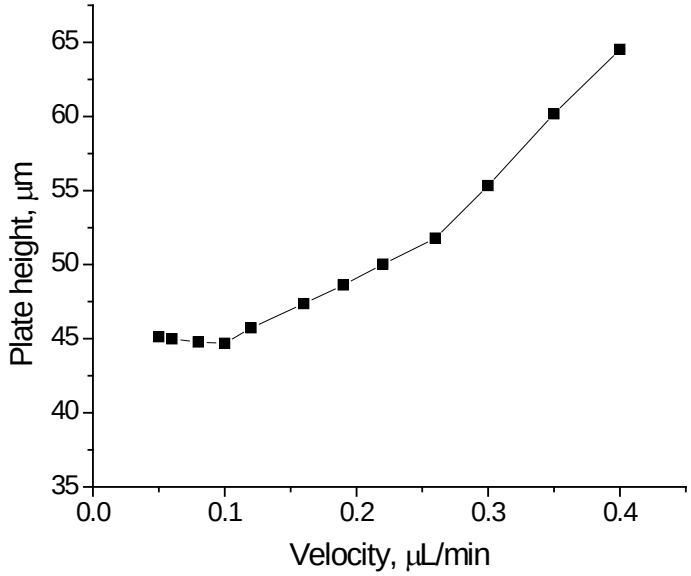

Figure 4.11. Plate height versus volumetric floe rate for a poly(BAEDA-4) monolithic column using uracil as an unretained compound. Conditions: 16 cm × 75 μm i.d. column; 70% A/30% B mobile phase.

unretained uracil was very likely due to disturbance from the valve movement which resulted in peak broadening.

4.3.4 Permeability

Column permeability was determined to evaluate the stability of the monolith. To obtain plots of back pressure versus flow rate, acetonitrile, methanol and water were pumped through a 15-cm long monolithic column at flow rates from 0.1 to 0.5 μL/min. Linear relationships between back pressure and flow rate ($R>0.999$ for all monoliths) clearly demonstrated the mechanical stability of all the monoliths. As an example, Figure 4.12 shows plots for three monolithic columns. The calculated permeabilities based on slopes of back pressure versus flow rate are listed in Tables 4.1 and 4.2. All monoliths were found to shrink slightly in polar solvents, resulting in higher permeability in water. BAEDA-2 and BAEDA-4 monoliths swelled slightly in acetonitrile, which contributed to the sharper peaks observed in Figures 4.7 and 4.8. The permeability values also revealed that variations in porogen nature or ratio altered the mechanical stability, which was demonstrated using the BADMA monoliths in Table 4.1 and comparison between the monoliths in Table 4.2.

4.3.5 Reproducibility and Stability

In addition to good chromatographic performance, reproducibility and stability are basic requirements for a monolithic column, especially when the column is supposed to be used in routine analysis. Run-to-run reproducibility was measured for all monolithic columns listed in Tables 4.1 and 4.2. The RSD values based on retention times were all within 1.2% and, in most cases, less than 0.50%. Several higher RSD values were mainly

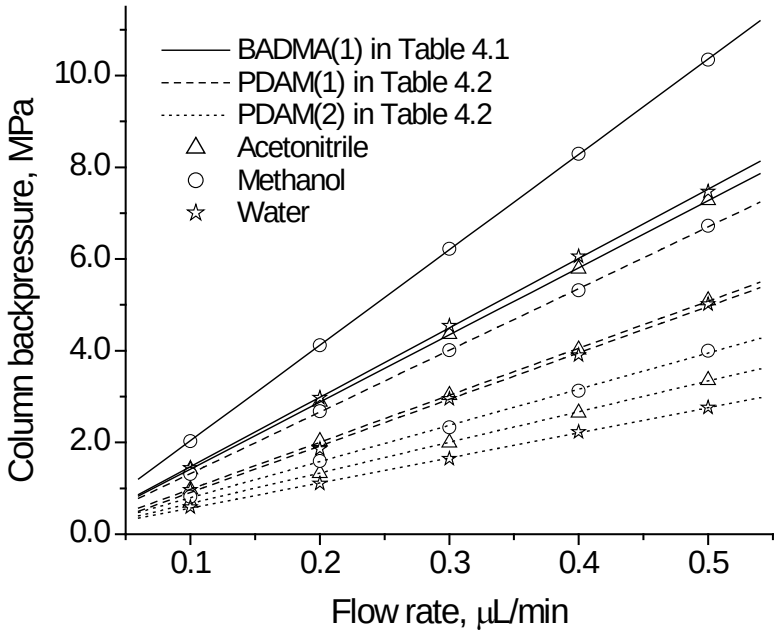

Figure 4.12. Effect of mobile phase flow rate on column back pressure. Conditions: 15 cm × 75 μm i.d. monolithic column.

caused by instability in the pumps or gradient mixing system based on observations during experiments. The RSD values for peak areas were larger, ranging between 2.5% and 6.8%. This was because slight changes in sample concentration and injection volume also contributed to the deviation in CLC. More than 60 runs were conducted to test the stability of BADMA(1) monolithic column in Table 4.1 and PDAM(1) monolithic column in Table 4.2. There was no noticeable change observed in column performance, indicating these two columns were stable for at least 60 runs.

Column-to-column reproducibility was investigated for the above two columns, and the results were quite good. The RSD values were within 1.2% based on retention times, and within 7.5% based on peak areas. Despite that fact that the pressure drop of the BADMA monolith was sensitive to the porogen ratio, the reproducibility of the column back pressure was acceptable, i.e., 8.2% RSD for BADMA(1) monolithic columns and 6.8% RSD for PDAM(1) monolithic columns. As an example, chromatographic performance of three independently prepared BADMA(1) monolithic columns were compared as shown in Figure 4.13. The RSD values for alkyl benzenes were between 0.18% and 0.38% for retention time, and between 1.2% and 7.4% for peak area. Both chromatographic performance and permeability provide strong evidence that monolith fabrication is highly reproducible.

Due to the highly crosslinked network, monoliths synthesized from single crosslinking monomers exhibited improved stability.[25] In this study, SEM images of BADMA(1) and PDAM(1) monolithic columns were taken before and after they were stored at room temperature for one week. There was no noticeable change observed for

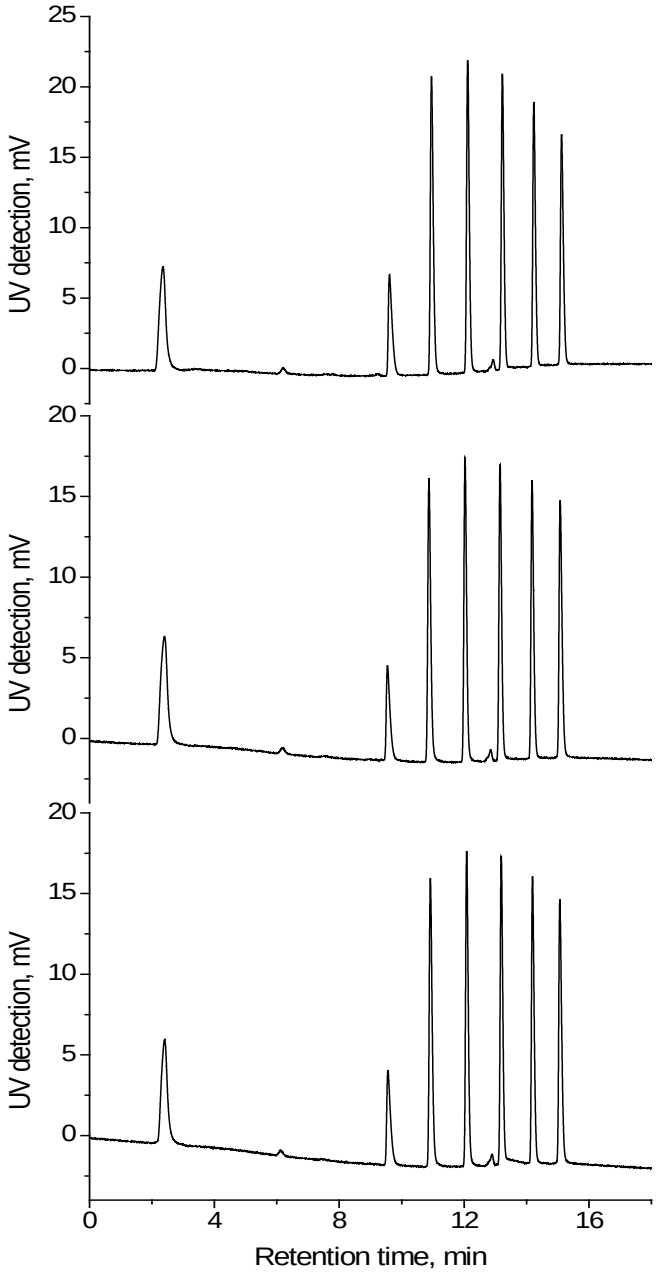

Figure 4.13. Separation of alkyl benzenes showing column-to-column reproducibility of three independently prepared poly(BADMA) monolithic columns. Conditions are the same as in Figure 4.7C.

either column, indicating that they can be stored without sealing the ends. Performance before and after being stored dry at room temperature will be investigated in future work.

4.4 Conclusions

Reversed-phase stationary phases possessing low flow resistance and separation efficiency of approximately 3500 plates for 16 cm length were produced by in situ UV-initiated polymerization of single crosslinking monomers BAEDA-4, BAEDA-2, BADMA and PDAM. Due to enhanced surface areas resulting from highly crosslinked structures, separations of alkyl benzenes and alkyl parabens were demonstrated using these columns. The single-monomer synthesis approach is promising for the preparation of polymer monoliths for chromatography of small molecules. The column-to-column reproducibility was good with RSD below 1.2% based on retention times and 7.4% based on peak areas. The good reproducibility of column fabrication was mainly attributed to the single-monomer synthesis. The monolithic columns demonstrated little shrinkage or swelling in solvents of different polarity, demonstrating their mechanical stability.

The strategy for porogen selection for preparation of the monoliths was investigated by evaluating different solvents for BADMA monolith synthesis. The proposed solvent properties of polarity and solubility were used as guidelines for porogen selection, and my investigations indicated that neither of them could be used alone to predict the porogen effects. To rationally select porogenic solvents, a more complicated strategy must be applied and additional solvent properties should be considered. However, when the porogenic solvents are similar in other properties, polarity can be a good characteristic to predict porogen behavior. Furthermore, a single-monomer system makes it easier to predict the effects of porogens than conventional multi-monomer systems.

4.5 References

1. Van Deemter, J. J.; Zuiderweg, F. J.; Klinkenberg, A. *Chem. Eng. Sci.* **1995**, *50*, 3869-3882.
2. MacNair, J. E.; Lewis, K. C.; Jorgenson, J. W. *Anal. Chem.* **1997**, *69*, 983-989.
3. Wu, N.; Collins, D. C.; Lippert, J. A.; Xiang, Y.; Lee, M. L. *J. Microcolumn Sep.* **2000**, *12*, 462-469.
4. Guiochon, G. *J. Chromatogr. A* **2007**, *1168*, 101-168.
5. Svec, F. *J. Chromatogr. A* **2010**, *1217*, 902-924.
6. Vlakh, E. G.; Tennikova, T. B. *J. Chromatogr. A* **2009**, *1216*, 2637-2650.
7. Vlakh, E. G.; Tennikova, T. B. *J. Sep. Sci.* **2007**, *30*, 2801-2813.
8. Svec, F. *J. Sep. Sci.* **2004**, *27*, 747-766.
9. Svec, F. *J. Sep. Sci.* **2004**, *27*, 1419-1430.
10. Cabrera, K. *J. Sep. Sci.* **2004**, *27*, 843-852.
11. Tanaka, N.; Kobayashi, H.; Ishizuka, N.; Minakuchi, H.; Nakanishi, K.; Hosoya, K.; Ikegami, T. *J. Chromatogr. A* **2002**, *965*, 35-49.
12. Nunez, O.; Ikegami, T.; Miyamoto, K.; Tanaka, N. *J. Chromatogr. A* **2007**, *1175*, 7-15.
13. Hara, T.; Kobayashi, H.; Ikegami, T.; Nakanishi, K.; Tanaka, N. *Anal. Chem.* **2006**, *78*, 7632-7642.
14. Premstaller, A.; Oberacher, H.; Huber, C. G. *Anal. Chem.* **2000**, *72*, 4386-4393.
15. Gu, B.; Chen, Z.; Thulin, C. D.; Lee, M. L. *Anal. Chem.* **2006**, *78*, 3509-3518.
16. Li, Y.; Tolley, H. D.; Lee, M. L. *Anal. Chem.* **2009**, *81*, 9416-9424.
17. Eeltink, S.; Herrero-Martinez, J. M.; Rozing, G. P.; Schoenmakers, P. J.; Kok, W. T. *Anal. Chem.* **2005**, *77*, 7342-7347.
18. Ueki, Y.; Umemura, T.; Iwashita, Y.; Odake, T.; Haraguchi, H.; Tsunoda, K. *J. Chromatogr. A* **2006**, *1106*, 106-111.
19. Huo, Y.; Schoenmakers, P. J.; Kok, W. T. *J. Chromatogr. A* **2007**, *1175*, 81-88.
20. Trojer, L.; Bisjak, C. P.; Wieder, W.; Bonn, G. K. *J. Chromatogr. A* **2009**, *1216*, 6303-6309.
21. Xu, Z.; Yang, L.; Wang, Q. *J. Chromatogr. A* **2009**, *1216*, 3098-3106.
22. Urban, J.; Svec, F.; Frechet, J. M. J. *Anal. Chem.* **2010**, *82*, 1621-1623.
23. Santora, B. P.; Gagne, M. R.; Moloy, K. G.; Radu, N. S. *Macromolecules* **2001**, *34*, 658-661.
24. Viklund, C.; Svec, F.; Frechet, J. M. J.; Irgum, K. *Chem. Mater.* **1996**, *8*, 744-750.
25. Li, Y.; Tolley, H. D.; Lee, M. L. *J. Chromatogr. A* **2010**, *1217*, 4934-4945.
26. Lubbad, S. H.; Buchmeiser, M. R. *J. Sep. Sci.* **2009**, *32*, 2521-2529.
27. Lubbad, S. H.; Buchmeiser, M. R. *J. Chromatogr. A* **2010**, *1217*, 3223-3230.
28. Greiderer, A.; Ligon, S. C.; Huck, C. W.; Bonn, G. K. *J. Sep. Sci.* **2009**, *32*, 2510-2520.

29. Greiderer, A.; Trojer, L.; Huck, C. W.; Bonn, G. K. *J. Chromatogr. A* **2009**, *1216*, 7747-7754.
30. Vidic, J.; Podgornik, A.; Strancar, A. *J. Chromatogr. A* **2005**, *1065*, 51-58.
31. Courtois, J.; Szumski, M.; Bystrom, E.; Iwasiewicz, A.; Shchukarev, A.; Irgum, K. *J. Sep. Sci.* **2006**, *29*, 325-325.
32. Okanda, F. M.; El Rassi, M. *Electrophoresis* **2005**, *26*, 1988-1995.
33. Jiang, Z.; Smith, N. W.; Ferguson, P. D.; Taylor, M. R. *J. Sep. Sci.* **2008**, *31*, 2774-2783.
34. Zhao, D.; Huo, Q.; Feng, J.; Chmelka, B. F.; Stucky, G. D. *J. Am. Chem. Soc.* **1998**, *120*, 6024-6036.
35. Li, Y.; Tolley, H. D.; Lee, M. L. *Anal. Chem.* **2009**, *81*, 4406-4413.
36. Courtois, J.; Bystrom, E.; Irgum, K. *Polymer* **2006**, *47*, 2603-2611.
37. Okay, O. *Prog. Polym. Sci.* **2000**, *25*, 711-779.
38. Hosoya, K.; Hira, N.; Yamamoto, K.; Nishimura, M.; Tanaka, N. *Anal. Chem.* **2006**, *78*, 5729-5735.

CHAPTER 5 FUTURE DIRECTIONS

5.1 Preparation of Monoliths with Improved Ligand Hydrophobicity for HIC of Proteins

HIC separations are based on mild hydrophobic interaction between the stationary phase and solute, as compared to RPLC where stronger interactions exist. These interactions are promoted through the use of a mobile phase containing high salt concentration, and programmed elution is achieved by decreasing the salt concentration. Compared to RPLC, HIC does not involve organic solvents or acidic conditions, and the stationary phase is less hydrophic, which makes HIC much less denaturing. Biomolecules can maintain their conformational structures that are responsible for the bioactivity. HIC is a valuable technique for protein separation and purification following IEC. In Chapters 2 and 3, a poly(HEA-*co*-PEGDA) monolith and monoliths from several PEGDA and PEGDMA monomers were successfully developed for HIC of proteins. A high salt concentration of 3 M $(NH_4)_2SO_4$ was required to promote hydrophobic interaction due to the weakly hydrophobic ligands in these monoliths. Although proteins dissolved in 3 M $(NH_4)_2SO_4$ were stable and no denaturation was observed for at least 48 h when kept on ice, this salt concentration is still considered to be high for many applications. Six protein standards could not be dissolved in higher concentrations than 0.5 M each. There is a need to develop monoliths with improved ligand hydrophobicity for HIC of proteins.

The overall hydrophobicity of an HIC stationary phase is determined by both ligand hydrophobicity and ligand density. The work described in Chapter 3 revealed that a hydrophilic matrix was important to avoid multi-point attachment of solutes to the stationary phase, which caused difficulty in eluting the solutes and resulted in peak tailing.

Thus, an ideal HIC stationary phase should contain a hydrophilic matrix, and the functionalities should be present in relatively low density. Short-chain alkyl groups and aryl groups are the most widely used functional ligands that are incorporated in silica-bound hydrophilic polymeric matrices. The hydrophobicity of alkyl groups increases with increasing chain length, e.g., pentyl > butyl > propyl > methyl.[1]

Based on the above discussion, I suggest that future work involve the design and synthesis of monoliths from monomers that contain more strongly hydrophobic functional ligands, such as propyl acrylate, butyl acrylate and pentyl acrylate. Since it has been demonstrated in Chapter 3 that PEGDA with three or more ethylene glycol units was effective in providing moderately hydrophilic backbone, PEGDA can be used as crosslinker. The density of the functional ligand can be adjusted by varying the ratio between the functional monomer and the crosslinker. Other potential cosslinking monomers that can be used to provide hydrophilic backbones include glycerol 1,3-diglyceralate diacrylate and OH-PEGDA (3 and 4 in Figure 5.1). Monolithic materials synthesized from these two monomers have been reported by Kubo et al.[2,3] These materials demonstrated hydrophilic characteristics based on contact angle measurements. Since the monomer and crosslinker are very different in polarity, whether or not rigid monoliths can be obtained will mainly depend on the selection of porogens. Monoliths prepared from BAEDA-4 in Chapter 4 were also found to be effective in HIC of proteins. Further characterization of this monolith for HIC is suggested.

5.2 Design of Functional Crosslinking Monomers for Various LC Modes

It has already been demonstrated in Chapters 3 and 4 that monoliths synthesized

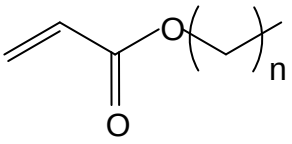

1
alkyl acrylate (n = 2, 3 and 4)

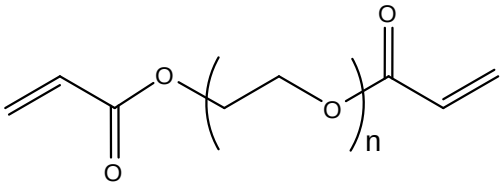

2
poly(ethylene glycol) diacrylate (n = 3 ~ 9)

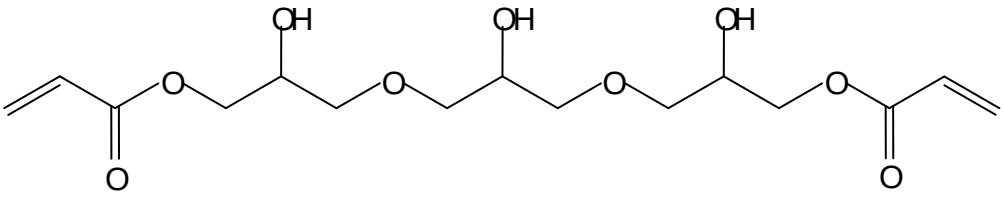

3
glycerol 1,3-diglyceralate diacrylate

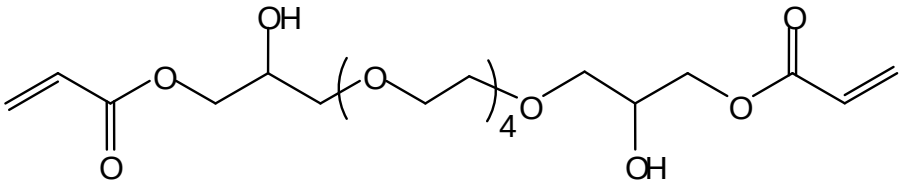

4
OH-PEGDA

Figure 5.1. Chemical structures of monomers for HIC stationary phases.

from single crosslinking monomers offered several advantages compared to monoliths prepared using conventional multi-monomer synthesis approaches, including improved column-to-column reproducibility, enhanced mesopores and surface area, higher rigidity and better mechanical stability. However, the available chemistry for single crosslinking monomers is not as abundant as for functional monomers. Several promising cosslinking monomers (Figure 5.2), such as alkyl diacrylates and dimethacrylates with different lengths of alkyl chains between the two acylic groups, e.g., *N*,*N*′-(1,2-dihydroxyethylene)bisacrylamide and *N*,*N*′-methylenebis(acrylamide), and bis[2-(methacryloyloxy)ethyl] phosphate, should be investigated to prepare monoliths for RPLC, HILIC and CEX.

With the intention of preparing more monoliths via single-monomer synthesis, the novel functional crosslinking monomers shown in Figure 5.3 could be synthesized for application in different separation modes. These diacrylates or dimethacrylates were designed to be symmetrical to ensure the same reactivity of the two acrylic ends. The presence of 4 or 6 ethylene glycol units is designed to provide a mildly hydrophilic backbone for the resulting monoliths. This is especially important for the analysis of biomolecules such as proteins or peptides, in which hydrophobic interactions often cause nonspecific interactions between analytes and stationary phase. The only exception would be stationary phases for RPLC, in which high functionality density is usually required to improve binding capacity. In this case, the PEG chain is not necessary.

5.3 Investigation of Porogen Selection

Despite observations that porogen nature and their percentage are the most powerful factors to adjust the porosity of the resulting monoliths, there is still no theory that leads to

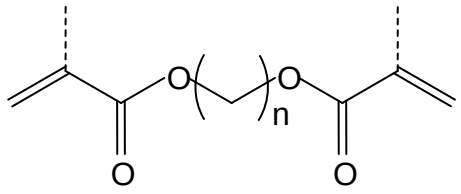

5

alkyl diacrylates and dimethacrylates (n ? 6)

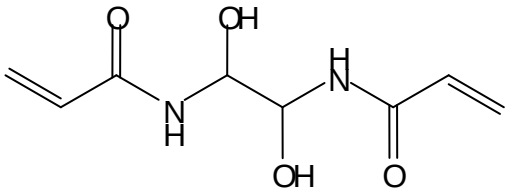

6

N,*N*?-(1,2-dihydroxyethylene)bisacrylamide

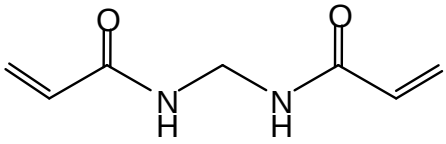

7

N,*N*?-methylenebis(acrylamide)

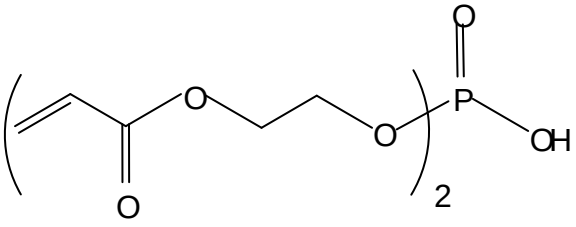

8

bis[2-(methacryloyloxy)ethyl] phosphate

Figure 5.2. Commercially available functional crosslinking monomers.

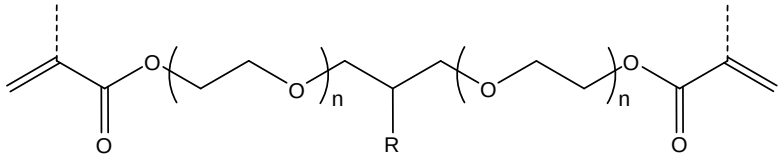

functional diacrylates or dimethacrylate (n = 2 or 3)

Reversed phase: R = —$CH_2(CH_2)_nCH_3$ (n = 2, 6 or 16)

Hydrophobic interaction: R = —$CH_2(CH_2)_nCH_3$ (n = 1, 2 or 3)

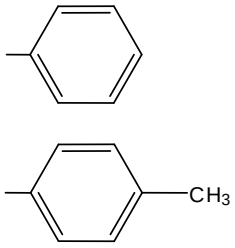

Cation exchange: R =

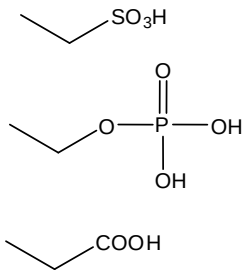

Anion exchange: R =

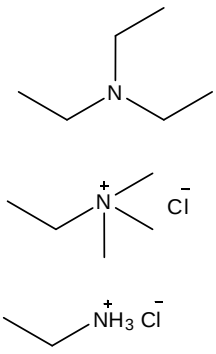

Hydrophilic interaction:

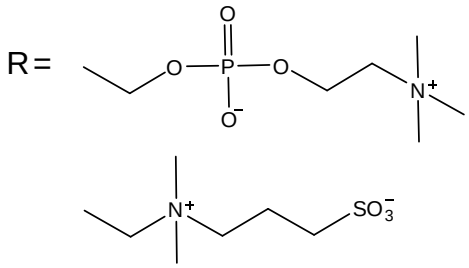

Reactive:

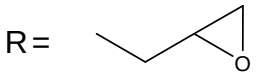

Figure 5.3. Chemical structures of proposed functional crosslinking monomers for different LC modes.

rational selection of porogenic solvents. The choice of porogens for the preparation of a porous polymer still depends on experience and trial and error. In Chapter 2, the strategy for porogen selection was systematically investigated through copolymerization between HEMA, HEA, EDMA and PEGDA. The results revealed that there were large differences in monolith morphologies of these copolymers when using the same porogens. Similarly, porogens suitable for formation of HEA/PEGDA monoliths were not effective for HEMA/PEGDA. As a continuing effort, selection of appropriate porogens was investigated using BADMA and PDAM as model monomers in Chapter 4. It was concluded that either dipole moment (i.e., polarity) or solubility parameter, which are the two solvent properties that have been proposed in the literature,[4,5] could be used as the a guide during porogen selection. However, solvent polarity could be a useful prediction if other properties are similar.

To further understand the strategy of porogen selection for a given monomer system, I propose that several representative crosslinking monomers be selected for the systematic study of porogen choice. For example, the hydrophilic monomers (PEGDA, PEGDMA or OH-PEGDA) in Figure 5.1, hydrophobic monomers (EDMA or alkyl diacrylate or dimethacrylate), and monomers containing hydrophobic and hydrophilic moieties such as PDAM can be potential candidates. Single monomer synthesis would make porogen selection more straightforward and the porogen effect easier to predict. Typical solvents as well as less widely used porogenic solvents should be explored. The morphologies and porosities should be characterized using SEM, mercury intrusion measurements, and BET measurements, as well as inverse size-exclusion chromatography.

5.4 References

1. Schmuck, M. N.; Nowlan, M. P.; Gooding, K. M. *J Chromatogr.* **1986,** *371*, 55-62.
2. Kubo, T.; Watanabe, F.; Kimura, N.; Kaya, K.; Hosoya, K. *Chromatographia* **2009,** *70*, 527-532.
3. Kubo, T.; Kimura, N.; Hosoya, K.; Kaya, K. *J. Polym. Sci. Pol. Chem.* **2007,** *45*, 3811-3817.
4. Courtois, J.; Bystrom, E.; Irgum, K. *Polymer* **2006,** *47*, 2603-2611.
5. Xu, Z. D.; Yang, L. M.; Wang, Q. Q. *J. Chromatogr. A* **2009,** *1216*, 3098-3106.